DISTRIBUTED COOPERATIVE STATE ESTIMATION AND CONTROL FOR MULTI-AGENT AUTONOMOUS SYSTEMS

Spine title: Distributed Cooperative State Estimation and Control for Multi-Agent Autonomous Systems

(Thesis format: Monograph)

by

MOUAAD BOUGHELLABA

Graduate Program
in
Electrical and Computer Engineering

A thesis submitted in partial fulfillment
of the requirements for the degree of
Doctor of Philosophy (Ph.D.)

The Faculty of Graduate Studies
Lakehead University
Thunderbay, Ontario, Canada

Abstract

This dissertation addresses several problems related to distributed cooperative state estimation and control design for multi-agent rigid-body autonomous systems, namely bearing-based distributed pose estimation, distributed attitude estimation on $SO(3)$, and global attitude synchronization on $SO(3)$.

We consider the distributed pose estimation problem for multi-agent rigid-body systems, under a directed graph topology, assuming that two agents have access to their respective poses. First, we consider the case where all agents have static positions and time-varying orientations, and propose two distributed pose estimation schemes evolving on $SO(3) \times \mathbb{R}^3$ and $SO(3) \times \mathbb{R}^3 \times \mathbb{R}^3$, with almost global asymptotic stability guarantees. Thereafter, we consider the case where the agents positions and orientations are time-varying, and propose a distributed pose observer evolving on $SO(3) \times \mathbb{R}^3$, with local exponential stability guarantees. The three proposed estimation schemes rely on individual angular velocity (and linear velocity in the case of agents with time-varying positions) measurements and local information exchange between neighboring agents (relative time-varying bearing measurements and estimated poses).

Next, we consider the problem of distributed attitude estimation of multi-agent systems, evolving on $SO(3)$, relying on individual angular velocity and relative attitude measurements, under an undirected, connected and acyclic communication graph topology. We propose two distributed attitude observers on $SO(3)$; a continuous version and a hybrid version, endowed respectively with almost global asymptotic stability and global asymptotic stability guarantees. In addition, the proposed hybrid attitude estimation scheme is used to solve the pose estimation problem of multi-agent rigid-body systems, with global asymptotic stability guarantees, relying on individual linear and angular velocity measurements as well as local relative bearing and relative orientation measurements.

Finally, we propose a distributed hybrid attitude synchronization scheme (with and without individual velocity measurements) for a group of rigid body systems evolving on $SO(3)$ under an undirected, connected and acyclic communication graph topology, with global asymptotic stability guarantees.

To all those whom I love...

Acknowledgements

First and foremost, I would like to express my deepest gratitude to my advisor, Prof. Abdelhamid Tayebi, for his invaluable guidance, unwavering support, and profound expertise throughout the journey of completing this PhD. His dedication to excellence, encouragement during challenging times, and insightful feedback have been instrumental in shaping this work. His mentorship has not only enriched my academic experience but has also inspired me to strive for excellence in all aspects of my research.

I would also like to thank the members of my doctoral examination committee: Prof. Xiaoping Liu and Prof. Kefu Liu for taking the time to serve as my PhD thesis examiners and for their constructive comments and feedback. I would especially like to thank Prof. Amir G. Aghdam from Concordia University for agreeing to review and examine my thesis.

I am grateful to my friends and colleagues who have supported me along this journey. Your encouragement and guidance have been invaluable, and I am truly grateful for your presence in my life.

I extend my deepest appreciation to my family. To my beloved mother, Alkhadem, and my siblings, Soulef, Wissal, and Ahmed, your prayers, encouragement, and understanding throughout this journey have been invaluable. Your love, patience, and belief in me have been the cornerstone of my perseverance and achievements.

Finally, I dedicate this thesis to the memory of my beloved father, Messaoud. His unwavering support, encouragement, and belief in my abilities have been the guiding lights at the beginning of my academic journey. Although he is no longer with us, his wisdom, love, and strength continue to inspire me every day.

Contents

Appendices   93

B   Proofs of Chapter 4   107

C   Proofs of Chapter 5   116

List of Figures

List of Abbreviations

MEMS	–	Micro Electro Mechanical Systems
AV	–	Autonomous Vehicle
PE	–	Persistently Exciting
BPE	–	Bearing Persistently Exciting
EA	–	Euler Angles
MRP	–	Modified Rodriguez Parameters
ISS	–	Input-to-State Stability
GAS	–	Globally Asymptotically Stable
AGAS	–	Almost Globally Asymptotically Stable
ES	–	Exponentially Stable
GES	–	Globally Exponentially Stable

List of Symbols

$\mathbb{R}$	–	the set of real numbers
$\mathbb{N}$	–	the set of natural numbers
$\mathbb{R}^n$	–	the set of n-dimensional vectors or n-dimensional Euclidean space
$\mathbb{R}^{n \times m}$	–	the set of real $n \times m$ matrices
$\mathbb{S}^{n-1}$	–	the set of n-dimensional unit vectors
$SO(3)$	–	the 3-dimensional Special Orthogonal group
$\mathfrak{so}(3)$	–	the Lie algebra of $\mathsf{SO}(3)$
$\mathcal{T}_x \mathcal{Q}$	–	the tangent space of smooth manifold $\mathcal{Q}$ at $x \in \mathcal{Q}$
$f : M \to N$	–	a mapping from M to N
$F : M \rightrightarrows N$	–	a set-valued mapping from M to N
$x \mapsto f(x)$	–	a mapping of an element x to a map $f(x)$
$\nabla_x f$	–	the gradient of f at x
df_x	–	the derivative of f at x
$\dot{x}$	–	the derivative, with respect to time, of the state x
x^+	–	the state of a hybrid system after a jump
$\mathrm{tr}(A)$	–	the trace of a matrix A
$\mathrm{diag}(\cdot)$	–	the block diagonal matrix
$\mathcal{E}(A)$	–	the set of unit eigenvectors of a matrix A
$\langle\langle A, B \rangle\rangle$	–	the Euclidean inner product of matrices $A, B \in \mathbb{R}^{m \times n}$
$\|x\|$	–	the Euclidean norm of a vector $x \in \mathbb{R}^n$
$\|X\|_F$	–	the Frobenius norm of a matrix $X \in \mathbb{R}^{m \times n}$
$\arg\min$	–	the argument of the minimum
$0_{n \times m}$	–	an $n \times m$ matrix of zero elements
I_n	–	an $n \times n$ identity matrix
λ_i^A	–	the i-th eigenvalue of matrix A
$\underline{\lambda}^A$	–	the smallest eigenvalue of matrix A
$\overline{\lambda}^A$	–	the largest eigenvalue of matrix A
$\otimes$	–	the Kronecker product

Chapter 1

Introduction

1.1 General Introduction

The past two decades have witnessed significant development and growth in Autonomous Vehicle (AV) technology, encompassing ground, maritime, and aerial vehicles. This rapid evolution has manifested itself in a wide range of civilian and military applications involving AVs, such as Intelligence, Security, and Reconnaissance (ISR) missions, inspection and monitoring operations, and transportation. The proliferation of AV technology has not only transformed conventional approaches to these applications, but has also paved the way for innovative solutions in areas considered dangerous or complex for human involvement. In addition, recent advances in micro-electro-mechanical systems (MEMS) have enabled the emergence of small AVs with high performance and capabilities. Making a group of AVs work together in a cooperative manner allows to achieve complex goals that are difficult of even impossible to achieve with a single AV. Among these applications, one can mention space-based interferometers, sensor networks, surveillance systems, *etc* (Ren and Cao, 2011).

The design of a robust multi-agent[1] autonomous system depends primarily on the development of reliable and efficient algorithms for cooperative state estimation and control. Unlike single-agent scenarios, the efficiency and robustness of these algorithms depend not only on the individual capabilities of each agent but also on their interaction capabilities. Therefore, two approaches are commonly considered for designing cooperative state estimation and control algorithms for multi-agent systems: distributed and non-distributed approaches. The non-distributed approach assumes either the availability of a central agent with global knowledge of all other agents (known as a centralized scheme), or that all agents have direct interactions with each other (known as a fully connected scheme). Unfortunately, the non-distributed scheme is not practical in terms of cost and robustness due to the single point of failure issue in the case of a centralized scheme, and the susceptibility to communication bottlenecks or delays that limit its scalability in the case of a fully connected scheme. In contrast, distributed approaches eliminate the need for a central agent or a direct interaction between all agents, with each agent interacting

---

[1]In this thesis, an agent denotes a dynamical rigid body system, *e.g.,* satellite, aircraft, ground vehicle, underwater vehicle.

solely with its neighbors. This yields significant advantages, including reduced operating costs, enhanced robustness, adaptability and scalability. Nevertheless, this approach increases the difficulty of designing cooperative control and estimation algorithms, especially for multi-agent systems with complex dynamics (*e.g.*, multi-agent systems evolving in non-Euclidean spaces). Although both approaches possess their own strengths and weaknesses, the distributed approach is preferred for practical applications because of the advantages mentioned above.

This thesis focuses on the design of distributed cooperative state estimation and control for multi-agent autonomous systems. In the following sections, we provide a general overview of the main approaches and results that have been proposed in this context.

1.2   Bearing-Based Distributed Cooperative Pose Estimation for Multi-agent Autonomous Systems

The distributed pose estimation problem for multi-agent networks consists of estimating the agents' poses (positions and orientations) in a distributed manner using some available absolute and relative measurements. Due to the importance of this problem in many applications related to multi-agent autonomous networks, significant research has been devoted to designing robust and reliable distributed pose localization schemes. According to the network's sensing capabilities, these schemes can be categorized as position-based (Ren and Atkins, 2007), distance-based (Oh and Ahn, 2011), and bearing-based schemes (Zhao and Zelazo, 2016). The latter category has recently gained in popularity due to the revolutionary development in bearing sensors and the fact that bearing information can be obtained from low-cost and simple sensor systems compared to distance-based or position-based solutions. For example, vision sensors (Tron et al., 2016) or wireless sensor arrays (Mao et al., 2007) can be used to obtain the bearing measurements.

Over the last decade, a number of interesting results dealing with distributed pose estimation of multi-agent systems, relying on the bearing rigidity theory, have been proposed in the literature. Roughly speaking, the basic idea behind the concept of bearing rigidity is that a set of relative static bearing vectors is sufficient to specify the geometric pattern of a multi-agent rigid-body system up to a translation and a scaling factor (Zhao and Zelazo, 2019). In early works, the authors in (Bishop et al., 2011; Eren, 2012) studied the theory of bearing rigidity in two-dimensional spaces. Later on, the authors in (Zhao and Zelazo, 2016; Zhao and Zelazo, 2015) developed the theory of bearing rigidity for spaces with arbitrary dimensions. As a result, bearing-based cooperative observers have made their appearances in the literature. For instance, the authors in (Zhao and Zelazo, 2016) formulated the problem of bearing-based network localization as a linear least-squares optimization problem. In solving this optimization problem, the authors provided the localization conditions and protocols for a static network in an n-dimensional space using only relative bearing measurements and the location of some anchors (agents with known positions). However, the aforementioned references assume that the bearings are expressed in a global reference frame (*i.e.*, knowledge of agents' orientations with respect to a global reference frame), which, unfortunately, is not the

case in most of the practical applications since the bearing measurements are usually obtained locally from a sensor (*e.g.*, a camera) mounted on the agent. This motivated many authors to design a distributed attitude observer that can be fed into a position estimation scheme together with local bearing measurements to obtain an overall cascaded bearing-based distributed pose estimation scheme (Li et al., 2020; Lee et al., 2019). The idea consists in using the estimated attitudes to transform the local relative bearing measurements into the global reference frame and then use the transformed bearings in the position estimation law. In (Lee and Ahn, 2016a; Lee and Ahn, 2016b; Van Tran et al., 2018; Lee et al., 2019; Van Tran et al., 2019; Van Tran and Ahn, 2020), the authors proposed several orientation estimation algorithms based on the consensus approach and the Gram-Schmidt orthonormalization procedure. However, most of these distributed attitude estimation schemes require relative attitude measurements, which are difficult to obtain since no low-cost setup can provide such measurements directly. To the best of the author's knowledge, there are very few results in the literature that address the distributed pose estimation problem for multi-agent networks relying on local relative bearing measurements without using the relative attitude information. Therefore, it is of great interest to design distributed pose observers for multi-agent systems using only bearing measurements. Reference (Tran et al., 2020) proposed distributed pose estimation schemes based on local relative bearing measurements and some absolute measurements (angular and linear velocities). Unfortunately, this work provides only convergence results, with some flaws in the proofs that have been pointed out in (Boughellaba and Tayebi, 2023b)[2]. This motivated the work is this dissertation on the design of distributed pose estimation schemes that rely only on local relative bearing measurements and some absolute measurements (angular and linear velocities) with AGAS.

On the other hand, dealing with time-varying bearings instead of static ones is more realistic and appropriate for applications involving networks of mobile agents. Therefore, some recent results have extended the concept of bearing rigidity by considering time-varying bearings. For instance, the authors in (Tang et al., 2020a; Tang et al., 2022) used the concept of persistence of excitation on bearing measurements to relax the conditions of bearing rigidity (Zhao and Zelazo, 2016) and bearing persistence[3] (Zhao and Zelazo, 2015). Based on the assumption that the bearings are persistently exciting, exponentially convergent bearing-based distributed position estimation algorithms have been proposed for multi-agent networks considering both undirected and directed graph topologies (Tang et al., 2020a; Tang et al., 2020b; Tang et al., 2021). Recently, the authors of the latter references further extended their research by considering undirected switching graph typologies and proposed bearing-based distributed position estimation algorithms that guarantee exponential convergence under the assumption that the formation is Bearing-Persistently-Exciting (BPE) (Tang and Loría, 2023a; Tang, 2023). However, these works also assume that the bearings are measured in the global reference frame. Therefore, the design of a bearing-based distributed pose estimation scheme with exponential stability guarantees, where the bearing measurements are time-varying and

---

[2]Authors' reply can be found in (Tran et al., 2023).

[3]A formation is bearing persistent when the null spaces of the bearing Laplacian matrix and the bearing rigidity matrix are the same (Zhao and Zelazo, 2015).

locally obtained, has been addressed in this dissertation.

1.3   Distributed Attitude Estimation for Multi-Agent Systems

A fundamental problem of great importance in the field of distributed cooperative state estimation for multi-agent autonomous systems, namely the distributed cooperative attitude estimation, consists of estimating the agents' attitudes using some absolute individual measurements and some inter-agent (relative) measurements according to a predefined interaction graph topology between the agents involved in the group. The importance of this problem stems from the fact that the available absolute individual measurements are not enough to allow each agent to estimate its orientation independently from other agents.

It is well known that the only representation that describes the attitude of a rigid body uniquely and globally is the rotation matrix belonging to the special orthogonal group $SO(3)$ which is a smooth manifold with group properties (*i.e.,* matrix Lie group). Since $SO(3)$ is boundaryless odd-dimensional compact manifold, it is non-diffeomorphic to any Euclidean space, and as such, it is not possible to achieve global asymptotic stability with time-invariant continuous vector fields on $SO(3)$ (Koditschek, 1989; Bhat and Bernstein, 2000), *i.e.,* in addition to the desired equilibrium there are other undesired equilibria. Since the use of classical cooperative schemes (on Euclidean spaces) for systems evolving on smooth manifolds is not trivial, appropriate cooperative control and estimation techniques needed to be developed. As such, some consensus-based attitude synchronization schemes on $SO(3)$ have been proposed in the literature (see, for instance, (Tron et al., 2012; Tron et al., 2013; Markdahl, 2021; Sarlette et al., 2009; Sarlette et al., 2007; Sarlette and Sepulchre, 2009a)). Motivated by the attitude synchronization schemes mentioned in the above references, some distributed cooperative attitude estimation schemes, designed directly on $SO(3)$, have been proposed in the literature. For instance, the authors in (Tron and Vidal, 2014) proposed a distributed attitude localization scheme for camera sensor networks endowed with an almost global convergence result. To achieve this, they introduced a reshaping function to the cost function, given in (Tron et al., 2011), such that the only stable equilibrium of the proposed scheme is the global minimizer of the reshaped cost function.

In a series of papers (Lee and Ahn, 2016a; Lee and Ahn, 2016b; Van Tran et al., 2018; Lee et al., 2019), the authors proposed some attitude estimation schemes relying on classical (Euclidean) consensus algorithms along with the Gram-Schmidt orthonormalization procedure. These attitude estimation algorithms have been extended to deal with time-varying orientations in n-dimensional Euclidean spaces (Van Tran et al., 2019; Van Tran and Ahn, 2020). Note that the attitude estimation schemes based on the Gram-Schmidt orthonormalization procedure may lead to problems when the estimated matrix (that does not belong to $SO(3)$) is singular. A more recent work (Li et al., 2020) suggests a similar algorithm as the one in (Lee and Ahn, 2016a; Van Tran et al., 2018), but without the Gram-Schmidt orthonormalization. As a result, the algorithm provides estimates of

the agents' orientations only when the time tends to infinity and not for all times, which makes the algorithm inappropriate for control applications requiring instantaneous orientations for feedback. The design of distributed attitude estimation schemes directly on a rotation manifold with global asymptotic stability guarantees is an open problem that has been solved in this thesis using hybrid techniques.

1.4   Attitude Synchronization

The attitude synchronization for multi-agent rigid body systems consists in aligning the agents orientations with a common desired orientation, using local information exchange. This problem has garnered considerable attention from the research community over the past few decades due to its significant implications in various areas. Many of the existing multi-agent rigid body formation control schemes assume that the agents' absolute orientations are known to allow the use of local relative measurements (*e.g.*, positions, distances, or bearings) in the formation control laws. However, if the agents' absolute attitudes are unknown, they can still achieve the desired formation up to a constant rotation by first synchronizing their attitudes to a common orientation and then using this common orientation together with local relative measurements in the formation control law. Note that the two tasks (*i.e.*, the attitude synchronization and formation control) can be performed simultaneously (Oh and Ahn, 2014; Moshtagh et al., 2009).

A number of works have investigated the problem of attitude synchronization using different attitude parameterizations such as the Euler Angles (EA), Modified Rodriguez Parameters (MRP), and unit quaternions. The authors in (Dimarogonas et al., 2009; Bayezit and Fidan, 2013; Ren, 2010; Jin et al., 2020; Meng et al., 2010; Chen et al., 2019) used EA and MRP representations to study the attitude synchronization problems. Unfortunately, these attitude representations evolve on the Euclidean space $\mathbb{R}^3$ and achieve only local results due to the singularity problem (Ren, 2010). Since the unit-quaternion represents the attitude of a rigid body globally (Shuster, 1993), several works have addressed the attitude synchronization problem using this representation (Ren, 2007; Bai et al., 2008; Liu and Huang, 2018; Pereira et al., 2020; Zhang et al., 2022). In the same context, the authors in (Abdessameud and Tayebi, 2009; Abdessameud et al., 2012) proposed quaternion-based attitude synchronization schemes that use the virtual dynamics approach, initially proposed in (Tayebi, 2008), to eliminate the need for the angular velocity measurements. Although the unit-quaternion representation does not suffer from the singularity problem, unit-quaternion space is a double cover of the special orthogonal group $SO(3)$. The use of unit-quaternion, without extra care, can result in the undesirable unwinding phenomenon. Motivated by this, the authors in (Mayhew et al., 2012; Gui and de Ruiter, 2018; Huang and Meng, 2021) proposed hybrid quaternion-based attitude synchronization schemes endowed with global asymptotic stability guarantees, while effectively avoiding the unwinding phenomenon through the use of an appropriately designed logic variable to determine the sign of the torque input.

Unlike other attitude parameterizations , the rotation matrix representation, which belongs to the special orthogonal group $SO(3)$, is the only representation that uniquely and globally represents the attitude of a rigid body. However, the topological obstruc-

tion to global asymptotic stability induced by the fact that $SO(3)$ not homeomorphic to any Euclidean space (Koditschek, 1989; Bhat and Bernstein, 2000), poses a challenge in extending the classical Euclidean consensus schemes to consensus schemes on smooth manifolds such as $SO(3)$. Despite this challenge, several attitude synchronization schemes on $SO(3)$ have been proposed in the literature (*e.g.*, (Maadani et al., 2020; Van Tran et al., 2022; Tron et al., 2012; Tron et al., 2013; Markdahl, 2021; Sarlette et al., 2009; Sarlette et al., 2007; Sarlette and Sepulchre, 2009a; Wei et al., 2018)). Unfortunately, none of these papers was able to provide global asymptotic stability results. Therefore, the design of attitude synchronization schemes (with and without angular velocity measurements) on $SO(3)$ with global asymptotic stability guarantees is an open problem addressed in this dissertation.

1.5 Thesis Contributions

In this dissertation, we address the problem of distributed cooperative state estimation and control design for multi-agent autonomous systems. The contributions can be summarized as follows:

- Chapter 3 deals with the design of bearing-based distributed pose observers, for multi-agent rigid body systems, under a directed graph topology. These observers rely on individual angular velocity (and linear velocity in the case of agents with time-varying positions) measurements and local information exchange between neighboring agents (relative time-varying bearing measurements and estimated poses). The following two main contributions summarize the results of this chapter:

  1. Assuming the agents have static positions and time-varying orientations, we first design an almost globally asymptotically stable stand-alone bearing-based distributed attitude observer evolving on $SO(3)$. We then extend this design by using filtered bearing measurements in the observer dynamics evolving on $SO(3) \times \mathbb{R}^3$, resulting in an AGAS distributed attitude estimation scheme. This state observer is more practical than the one proposed in the first design, since it helps filtering out bearing measurements noise. Finally, relying on the attitude estimates, provided by the distributed rotational state observer, together with local relative (time-varying) bearing measurements, we design an AGAS distributed pose observer. Note that the authors in (Tran et al., 2020) dealt with the same problem and provided convergence results with some flaws in their proof as pointed out in (Boughellaba and Tayebi, 2023b). To the best of the author's knowledge, no such strong stability result has been reported in the available literature for the problem under consideration.

  2. Considering the case where the agents are assumed to have both time-varying positions and orientations, we propose an exponentially stable bearing-based distributed nonlinear pose estimation scheme on $SO(3) \times \mathbb{R}^3$. The overall bearing-based distributed pose estimation scheme is a cascade of a standalone bearing-based distributed attitude observer, endowed with local exponential

stability, and a bearing-based distributed position observer relying on the attitude estimates provided by the rotational observer. Local exponential stability of the overall distributed pose estimation scheme is established. This local stability result is mainly due to the fact that the agents' positions are allowed to be time-varying. Moreover, unlike the design proposed in (Tang and Loría, 2023b; Tang et al., 2020a; Tang et al., 2021), our distributed pose localization scheme relies on local time-varying bearing measurements.

The results presented in this chapter are reported in (Boughellaba and Tayebi, 2022; Boughellaba and Tayebi, 2023b; Boughellaba and Tayebi, 2023a).

- In Chapter 4, two distributed attitude estimation schemes on $SO(3)$ are proposed for a group of rigid body systems under an undirected, connected and acyclic graph topology. Each agent measures its own angular velocity in the respective body-frame, measures the relative orientation with respect to its neighbors, and receives information from its neighbors. The attitude observers designed in this Chapter do not rely on relative bearing measurements as in Chapter 3 but on relative orientation measurements. Note that both estimation schemes provide attitude estimates up to a constant orientation which can be determined in the presence of a leader in the group (knowing its absolute orientation). Furthermore, a distributed pose estimation law is proposed, providing global estimates of the individual poses up to a constant translation and orientation. It relies on the estimated attitudes, provided by the distributed attitude observer, the local relative (time-varying) bearing information, and the individual linear velocities.

    1. Inspired by the consensus optimization framework on manifolds introduced in (Sarlette and Sepulchre, 2009b), we propose a continuous distributed attitude estimation scheme on $SO(3)$. Moreover, we provide a rigorous stability analysis that shows that the proposed continuous attitude observer is AGAS. Compared to the existing results, such as (Lee and Ahn, 2016a; Lee et al., 2019; Van Tran et al., 2019; Van Tran and Ahn, 2020), the proposed continuous distributed attitude observer, in addition of being designed directly on $SO(3)$ and endowed with asymptotic stability (not only convergence) results, is much simpler and does not require any auxiliary matrices and orthonormalization procedures (*e.g.*, Gram-Schmidt orthonormalization), which may complicate the implementation of the observer and add extra computational overhead.

    2. To overcome the topological obstruction that precludes global asymptotic stability on $SO(3)$ with smooth vector fields, a new hybrid distributed attitude observer, with global asymptotic stability guarantees, is developed.

    3. A globally asymptotically stable bearing-based hybrid distributed pose estimation scheme for n-agent rigid-body systems is developed. To the best of the author's knowledge, there is no existing work in the literature providing such strong stability results for the problem dealt with in this dissertation.

The results presented in Chapter 4 have been published in (Boughellaba and Tayebi, 2023c; Boughellaba and Tayebi, 2023d).

- In Chapter 5, a new distributed hybrid feedback control scheme, for the global attitude synchronization of a group of rigid body systems, is developed. The proposed distributed control scheme, relying on individual angular velocity measurements and relative attitude information, ensures global convergence of the individual orientations to a common orientation under undirected, connected, and acyclic graph topologies. In contrast to (Mayhew et al., 2012; Gui and de Ruiter, 2018; Huang and Meng, 2021), the proposed distributed attitude synchronization scheme is designed directly on $SO(3)$. Furthermore, a velocity-free distributed hybrid attitude synchronization scheme, with global asymptotic stability guarantees, relying on relative attitude measurements, is proposed. Inspired by (Tayebi, 2008) and (Wang and Tayebi, 2022), the proposed velocity-free control law uses, in addition to the generic multi-agent switching mechanism introduced in Chapter 4, an auxiliary dynamical system for each agent to generate the necessary damping that compensates for the lack of angular velocity information. To the best of the author's knowledge, this is the first result in the literature dealing with velocity-free global attitude synchronization on $SO(3)$. The results of this chapter are presented in (Boughellaba and Tayebi, 2024).

List of Publications

The materials presented in this dissertation are based on the following publications:

Journal Articles:

- M. Boughellaba and A. Tayebi, "Distributed attitude estimation for multi-agent systems on SO(3)", *IEEE Transactions on Automatic Control*, Conditionaly accepted, 2023.

- M. Boughellaba and A. Tayebi, "Bearing-based distributed pose estimation for multi-agent networks", *IEEE Control Systems Letters*, vol. 7, pp. 2617–2622, 2023.

- M. Boughellaba and A. Tayebi, "Comments on "pose localization of leader–follower networks with direction measurements" [automatica 120 (2020) 109125]", *Automatica*, vol. 151, p. 110 949, 2023, issn: 0005-1098.

Peer-Reviewed Conference Proceedings:

- M. Boughellaba and A. Tayebi, "Global attitude alignment for multi-agent systems on $SO(3)$ without angular velocity measurements", In *proc. of the American Control Conference (ACC)*, Toronto, Canada, Accepted, 2024.

- M. Boughellaba and A. Tayebi, "Bearing-based distributed pose estimation for multi-agent networks", In *Proc. of the 62nd IEEE Conference on Decision and Control (CDC)*, Singapore, pp. 1394-1399, 2023.

- M. Boughellaba and A. Tayebi, "Distributed hybrid attitude estimation for multi-agent systems on $SO(3)$", In *proc. of the American Control Conference (ACC)*, San Diego, CA, USA, pp. 1048–1053, 2023.

- M. Boughellaba and A. Tayebi, "Leader-follower bearing-based distributed pose estimation for multi-vehicle networks", In *Proc. of the 61st IEEE Conference on Decision and Control (CDC)*, Cancun, Mexico, pp. 6562–6567, 2022.

1.6   Thesis Outline

This thesis is organized as follows:

Chapter 2 presents the notations, background and preliminaries used throughout the thesis. Section 2.1 contains the general notations used in this thesis. Section 2.2 and Section 2.3 present some tools related to differential manifolds and graph theory. Fundamental consensus algorithms are presented in Section 2.4. Section 2.5 describes the attitude representation and some useful related identities and lemmas. Section 2.6 presents the hybrid systems framework used in this dissertation. Finally, Section 2.7 presents the notion of almost global input-to-state stability and some useful related results.

Chapter 3 is devoted to the problem of bearing-based distributed cooperative pose estimation for multi-agent autonomous. Section 3.2 deals with the design of bearing-based distributed pose estimation schemes, assuming that agents have fixed positions and time-varying orientations. The case where the agents have time-varying positions and orientations is dealt with in Section 3.3. Concluding remarks are presented in Section 3.4.

Chapter 4 is dedicated to the design of distributed attitude estimation observers for multi-agent rigid-body systems, relying on relative orientation measurements, with application to distributed pose estimation. In Section 4.2, the distributed attitude estimation problem for multi-agent systems, with relative attitude measurements, is formulated. Section 4.3 provides the design of continuous and hybrid distributed attitude estimation schemes. Section 4.4 deals with the design of a hybrid distributed pose estimation scheme. Simulation results and concluding remarks are presented in Section 4.5 and Section 4.6, respectively.

Chapter 5 considers the problem of global attitude synchronization on $SO(3)$ for multi-agent rigid body systems. Section 5.2 formulates the problem of attitude synchronization on $SO(3)$. Section 5.3 presents the (generic) distributed hybrid feedback control scheme for the global attitude synchronization relying on angular velocity and relative attitude measurements. This generic feedback control scheme is extended in Section 5.4 to the case where only relative attitude measurements are available. Section 5.5 provides an explicit design for both feedback control schemes presented in Sections 5.3 and 5.4. Finally, Sections 5.6 and 5.7 present some simulation results and concluding remarks,

respectively.

Chapter 6 summarizes the findings of this thesis and presents some possible future directions.

Appendix A, B, C contain the detailed proofs of lemmas and theorems stated throughout this thesis.

Chapter 2

Background and Preliminaries

2.1 General Notations

The sets of real numbers and the n-dimensional *Euclidean* space are denoted by $\mathbb{R}$ and $\mathbb{R}^n$, respectively. Consider a matrix A with dimensions $n \times m$ (*i.e.*, $A \in \mathbb{R}^{n \times m}$), where n represents the number of rows and m represents the number of columns. Each entry in the matrix is denoted by a_{ij}, representing the value in the i-th row and the j-th column. For any square matrix $A \in \mathbb{R}^{n \times n}$, the trace of the matrix is denoted as $\text{tr}(A)$ and is calculated by summing the values of its diagonal elements, *i.e.*, $\text{tr}(A) = \sum_{i=1}^{n} a_{ii}$. The determinant of the matrix A is denoted by $\det(A)$. The set of unit vectors in $\mathbb{R}^n$ is defined as $\mathbb{S}^{n-1} := \{x \in \mathbb{R}^n \mid x^T x = 1\}$. Let A^T be the transpose of the matrix A. Given two matrices $A,B \in \mathbb{R}^{n \times m}$, their *Euclidean* inner product is defined as $\langle\langle A, B \rangle\rangle = \text{tr}(A^T B)$. The *Euclidean* norm of a vector $x \in \mathbb{R}^n$ is defined as $||x|| = \sqrt{x^T x}$, and the *Frobenius* norm of a matrix $A \in \mathbb{R}^{n \times n}$ is given by $||A||_F = \sqrt{\langle\langle A, A \rangle\rangle}$. The dot product of two vectors x and y in $\mathbb{R}^3$ is given by $x \cdot y = ||x|| ||y|| \cos\langle x, y \rangle$, where $\langle x, y \rangle$ denotes the angle between the vectors x and y. Let A be a square matrix of size $n \times n$ over the real numbers. We use λ_i^A to represent the i-th eigenvalue of matrix A. In addition, $\underline{\lambda}^A$ and $\overline{\lambda}^A$ denote the smallest and largest eigenvalues of A, respectively. Furthermore, $\mathcal{E}(A)$ denotes the collection of all eigenvectors associated with matrix A. The matrix $I_n \in \mathbb{R}^{n \times n}$ denotes the identity matrix, and $\mathbf{1}_n = [1 \dots 1]^T \in \mathbb{R}^n$. Given a subset $\mathcal{S}_\mathbb{N} \subset \mathbb{N}$, where $\mathbb{N}$ is the set of natural numbers, the cardinality of $\mathcal{S}_\mathbb{N}$ is denoted by $|\mathcal{S}_\mathbb{N}|$. Let $\mathcal{S}$ be a subset, $\overline{\mathcal{S}}$ denotes the closure[1] of $\mathcal{S}$. Given two matrices $A := [a_{ij}] \in \mathbb{R}^{n \times m}$ and $B \in \mathbb{R}^{p \times q}$, the Kronecker product of A and B is defined as the matrix

$$A \otimes B := \begin{bmatrix} a_{11}B & a_{12}B & \dots & a_{1m}B \\ a_{21}B & a_{22}B & \dots & a_{2m}B \\ \vdots & \vdots & \ddots & \vdots \\ a_{n1}B & a_{n2}B & \dots & a_{nm}B \end{bmatrix} \in \mathbb{R}^{np \times mq}. \tag{2.1}$$

---

[1]The closure of a set contains all the points of the set itself and any limit points of the set. A limit point of a set is a point such that every neighborhood of that point contains at least one point from the set different from the point itself.

2.2   Differential Manifold

A differential manifold is a more general mathematical object that includes spaces that are locally similar to *Euclidean* space, but can have more complicated global structures and curvatures. Unlike *Euclidean* spaces, differential manifolds can have variable curvature and need not be flat on a large scale. A classic example of a differential manifold is the unit sphere, defined as $\mathbb{S}^{n-1} := \left\{(x_1, x_2, \ldots, x_n) \in \mathbb{R}^n : \quad x_1^2 + x_2^2 + \ldots + x_n^2 = 1\right\}$, which is a differential manifold embedded in $\mathbb{R}^n$. It is important to note that the standard definition of a derivative for functions in *Euclidean* spaces, relying on vector space structures, does not directly apply to smooth maps between manifolds. This limitation arises because manifolds are more general geometric objects that may lack a simple vector space structure, particularly when embedded in higher-dimensional spaces. Therefore, a new notion of the derivative of a map on a smooth manifold needs to be defined (Darryl D Holm., 2009).

Let $\mathcal{Q}$ be a smooth manifold, and consider an open interval $\mathbb{I} \subset \mathbb{R}$ containing zero in its interior. Let $\zeta : \mathbb{I} \to \mathcal{Q}$ be a smooth curve with $\zeta(0) = x$. The *tangent vector* at $x \in \mathcal{Q}$ is defined as the derivative of the curve ζ evaluated at zero:

$$\dot{\zeta}(0) := \left.\frac{d}{dt}\right|_{t=0} \zeta(t).$$

Definition 2.1 *(Darryl D Holm., 2009) The set of all tangent vectors at a given point x, corresponding to all possible paths in $\mathcal{Q}$ through x, is called the* tangent space *to $\mathcal{Q}$ at point x, denoted by $\mathcal{T}_x\mathcal{Q}$.*

Definition 2.2 *(Darryl D Holm., 2009) The disjoint union of all tangent spaces represents the* tangent bundle *of $\mathcal{Q}$, given as*

$$\mathcal{T}\mathcal{Q} = \bigcup_{x \in \mathcal{Q}} \mathcal{T}_x\mathcal{Q}.$$

Definition 2.3 *Consider two smooth manifolds $\mathcal{Q}$ and $\mathcal{O}$. The map $f : \mathcal{Q} \to \mathcal{O}$ is said to be a* differentiable *map if it is differentiable at all points in its domain.*

Remark 2.1 *The inverse image of a subset $\mathcal{S}_\mathcal{O} \subset \mathcal{O}$ under the map f is the subset of $\mathcal{Q}$ given by $f^{-1}(\mathcal{S}_\mathcal{O}) = \{x \in \mathcal{Q} : f(x) \in \mathcal{S}_\mathcal{O}\}$.*

Remark 2.2 *The map f is a* diffeomorphism *map if it is differentiable and its inverse is also differentiable.*

Definition 2.4 *(Darryl D Holm., 2009) Let $f : \mathcal{Q} \to \mathcal{O}$ be a differentiable map between two smooth manifolds $\mathcal{Q}$ and $\mathcal{O}$. The* tangent map *of f at point $x \in \mathcal{Q}$ denoted by $df_x : \mathcal{T}_x\mathcal{Q} \to \mathcal{T}_{f(x)}\mathcal{O}$ is defined as*

$$df_x(\eta) := \left.\frac{d}{dt}\right|_{t=0} f\left(\zeta(t)\right),$$

where $\zeta(t)$ is a smooth curve in $\mathcal{Q}$ with $\zeta(0) = x$ and $\eta = \dot{\zeta}(0) \in \mathcal{T}_x\mathcal{Q}$.

Consider a smooth manifold $\mathcal{Q}$ with $\mathcal{T}_x\mathcal{Q}$ being its tangent space at point $x \in \mathcal{Q}$. Let $f : \mathcal{Q} \to \mathbb{R}_{\geq 0}$ be a continuously differentiable real-valued function. The function f is a potential function on $\mathcal{Q}$ with respect to set $\mathcal{B} \in \mathcal{Q}$ if

$$\begin{cases} f(x) & = 0, & \forall x \in \mathcal{B} \\ f(x) & > 0, & \forall x \notin \mathcal{B} \end{cases}$$

The gradient of f at $x \in \mathcal{Q}$, denoted by $\nabla_x f(x)$, is defined as the unique element of $\mathcal{T}_x\mathcal{Q}$ such that (Absil et al., 2007):

$$df_x(\eta) = \langle \nabla_x f(x), \eta \rangle_x, \qquad \forall \eta \in \mathcal{T}_x\mathcal{Q},$$

where $\langle \ , \ \rangle_x : \mathcal{T}_x\mathcal{Q} \times \mathcal{T}_x\mathcal{Q} \to \mathbb{R}$ is *Riemannian* metric on manifold $\mathcal{Q}$ at point x. The point $x \in \mathcal{Q}$ is said to be a critical point of f if $\nabla_x f(x) = 0$.

2.3 Graph Theory

Graph theory plays a crucial role in designing and analyzing cooperative control and state estimation schemes since it provides a mathematical framework and a set of tools for modeling and studying the relationships and interactions between different entities or agents in a system. Therefore, in this section, we will present some important definitions and properties related to the graph theory used throughout this thesis. The reader is referred to (Ren and Beard, 2007; Mesbahi and Egerstedt, 2010) for more details.

Consider a network of n agents. The interaction topology between the agents can be described either by the undirected graph $\mathcal{G}_u = (\mathcal{V}, \mathcal{E}_u)$ or by the directed graph $\mathcal{G}_d = (\mathcal{V}, \mathcal{E}_d)$ where $\mathcal{V} = \{1, \ldots, n\}$ represents the vertex (or agent) set and $\mathcal{E}_u \subseteq \mathcal{V} \times \mathcal{V}$ (resp. $\mathcal{E}_d \subseteq \mathcal{V} \times \mathcal{V}$) represents the edge set of $\mathcal{G}_u$ (resp. $\mathcal{G}_d$). In undirected graphs, if $(i, j) \in \mathcal{E}_u$, then $(j, i) \in \mathcal{E}_u$. In other words, if j is a neighbor of i, then i is also a neighbor of j. However, in directed graphs, $(i, j) \in \mathcal{E}_d$ does not necessarily imply $(j, i) \in \mathcal{E}_d$. The set of neighbors of agent i is defined as $\mathcal{N}_i = \{j \in \mathcal{V} : (i, j) \in \mathcal{E}\}$, where $\mathcal{E}$ is either equal to $\mathcal{E}_u$ or $\mathcal{E}_d$ depending on whether the graph is directed or undirected, respectively. The undirected path is a sequence of edges in an undirected graph $\mathcal{G}_u$. An undirected graph $\mathcal{G}_u$ is connected if there is an undirected path between every pair of distinct vertices. An undirected graph has a cycle if there exists an undirected path that starts and ends at the same agent. An acyclic undirected graph is an undirected graph without a cycle. An undirected tree is an undirected graph in which any two agents are connected by exactly one path (*i.e.*, an undirected tree is an undirected, connected, and acyclic graph). An oriented graph is obtained from an undirected graph by assigning an arbitrary direction to each edge.

The adjacency matrix is a square matrix used to represent the relationships of the graph's vertices in a 2D array. The adjacency matrix $D := [d_{ij}] \in \mathbb{R}^{n \times n}$ of an undirected graph $\mathcal{G}_u$ is defined such that $d_{ii} = 0$ and

$$\begin{cases} d_{ij} = d_{ji} = 1, & \text{if } (i, j) \in \mathcal{E}_u \\ d_{ij} = d_{ji} = 0, & \text{otherwise} \end{cases} \tag{2.2}$$

Note that the presence or absence of an edge between two vertices is represented by the values 1 and 0, respectively, in the adjacency matrix. For example, the unweighted adjacency matrix of the undirected graph in Figure 2.1 is given by

$$D = \begin{bmatrix} 0 & 1 & 0 & 0 & 1 \\ 1 & 0 & 1 & 0 & 0 \\ 0 & 1 & 0 & 1 & 0 \\ 0 & 0 & 1 & 0 & 1 \\ 1 & 0 & 0 & 1 & 0 \end{bmatrix} \tag{2.3}$$
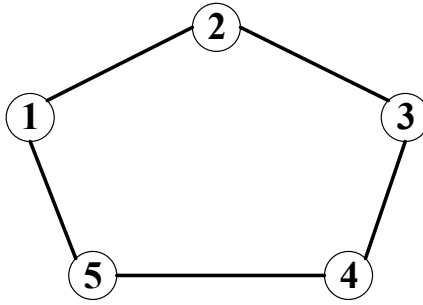
Figure 2.1: Example of an undirected graph with five vertices.

Property 2.1 *For an undirected graph, the adjacency matrix is always symmetric since if there is an edge from vertex i to vertex j, there is also an edge from vertex j to vertex i.*

Consider an oriented graph where each edge is indexed by a number. Let $m = |\mathcal{E}|$ and $\mathcal{M} = \{1, \ldots, m\}$ be the total number of edges and the set of edge indices, respectively. The incidence matrix of an oriented graph is denoted by $H \in \mathbb{R}^{n \times m}$, where the rows are indexed by the vertex numbers and the columns are indexed by the edge numbers. The entry indexed by (i, k) equals 1 if vertex i is the head of edge k, -1 if it is the tail, and 0 otherwise. Define $\mathcal{M}_i^+ \subset \mathcal{M}$ as the subset of edge indices in which agent i is the head of the edges and $\mathcal{M}_i^- \subset \mathcal{M}$ as the subset of edge indices in which agent i is the tail of the edges. Using these definitions, the incidence matrix can be expressed as follows:

$$H := [h_{ik}]_{n \times m} \quad \text{with } h_{ik} = \begin{cases} +1 & k \in \mathcal{M}_i^+ \\ -1 & k \in \mathcal{M}_i^- \\ 0 & \text{otherwise} \end{cases}, \tag{2.4}$$

For instant, assigning an arbitrary orientation to the undirected graph given in Figure 2.1, one gets the oriented graph in Figure 2.2.
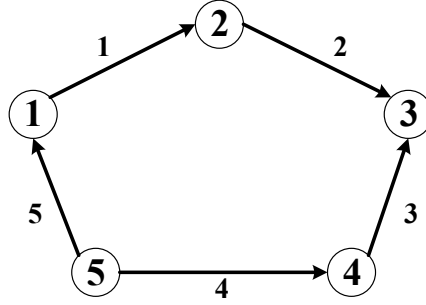
Figure 2.2: Example of an oriented graph with five vertices.

The incidence matrix related to the oriented graph presented in Figure 2.2 is found to be

$$H = \begin{bmatrix} -1 & 0 & 0 & 0 & 1 \\ 1 & -1 & 0 & 0 & 0 \\ 0 & 1 & 1 & 0 & 0 \\ 0 & 0 & -1 & 1 & 0 \\ 0 & 0 & 0 & -1 & -1 \end{bmatrix} \tag{2.5}$$

Property 2.2 *Given a connected graph, one verifies that $H^T \mathbf{1}_n = 0$ and rank(H)=$n-1$. Moreover, the columns of H are linearly independent if the graph is an undirected tree.*

Moreover, having an oriented graph, the *Laplacian* matrix $L := [l_{ij}] \in \mathbb{R}^{n \times n}$ is defined such that $l_{ij} = -d_{ij} = 0$, for every $(i, j) \notin \mathcal{E}_u$, and

$$\begin{cases} l_{ii} = \sum_{j=1, j\neq i}^{n} d_{ij}, \\ l_{ij} = -d_{ij}, \end{cases} \tag{2.6}$$

for every $(i, j) \in \mathcal{E}_u$, where d_{ij} is (i, j)-th entry of the adjacency matrix given in (2.2). According to the incidence matrix (2.4), the *Laplacian* matrix can also be defined as follows

$$L := H^T H. \tag{2.7}$$

The *Laplacian* matrix of the oriented graph shown in Figure 2.2 is given by

$$L = \begin{bmatrix} 2 & -1 & 0 & 0 & -1 \\ -1 & 2 & -1 & 0 & 0 \\ 0 & -1 & 2 & -1 & 0 \\ 0 & 0 & -1 & 2 & -1 \\ -1 & 0 & 0 & -1 & 2 \end{bmatrix} \tag{2.8}$$

It follows from (2.6) and (2.7) that the *Laplacian* matrix enjoys the following properties:

Property 2.3 *The Laplacian matrix is symmetric and positive semidefinite.*

Property 2.4 *The Laplacian matrix has zero row summation, which means that the zero is an eigenvalue of the Laplacian matrix with the associated eigenvector $\mathbf{1}_n$.*

Lemma 2.1 *(Ren and Beard, 2007) The Laplacian matrix is diagonally dominant and has nonnegative diagonal entries. Consequently, all non-zero eigenvalues of the Laplacian matrix are positive (i.e., the Laplacian matrix is positive semidefinite). Furthermore, if the undirected graph is connected, zero is a simple eigenvalue of the Laplacian matrix.*

2.4 Fundamental Consensus Algorithms

Consensus algorithms are protocols used in distributed systems to achieve agreement among multiple agents. These algorithms ensure that all agents in a multi-agent system agree on a single value or a specific state of the system. This section presents some basic consensus algorithm, which can be extended to more complicated ones according to the problems at hand.

Consider a network of n agents that can interact with each other according to an undirected graph topology $\mathcal{G}_u = (\mathcal{N}, \mathcal{E}_u)$. Let the following single-integrator system describe the dynamics of agent i:

$$\dot{x}_i = u_i, \tag{2.9}$$

where $i \in \mathcal{V}$, $x_i \in \mathbb{R}^d$, $d \geq 1$, is the state of agent i, and $u_i \in \mathbb{R}^d$ is the control input of agent i. The most common continuous-time consensus protocol for the above multi-agent system is (Mesbahi and Egerstedt, 2010)

$$u_i = -\sum_{j=1}^{n} d_{ij}(x_i - x_j), \tag{2.10}$$

where d_{ij} is the (i,j)-th entry of the adjacency matrix D associated with the graph $\mathcal{G}_u$. Note that $d_{ij} = 0$ indicates that agent i cannot interact with agent j. By defining $x := \left[x_1^T, x_2^T, \ldots, x_n^T\right]^T \in \mathbb{R}^{dn}$ and from the definition of *Laplacian* matrix (2.7), one can derive the following compact matrix form of system (2.9)-(2.10):

$$\dot{x} = -(L \otimes I_d)x. \tag{2.11}$$

It follows from Lemma 2.1, when considering a connected undirected graph topology, that the consensus algorithm (2.9)-(2.10) achieves the average consensus, *i.e.*, $x_i \rightarrow \frac{1}{n}\sum_{j=1}^{n} x_j(0)$, for each $i \in \mathcal{V}$ (Ren and Beard, 2007). The following lemma establishes a connection between the convergence of the consensus algorithm (2.9)-(2.10) and the eigenvalues of the *Laplacian* matrix.

Lemma 2.2 *(Mesbahi and Egerstedt, 2010) The convergence properties of the consensus algorithm (2.9)-(2.10) depend on the value of the lowest non-zero eigenvalue of the Laplacian matrix.*

2.5 Rigid Body Attitude Representation

There are several commonly used attitude representations, such as EA, MRP, axis-angle parameterization, unit quaternion, and rotation matrix. Each of these representations has its advantages and disadvantages. However, the rotation matrix representation is the only one that is global and unique. Therefore, in this thesis, we will use the rotation matrix representation in the design of our attitude estimation and control schemes.
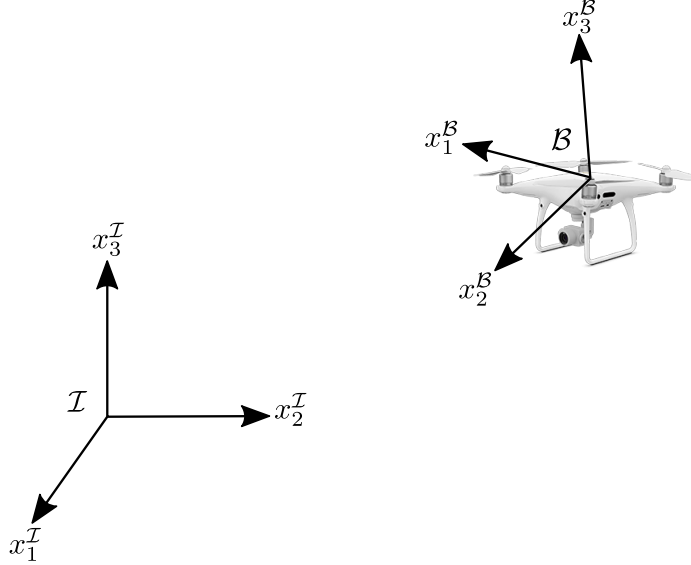
Figure 2.3: Coordinate systems: $\mathcal{I}$ is the inertial frame and $\mathcal{B}$ is the body-fixed frame attached to the center of mass of the VTOL aircraft.

In Figure 2.3, frame $\mathcal{I}$ denotes the inertial frame and frame $\mathcal{B}$ denotes the body-fixed frame attached to the vehicle's center of mass. The attitude of the vehicle is the orientation of its body-fixed frame with respect to the inertial frame. This orientation can be described by a rotation matrix, namely $R \in \mathbb{R}^{3\times3}$, which relates the axes of the two frames as follows:

$$x_i^{\mathcal{B}} = R^T x_i^{\mathcal{I}}, \tag{2.12}$$

where $i \in \{1, 2, 3\}$. According to the above equation and the fact that the axes of the two frames are unit vectors, one can derive the following form of the rotation matrix:

$$R := \begin{bmatrix} x_1^{\mathcal{B}} \cdot x_1^{\mathcal{I}} & x_2^{\mathcal{B}} \cdot x_1^{\mathcal{I}} & x_3^{\mathcal{B}} \cdot x_1^{\mathcal{I}} \\ x_1^{\mathcal{B}} \cdot x_2^{\mathcal{I}} & x_2^{\mathcal{B}} \cdot x_2^{\mathcal{I}} & x_3^{\mathcal{B}} \cdot x_2^{\mathcal{I}} \\ x_1^{\mathcal{B}} \cdot x_3^{\mathcal{I}} & x_2^{\mathcal{B}} \cdot x_3^{\mathcal{I}} & x_3^{\mathcal{B}} \cdot x_3^{\mathcal{I}} \end{bmatrix} = \begin{bmatrix} \cos\langle x_1^{\mathcal{B}}, x_1^{\mathcal{I}}\rangle & \cos\langle x_2^{\mathcal{B}}, x_1^{\mathcal{I}}\rangle & \cos\langle x_3^{\mathcal{B}}, x_1^{\mathcal{I}}\rangle \\ \cos\langle x_1^{\mathcal{B}}, x_2^{\mathcal{I}}\rangle & \cos\langle x_2^{\mathcal{B}}, x_2^{\mathcal{I}}\rangle & \cos\langle x_3^{\mathcal{B}}, x_2^{\mathcal{I}}\rangle \\ \cos\langle x_1^{\mathcal{B}}, x_3^{\mathcal{I}}\rangle & \cos\langle x_2^{\mathcal{B}}, x_3^{\mathcal{I}}\rangle & \cos\langle x_3^{\mathcal{B}}, x_3^{\mathcal{I}}\rangle \end{bmatrix} \tag{2.13}$$

The rotation matrix R is an element of the *Special Orthogonal group* of order three defined by

$$SO(3) := \left\{ R \in \mathbb{R}^{3\times3} : \det(R) = 1, \ \ RR^T = R^T R = I_3 \right\}. \tag{2.14}$$

Note that $SO(3)$ is a matrix Lie group where the group operation is defined by ordinary matrix multiplication. The associated *Lie algebra*, denoted by $\mathfrak{so}(3)$, is composed of all

skew-symmetric 3-by-3 matrices defined as

$$\mathfrak{so}(3) := \{\Omega \in \mathbb{R}^{3\times3} : \Omega^T = -\Omega\}. \tag{2.15}$$

The skew-symmetric map $[.]^\times : \mathbb{R}^3 \to \mathfrak{so}(3)$ is defined such that $[x]^\times y = x \times y$ for any $x, y \in \mathbb{R}^3$, where $\times$ denotes the vector cross product in $\mathbb{R}^3$. This map establishes an isomorphism between the *Lie algebra* $\mathfrak{so}(3)$ and $\mathbb{R}^3$. For example, given $\omega = [\omega_1\ \omega_2\ \omega_3]^T \in \mathbb{R}^3$, one can map the vector ω to the *Lie algebra* $\mathfrak{so}(3)$ using the skew-symmetric map as follows:

$$[\omega]^\times = \begin{bmatrix} 0 & -\omega_3 & \omega_2 \\ \omega_3 & 0 & -\omega_1 \\ -\omega_2 & \omega_1 & 0 \end{bmatrix}. \tag{2.16}$$

Now, Let us introduce some useful identities related to the skew-symmetric map. Given $x, y \in \mathbb{R}^3$, $A \in \mathbb{R}^{3\times3}$ and $R \in SO(3)$, one has

$$[x]^\times x = 0, \tag{2.17}$$

$$\left([x]^\times\right)^3 = -||x||^2[x]^\times, \tag{2.18}$$

$$[x]^\times y = -[y]^\times x, \tag{2.19}$$

$$[x + y]^\times = [x]^\times + [y]^\times, \tag{2.20}$$

$$[y]^\times[y]^\times = yx^T - (x^Ty)I_3, \tag{2.21}$$

$$\left[[x]^\times y\right]^\times = [x]^\times[y]^\times - [y]^\times[x]^\times, \tag{2.22}$$

$$\langle\langle[x]^\times, [y]^\times\rangle\rangle = 2x^Ty, \tag{2.23}$$

$$A[x]^\times + [x]^\times A = \left[(\operatorname{tr}(A)I_3 - A^T)x\right]^\times, \tag{2.24}$$

$$(Rx) \times (Ry) = R(x \times y), \tag{2.25}$$

$$[Rx]^\times = Rx^\times R^T. \tag{2.26}$$

The inverse map of $[.]^\times$ is the vex map defined as $\operatorname{vex} : \mathfrak{so}(3) \to \mathbb{R}^3$ such that $\operatorname{vex}([\omega]^\times) = \omega$, and $[\operatorname{vex}(\Omega)]^\times = \Omega$ for all $\omega \in \mathbb{R}^3$ and $\Omega \in \mathfrak{so}(3)$. In addition, let $\mathbb{P}_a : \mathbb{R}^{3\times3} \to \mathfrak{so}(3)$ be the projection map on the *Lie algebra* $\mathfrak{so}(3)$ such that $\mathbb{P}_a(A) := (A - A^T)/2$. Given a 3-by-3 matrix $C := [c_{ij}]_{i,j=1,2,3}$, one can define the following map, which is a composition of the projection map and the skew-symmetric map:

$$\psi(C) := \operatorname{vex} \circ \mathbb{P}_a(C) = \operatorname{vex}(\mathbb{P}_a(C)) = \frac{1}{2}\begin{bmatrix} c_{32} - c_{23} \\ c_{13} - c_{31} \\ c_{21} - c_{12} \end{bmatrix}. \tag{2.27}$$

Accordingly, for any $x, y \in \mathbb{R}^3$, $A \in \mathbb{R}^{3\times3}$ and $R \in SO(3)$, one has the following identities:

$$\langle\langle A, x^\times\rangle\rangle = \langle\langle\mathbb{P}_a(A), x^\times\rangle\rangle, \tag{2.28}$$

$$\langle\langle A, x^\times\rangle\rangle = 2x^T\psi(A), \tag{2.29}$$

$$\psi(AR) = R^T\psi(RA), \tag{2.30}$$

$$[x \times y]^\times = \mathbb{P}_a(yx^T), \tag{2.31}$$

$$x \times y = 2\psi(yx^T), \tag{2.32}$$

$$\text{tr}(Ax^\times) = \text{tr}(\mathbb{P}_a(A)x^\times). \tag{2.33}$$

Now, we will introduce an important concept related to the metrics on $SO(3)$. A metric on $SO(3)$ is a function $d_{SO(3)} : SO(3) \times SO(3) \to \mathbb{R}_{\geq 0}$ that measures the disparity between two given rotations. This function should satisfy the following properties:

- $d_{SO(3)}(R_1, R_2) \geq 0$.

- $d_{SO(3)}(R_1, R_2) = d_{SO(3)}(R_2, R_1)$.

- $d_{SO(3)}(R_1, R_2) = 0$ if and only if $R_1 = R_2$.

- $d_{SO(3)}(R_1, R_3) \leq d_{SO(3)}(R_1, R_2) + d_{SO(3)}(R_2, R_3)$.

A commonly used metric on SO(3) is the *Frobenius* distance, also known as the *Euclidean* (Chordal) distance on $SO(3)$. Given two rotations R_1 and R_2 in $SO(3)$, the *Frobenius* distance between them can be found as follows:

$$d_{SO(3)}(R_1, R_2) = ||R_1 - R_2||_F. \tag{2.34}$$

From the fact that $\text{tr}(R) \geq -1$, for any $R \in SO(3)$, one can derive the upper bound of the *Frobenius* distance for any $R_1, R_2 \in SO(3)$ as

$$d_{SO(3)}(R_1, R_2) = d_{SO(3)}(I_3, R_1 R_2^T) = \sqrt{2\text{tr}(I_3 - R_1 R_2^T)} \leq \sqrt{8}. \tag{2.35}$$

The above inequality shows that the $SO(3)$ group has a compact manifold structure. In this thesis, we will mostly use the normalized version of the *Frobenius* distance (known as the normalized attitude norm), which is given by

$$|R|_I = \frac{d_{SO(3)}(I_3 - R)}{\sqrt{8}} = \frac{||I_3 - R||_F}{\sqrt{8}} = \frac{\sqrt{\text{tr}(I_3 - R)}}{\sqrt{4}}. \tag{2.36}$$

Note that the normalized attitude norm measures the disparity of a given rotation with respect to I_3. Also, note that this norm ranges between zero and one, *i.e.*, $0 \leq |R|_I \leq 1$.

Another interesting metric on $SO(3)$ is the *Riemannian* metric. Recall that a *Riemannian* metric on a smooth manifold assigns a positive definite inner product to each tangent space at every point on the manifold. Therefore, before proceeding with this metric on $SO(3)$, it is necessary to first introduce the tangent space of $SO(3)$. The tangent space of $SO(3)$ at any given rotation R is defined as follows:

$$\mathcal{T}_R SO(3) := \{R\,\Omega \mid \Omega \in \mathfrak{so}(3)\}. \tag{2.37}$$

Note that the vector space $\mathfrak{so}(3)$ can be seen as the tangent space of $SO(3)$ at the identity matrix, *i.e.*, $\mathfrak{so}(3) = \mathcal{T}_I SO(3)$. Consequently, the *Riemannian* metric can be defined as the map $\langle\,,\,\rangle_R : \mathcal{T}_R SO(3) \times \mathcal{T}_R SO(3) \to \mathbb{R}_{\geq 0}$ such that

$$\langle R\Omega_1, R\Omega_2 \rangle_R = \langle\langle \Omega_1, \Omega_2 \rangle\rangle, \tag{2.38}$$

where $R \in SO(3)$ and $\Omega_1, \Omega_2 \in \mathfrak{so}(3)$. Furthermore, given a differentiable smooth function $f : SO(3) \to \mathbb{R}$, the gradient of f at $R \in SO(3)$, denoted by $\nabla_R f \in \mathcal{T}_R SO(3)$, is defined as the unique element of $\mathcal{T}_R SO(3)$ such that

$$df \cdot R\Omega = \langle \nabla_R f, R\Omega \rangle_R = \langle\langle R^T \nabla_R f, \Omega \rangle\rangle, \tag{2.39}$$

for all $R \in SO(3)$ and $\Omega \in \mathfrak{so}(3)$. A point $R \in SO(3)$ is called a critical point of f if the gradient of f at point $R \in SO(3)$ is zero, *i.e.*, $\nabla_R f(R) = 0$.

For any $A, B \in \mathbb{R}^{3\times3}$, $x, y \in \mathbb{R}^3$ and $a \in \mathbb{R}$, one has the following identities:

$$\mathrm{tr}(A^T) = \mathrm{tr}(A), \tag{2.40}$$
$$\mathrm{tr}(A + B) = \mathrm{tr}(A) + \mathrm{tr}(B), \tag{2.41}$$
$$\mathrm{tr}(aA) = a\,\mathrm{tr}(A), \tag{2.42}$$
$$\mathrm{tr}(AB) = \mathrm{tr}(BA), \tag{2.43}$$
$$\mathrm{tr}(AB) = 0 \quad \text{if} \quad A = A^T \text{ and } B = -B^T, \tag{2.44}$$
$$\mathrm{tr}(xy^T) = x^T y. \tag{2.45}$$

Lemma 2.3 *(Berkane, 2017) Consider a symmetric positive semi-definite matrix $A \in \mathbb{R}^{3\times3}$ such that $\bar{A} := \frac{1}{2}(\mathrm{tr}(A)I_3 - A)$ is positive definite. Then, for any $x, y \in \mathbb{R}^3$, the following properties are satisfied for all $R \in SO(3)$:*

$$4\underline{\lambda}^{\bar{A}}|R|_I^2 \leq \mathrm{tr}\left((I_3 - R)A\right) \leq 4\bar{\lambda}^{\bar{A}}|R|_I^2, \tag{2.46}$$
$$||\psi(AR)||^2 = \alpha(A, R)\,\mathrm{tr}\left((I_3 - R)\underline{A}\right), \tag{2.47}$$
$$||\psi(R)||^2 = 4(1 - |R|_I^2)|R|_I^2 \leq 1, \tag{2.48}$$
$$\psi(R)^T \psi(AR) = \psi(R)^T \bar{A}\psi(R), \tag{2.49}$$
$$||E(AR)||_F \leq ||\bar{A}||_F, \tag{2.50}$$

where $\underline{A} := \mathrm{tr}(\bar{A}^2)I_3 - 2\bar{A}^2$, $E(AR) := \frac{1}{2}\left(\mathrm{tr}(AR)I_3 - R^T A\right)$ and $\alpha(A, R) := 1 - |R|_I^2 \cos\langle u, \bar{M}u \rangle$ with $u \in \mathbb{S}^2$ denoting the axis of the rotation R and $\langle u, \bar{M}u \rangle$ denoting the angle between two vectors. Furthermore, consider the trajectories generated by $\dot{R} = R[\omega]^\times$ with $R(0) \in SO(3)$ and $\omega \in \mathbb{R}^3$. One can get the following derivatives:

$$\nabla \mathrm{tr}(A(I_3 - R)) = R\mathbb{P}_a(AR), \tag{2.51}$$
$$\frac{d}{dt}\mathrm{tr}((I_3 - R)A) = 2\omega^T \psi(AR), \tag{2.52}$$
$$\frac{d}{dt}\psi(AR) = E(AR)\omega, \tag{2.53}$$

Lemma 2.4 *(Mayhew and Teel, 2011b) Let $A = A^T$ be a positive semi-definite matrix with three distinct eigenvalues. Then, the solution of $||\psi(AR)|| = 0$ with $R \in SO(3)$ belongs to the following set*

$$\mathcal{W} = \{I_3\} \cup \{R = \mathcal{R}_\alpha(\pi, v_i)|v_i \in \mathcal{E}(A)\}. \tag{2.54}$$

where $\mathcal{E}(A) \subset \mathbb{S}^2$ is the set of unit eigenvectors of matrix A.

2.6 Hybrid Dynamical Systems

In this section we will present some concepts and stability tools related hybrid dynamical systems. For further details, the reader is referred to (Goebel et al., 2009; Goebel et al., 2012).

2.6.1 Hybrid Dynamical Systems Models

Consider a manifold $\mathcal{Y}$ embedded in $\mathbb{R}^n$. A general model for hybrid systems, denoted by $\mathcal{H}$, is represented by the following compact form, for every $y \in \mathcal{Y}$:

$$\mathcal{H} : \begin{cases} \dot{y} \in F(y) & y \in \mathcal{F} \\ y^+ \in G(y) & y \in \mathcal{J} \end{cases} \tag{2.55}$$

where $F : \mathcal{Y} \rightrightarrows \mathcal{T}\mathcal{Y}$, $G : \mathcal{Y} \rightrightarrows \mathcal{Y}$, $\mathcal{F}$ and $\mathcal{J}$ denote the flow map (governing the continuous evolution of the state by a differential inclusion), the jump map (governing the discrete evolution of the state by a difference inclusion), the flow set (indicating where the continuous state evolution is allowed), and the jump set (indicating where the discrete state evolution is allowed), respectively.

Remark 2.3 *The symbol $\rightrightarrows$ represents a set-valued mapping, and x^+ denotes the value of x after an immediate jump, specifically defined as $x^+ := x(t, j+1)$, where $x(t, j)$ is the value of x before the jump occurs.*

Remark 2.4 *The hybrid system model (2.55) is generic since it can represent the dynamics of a purely continuous system by letting the flow set equal to $\mathcal{Y}$ and the jump set to be empty, or vice versa to represent a purely discrete system.*

2.6.2 Hybrid Systems Solutions

In this subsection, we introduce some concepts related to hybrid systems solutions. According to the nature of the hybrid system dynamics, which allows continuous flow and discrete jumps, it is evident that the solutions of the hybrid system are parameterized by $t \in \mathbb{R}_{\geq 0}$ to indicate the amount of time spent in the flow set and $j \in \mathbb{N}$ to track the number of jumps that occur. The structure that represents this parameterization is known as a *hybrid time domain*.

Definition 2.5 *(Goebel et al., 2012) A subset $E \subset \mathbb{R}_{\geq 0} \times \mathbb{N}$ is a compact hybrid time domain if*

$$E = \bigcup_{j=0}^{J-1} ([t_j, t_{j+1}], j)$$

for some finite sequence of time $0 = t_0 \leq t_1 \leq t_2 \leq \ldots \leq t_J$. It is a hybrid time domain if for all $(T, J) \in E$, $E \cap ([0, T] \times \{0, 1, \ldots, J\})$ is a compact hybrid domain.

Remark 2.5 *For any (t, j) and (t', j') belonging to a hybrid time domain, one has $(t, j) \leq (t', j')$ if and only if $t \leq t'$ and $j \leq j'$.*

Definition 2.6 *(Goebel et al., 2012) A hybrid arc is a function* $y : \text{dom } y \to \mathcal{Y}$, *where* dom y *is a hybrid time domain, for each fixed* j, $t \to y(t,j)$ *is a locally absolutely continuous function on the interval*

$$I^j = \{t : (t,j) \in E\}$$

The hybrid arc y is a solution to the hybrid system $\mathcal{H}$, given in (2.55), if $y(0,0) \in \mathcal{F} \cup \mathcal{J}$ and the following conditions are satisfied (Goebel et al., 2012):

- Flow condition: for each $j \in \mathbb{N}$ such that I^j has nonempty interior with

$$\dot{y}(t,j) \in F(y(t,j)), \qquad \text{for almost all } t \in I^j, \qquad (2.56)$$
$$y(t,j) \in \mathcal{F}, \qquad \text{for all } t \in [\min I^j, \sup I^j). \qquad (2.57)$$

- Jump condition: for each $(t,j) \in \text{dom } y$ such that $(t,j+1) \in \text{dom } y$ with

$$y(t,j+1) \in G(y(t,j)), \qquad (2.58)$$
$$y(t,j) \in \mathcal{J}. \qquad (2.59)$$

The following definitions characterize the nature of a hybrid system solution:

Definition 2.7 *(Goebel et al., 2012) A solution* y *to* $\mathcal{H}$ *is said to be* maximal *if there is no other solution* y^* *to* $\mathcal{H}$ *such that* dom y *is a proper subset of* dom y^* *and* $y(t,j) = y^*(t,j)$ *for all* $(t,j) \in \text{dom } y$.

Definition 2.8 *(Goebel et al., 2012) A solution* y *to* $\mathcal{H}$ *is said to be* complete *if its domain, namely* dom y, *is unbounded.*

Definition 2.9 *(Goebel et al., 2012) A solution* y *to* $\mathcal{H}$ *is said to be* precompact *if it is complete and bounded.*

Remark 2.6 *It follows from the above definitions that every complete solution of* $\mathcal{H}$ *is maximal, but the opposite is not true.*

To ensure the existence of the solution, the robustness of stability in the presence of small perturbations, and other important properties, the hybrid system $\mathcal{H}$ given in (2.55) should satisfy the following three hybrid basic conditions (Goebel et al., 2012):

- The flow map $\mathcal{F}$ and the jump set $\mathcal{J}$ are closed sets in $\mathcal{Y}$.

- The flow map $F : \mathcal{Y} \rightrightarrows \mathcal{T}\mathcal{Y}$ is outer semicontinuous [2] and locally bounded[3] relative to $\mathcal{F}$, and the set $F(y)$ is nonempty and convex[4] for every $y \in \mathcal{F}$.

---

[2]This means that for every $y_0 \in \mathcal{Y}$, one has $\limsup_{y \to y_0} F(y) \subseteq F(y_0)$.

[3]This means that for each $y_0 \in \mathcal{F}$, there exists a neighborhood N_{y_0} of y_0 such that all sets in the range of F (*i.e.*, $F(y)$ for $y \in N_{y_0}$) are bounded sets.

[4]A set $\mathcal{B}$ is said to be convex if, for every pair of points x and y in the set, the line segment connecting x and y is completely inside the set. In other words, if one takes any two points inside the set, all the points along the line segment connecting them are also inside the set.

- The jump map $G : \mathcal{Y} \rightrightarrows \mathcal{Y}$ is outer semicontinuous and locally bounded relative to $\mathcal{J}$, and G nonempty for every $x \in \mathcal{J}$.

Proposition 2.1 *(Goebel et al., 2012) Consider a hybrid system $\mathcal{H}$ satisfying the hybrid basic conditions. Take an arbitrary $\zeta \in \mathcal{F} \cup \mathcal{J}$. If $\zeta \in \mathcal{J}$ or*

(VC) *there exists a neighborhood $\mathcal{U}$ of ζ such that for every $y \in \mathcal{U} \cap \mathcal{F}$,*

$$F(y) \cap T_{\mathcal{F}}(y) = \varnothing,$$

where $T_{\mathcal{F}}(y)$ denotes the tangent cone to $\mathcal{F}$ at the point y, then there exists a nontrivial solution ϕ to $\mathcal{H}$ with $\phi(0,0) = \zeta$. If (VC) holds for every $\zeta \in \mathcal{F} \setminus \mathcal{J}$, then there exists a nontrivial solution to $\mathcal{H}$ from every initial point in $\mathcal{F} \cup \mathcal{J}$, and every $\phi \in \mathcal{S}_{\mathcal{H}}$, where $\mathcal{S}_{\mathcal{H}}$ denotes the set of all maximal solutions of $\mathcal{H}$, satisfies exactly one of the following conditions:

i) ϕ *is complete.*

ii) $\mathrm{dom}\ \phi$ *is bounded and the interval I^J, where $J = \sup_j \mathrm{dom}\phi$, has nonempty interior and $t \to \phi(t, J)$ is a maximal solution to $\dot{z} \in F(z)$, in fact $\lim_{t \to T} |\phi(t, J)| = \infty$, where $T = \sup_t \mathrm{dom}\phi$.*

iii) $\phi(T, J) \notin \mathcal{F} \cup \mathcal{J}$, *where $(T, J) = \sup \mathrm{dom}\phi$.*

Remark 2.7 *If $G(\mathcal{J}) \subset \mathcal{F} \cup \mathcal{J}$, then case (iii) does not occur. Furthermore, case (ii) can also be excluded if every solution is bounded (Goebel et al., 2012).*

2.6.3 Stability Analysis for Hybrid Systems

In this subsection, we will present some definitions and stability theorems for hybrid dynamical systems that will be used in this dissertation.

Definition 2.10 *Let $y \in \mathcal{Y}$ and $\mathcal{A} \subset \mathcal{Y}$ be a closed set. The distance from y to $\mathcal{A}$, denoted $|y|_{\mathcal{A}}$, is defined as*

$$|y|_{\mathcal{A}} := \inf_{x \in \mathcal{A}}\ d_{\mathcal{Y}}(y, x),$$

where $d_{\mathcal{Y}} : \mathcal{Y} \times \mathcal{Y} \to \mathbb{R}_{\geq 0}$ is the distance between two given elements in $\mathcal{Y}$.

Definition 2.11 *(Goebel et al., 2012) Consider a hybrid system $\mathcal{H}$ on $\mathcal{Y}$. A compact set $\mathcal{A} \subset \mathcal{Y}$ is said to be*

- *uniformly globally stable for $\mathcal{H}$ if there exists a class $\mathcal{K}_{\infty}$ function α such that any solution ϕ to $\mathcal{H}$ satisfies $|\phi(t, j)|_{\mathcal{A}} \leq \alpha(|\phi(0, 0)|_{\mathcal{A}})$ for all $(t, j) \in \mathrm{dom}\ \phi$.*

- *uniformly globally pre-attractive for $\mathcal{H}$ if for each $\epsilon > 0$ and $r > 0$ there exists $T > 0$ such that, for any solution ϕ to $\mathcal{H}$ with $|\phi(0, 0)|_{\mathcal{A}} \leq r$, $(t, j) \in \mathrm{dom}\ \phi$ and $t + j \geq T$ imply $|\phi(t, j)|_{\mathcal{A}} \leq \epsilon$.*

- *uniformly globally pre-asymptotically stable for $\mathcal{H}$ if it is both uniformly globally stable and uniformly globally pre-attractive.*

Remark 2.8 *The term "pre-" is added in stating the above results only to indicate that maximal solutions to $\mathcal{H}$ are not required to be complete solutions. Furthermore, if every maximal solution of $\mathcal{H}$ is complete, then the compact set $\mathcal{A}$ is said to be globally attractive for $\mathcal{H}$ if $\lim_{t+j\to\infty} |\phi(t,j)| = 0$ and asymptotically stable if it is stable and attractive (Sanfelice et al., 2007).*

Using Definition 2.11 directly to deduce the stability properties of the hybrid system (2.55) with respect to the compact set $\mathcal{A}$ is a quite daunting task, since it requires finding the explicit solutions of the system. Therefore, in the following, we will present some *Lyapunov*-based techniques that can be used to establish the stability properties of system (2.55) without explicitly determining its solutions.

Definition 2.12 *(Goebel et al., 2009) Consider the hybrid system $\mathcal{H}$, given in (2.55), and a compact set $\mathcal{A} \subset \mathcal{Y}$. The function $\mathcal{L} : \operatorname{dom} \mathcal{L} \to \mathbb{R}$ is a* Lyapunov function candidate *for $(\mathcal{H}, \mathcal{A})$ if:*

- *$\mathcal{L}$ is continuous and nonnegative on $(\mathcal{F} \cup \mathcal{J}) \setminus \mathcal{A} \subset \operatorname{dom} \mathcal{L}$.*

- *$\mathcal{L}$ is continuous differentiable on an open set $\mathcal{O}$ satisfying $\mathcal{F} \setminus \mathcal{A} \subset \mathcal{O} \subset \operatorname{dom} \mathcal{L}$.*

- *$\lim_{\{y \to \mathcal{A},\ y \in \operatorname{dom}\ \mathcal{L} \cap (\mathcal{F} \cup \mathcal{J})\}} \mathcal{L}(y) = 0$.*

The following theorem provides a simple way to show the stability of a set $\mathcal{A}$ using the *Lyapunov* function:

Theorem 2.1 *(Goebel et al., 2009) Consider a hybrid system $\mathcal{H}$ satisfying the hybrid basic conditions and a compact set $\mathcal{A} \subset \mathcal{Y}$ satisfying $G(\mathcal{J} \cap \mathcal{A}) \subset \mathcal{A}$. If there exists a* Lyapunov *function candidate $\mathcal{L}$ for $(\mathcal{H}, \mathcal{A})$ that is positive on $(\mathcal{F} \cup \mathcal{J}) \setminus \mathcal{A}$ and satisfies*

$$\langle \nabla \mathcal{L}(y), f \rangle \leq 0 \quad \text{for all } y \in \mathcal{F} \setminus \mathcal{A},\ f \in F(y),$$
$$\mathcal{L}(g) - \mathcal{L}(y) \leq 0 \quad \text{for all } y \in \mathcal{J} \setminus \mathcal{A},\ g \in G(y),$$

then the set $\mathcal{A}$ is stable.

Now, we present a version of the *invariance principle* for hybrid dynamical systems, which will be used to establish asymptotic stability of the set $\mathcal{A}$. Consider the following two functions:

$$\mu_{\mathcal{J}}(y) = \begin{cases} \max_{y^+ \in G(y)} \{V(y^+) - V(y)\} & \text{if } y \in \mathcal{J} \\ -\infty & \text{otherwise,} \end{cases} \tag{2.60}$$

$$\mu_{\mathcal{F}}(y) = \begin{cases} \max_{v \in F(y)} \langle \nabla V(y), v \rangle & \text{if } y \in \mathcal{F} \\ -\infty & \text{otherwise,} \end{cases} \tag{2.61}$$

where the continuous function $V : \mathcal{Y} \to \mathbb{R}$ is a continuously differentiable function on a neighborhood of $\mathcal{F}$. Under certain conditions on the functions $\mu_{\mathcal{F}}(y)$ and $\mu_{\mathcal{J}}(y)$, the following theorem introduces the invariance principle for the hybrid system $\mathcal{H}$.

Theorem 2.2 *(Goebel et al., 2012) Consider a continuous function $V : \mathcal{Y} \to \mathbb{R}$, continuously differentiable on a neighborhood of $\mathcal{F}$. Suppose that for a given set $U \subset \mathcal{Y}$,*

$$\begin{cases} \mu_{\mathcal{F}}(z) \leq 0, \\ \mu_{\mathcal{J}}(z) \leq 0, \end{cases} \tag{2.62}$$

for all $z \in U$. Let a precompact $y^* \in \mathcal{S}_{\mathcal{H}}$ be such that $\overline{\mathrm{rge}\ y^*} \subset U$, with $\mathrm{rge}\ y := y(\mathrm{dom}\ y)$ being the range of y. Then, for some $r \in V(U)$, y^* approaches the nonempty set which is the largest weakly invariant subset of

$$V^{-1}(r) \cap U \cap \left[\overline{\mu_{\mathcal{F}}^{-1}(0)} \cup \left(\mu_{\mathcal{J}}^{-1}(0) \cap G(\mu_{\mathcal{J}}^{-1}(0)) \right) \right]. \tag{2.63}$$

Remark 2.9 *Note that the Lyapunov function candidate $\mathcal{L}$ can be used instead of V since it satisfies the requirements in Theorem 2.2.*

The following theorem provides a useful result for asymptotic stability of a compact set.

Theorem 2.3 *(Goebel et al., 2012) Let $\mathcal{A} \subset \mathcal{Y}$ be compact. If*

(a) $G(\mathcal{J}) \subset \overline{\mathcal{F}} \cup \mathcal{J}$ and there exists a continuous $V : \mathcal{Y} \to \mathbb{R}$ which is positive definite on $\overline{\mathcal{F}} \cup \mathcal{J}$ with respect to $\mathcal{A}$ and continuously differentiable on a neighborhood of $\mathcal{F}$, and a neighborhood $U \subset \mathcal{Y}$ of $\mathcal{A}$ such that the bounds in (2.62) hold,

then $\mathcal{A}$ is stable. If, additionally,

(b) there exists $r^* > 0$ such that, for every $r \in (0, r^*)$, the largest weakly invariant subset in (2.63) is empty,

then $\mathcal{A}$ is locally pre-asymptotically stable.

2.7 Almost Global Input-to-State Stability

The notion of Input-to-State Stability (ISS) is a key tool for establishing the stability properties of nonlinear systems with exogenous signals, including inputs or disturbances. As a result, the literature is replete with theories dealing with the notion of ISS. However, most of these theories are proposed for nonlinear systems evolving on Euclidean spaces. In this section, we present some results related to the notion of almost global ISS (Angeli, 2004; Angeli and Praly, 2011) which deals with nonlinear systems evolving on manifolds (non-Euclidean spaces).

Consider the following autonomous nonlinear system:

$$\dot{x} = f(x, u), \tag{2.64}$$

where the state x belongs to the manifold $\mathcal{Q}$. Let $X(t, x_0; u)$ denote the solution of (2.64) with initial condition x_0. The following autonomous ordinary differential equation represents the unperturbed dynamics of (2.64):

$$\dot{x} = f(x, 0) := f_0(x). \tag{2.65}$$

Before presenting the results related to the ISS, let us first consider the following assumptions adopted from (Angeli and Praly, 2011):

Assumption 2.1 *Let $\mathcal{Q}$ be an $n-$dimensional $\mathcal{C}^2$ connected, orientable, Riemannian manifold without boundary, $f : \mathcal{Q} \times U \to \mathcal{T}_x \mathcal{Q}$ be a $\mathcal{C}^1-$Lipschitz function and U be a closed subset of $\mathbb{R}^m$.*

Assumption 2.2 *There exists a nonnegative and proper[5] $\mathcal{C}^1$ function $V : \mathcal{Q} \to \mathbb{R}$ such that*

$$L_{f_0} V|_x < 0, \qquad \forall x \in \mathcal{Q} : \ f_0(x) \neq 0, \tag{2.66}$$

where the notation $L_f V|_x$ denotes the Lie derivative of V along f at x.

Assumption 2.3 *Any equilibrium x_e which is not asymptotically stable, is isolated and such that at least one eigenvalue of $\mathcal{D}f_0(x_e) : \mathcal{T}_{x_e}\mathcal{Q} \to \mathcal{T}_{x_e}\mathcal{Q}$ has strictly positive real part, where $\mathcal{D}f_0(x)$ denotes the differential of f_0 at x.*

In the following definition, we will introduce the formal definition of the almost global ISS concept according to (Angeli, 2004).

Definition 2.13 *(Angeli, 2004) System (2.64) is almost globally ISS with respect to the set $\mathcal{A}$, if $\mathcal{A}$ is locally asymptotically stable for system (2.65) and there exists a class $\mathcal{K}$ function[6] γ such that for each locally essentially bounded and measurable input $u : \mathbb{R}_{\geq 0} \to U$, there exists a zero Lebesgue measure subset $\mathcal{N} \subset \mathcal{Q}$ such that*

$$\limsup_{t \to \infty} |X(t, x(t_0); u)|_{\mathcal{A}} \leq \gamma(||u||_\infty), \qquad \forall x(t_0) \in \mathcal{Q} \setminus \mathcal{N}. \tag{2.67}$$

Recall that the notation $|.|_{\mathcal{A}}$ is defined in Definition 2.10. Unfortunately, it is sometimes challenging to use the result of Definition 2.13 to conclude almost global ISS because an explicit solution is required. Therefore, next, we will present a useful result that relies on some sufficient conditions, that do not depend on explicit solutions, to conclude the almost global ISS. But first, let us introduce the following lemma:

Lemma 2.5 *(Angeli and Praly, 2011) Consider the system (2.64) and let $W : \mathcal{Q} \to \mathbb{R}_{\geq 0}$ be a class $\mathcal{C}^1$ and proper function satisfying*

$$L_f W|_{x,u} \leq -\alpha(W(x)) + c + \delta(|u|), \tag{2.68}$$

for all $x \in \mathcal{Q}$ and all $u \in U$, where α and δ are class $\mathcal{K}$ functions. Then, system (2.64) fulfills the ultimate boundedness property.

Theorem 2.4 *(Angeli and Praly, 2011) Consider system (2.64) and let Assumptions 2.1-2.3 hold. Assume that the set of asymptotically stable equilibria of (2.65), denoted by E_s, is finite. If the ultimate boundedness (as per Lemma 2.5) holds, then, system (2.64) is almost globally ISS with respect to the set E_s.*

---

[5]We recall that a function V is proper provided $V^{-1}(K)$ is compact for all compacts K included in the domain of V.

[6]A continuous function $\gamma : [0, a) \to [0, \infty)$ is said to be a class $\mathcal{K}$ function if it is strictly increasing and $\gamma(0) = 0$. It is said to be a class $\mathcal{K}_\infty$ function if $a = \infty$ and $\gamma(r) \to \infty$ as $r \to \infty$.

Almost global ISS can be used to study the stability properties of a cascaded nonlinear system, as shown in the following theorem.

Theorem 2.5 *(Angeli, 2004) Consider the following cascaded system:*

$$\dot{x} = f(x, y) \tag{2.69}$$
$$\dot{y} = g(y), \tag{2.70}$$

where $(x, y) \in \mathcal{Q} \times \mathcal{N}$, $f : \mathcal{Q} \times \mathcal{N} \to \mathcal{T}\mathcal{Q}$ and $g : \mathcal{N} \to \mathcal{T}\mathcal{N}$ are locally Lipschitz with $f(x, y) \in \mathcal{T}_x\mathcal{Q}$ and $g(y) \in \mathcal{T}_y\mathcal{N}$ for all $(x, y) \in \mathcal{Q} \times \mathcal{N}$. Suppose that

- *the $x-$subsystem (2.69) is almost globally ISS with respect to $\mathcal{A}_x \subset \mathcal{Q}$ and input y.*

- *the equilibrium set $\mathcal{A}_y \subset \mathcal{N}$ is Almost Globally Asymptotically Stable[7] (AGAS) for the $y-$subsystem (2.70).*

Then, the cascaded system (2.69)-(2.70) is AGAS at $\mathcal{A} := \mathcal{A}_x \times \mathcal{A}_y$.

Remark 2.10 *Considering the cascaded system (2.69)-(2.70), one can conclude the AGAS of $\mathcal{A}$ if the $x-$subsystem (2.69) is almost globally ISS with respect to $\mathcal{A}_x \subset \mathcal{Q}$ and input y, and the $y-$subsystem (2.70) is globally asymptotically stable at $\mathcal{A}_y \subset \mathcal{N}$ (Wang and Tayebi, 2021).*

---

[7]An equilibrium set is said to be almost globally asymptotically stable if it is stable, and attractive from all initial conditions except a set of zero Lebesgue measure.

Chapter 3

Bearing-Based Distributed Pose Estimation for Multi-Agent Rigid-Body Systems

3.1 Introduction

In this chapter, we address the problem of distributed pose estimation for multi-agent rigid-body systems, using local time-varying relative bearing measurements between neighboring agents. The use of bearing measurements in the design of distributed pose estimation schemes is interesting since these measurements can be easily obtained from low-cost sensors such as cameras. Several bearing-based distributed pose estimation schemes have been proposed in the literature (Zhao and Zelazo, 2016; Li et al., 2020; Lee et al., 2019; Lee and Ahn, 2016b; Lee et al., 2019; Tran et al., 2020). However, most of these works assume the availability of the relative attitude, which can be restrictive since there is no readily available low-cost setup to directly provide this information. This motivated us to design distributed pose observers for multi-agent rigid-body systems that rely solely on individual angular velocity measurements and local information exchange between neighboring agents (relative time-varying bearing measurements and estimated poses), available according to a directed graph topology, assuming that two agents have access to their respective poses.

The first part of this chapter explores multi-agent rigid-body systems with fixed positions and time-varying orientations. Motivated by the recent work in (Tran et al., 2020), a new AGAS bearing-based distributed pose estimation scheme has been proposed. To the best of our knowledge, no such strong stability result has been reported in the available literature for the problem considered in this part.

In the second part, a bearing-based distributed pose estimation scheme multi-agent rigid-body systems with time-varying positions and orientations. The proposed estimation scheme is a cascade of two subsystems. The first subsystem is a stand-alone bearing-based distributed attitude observer endowed with local exponential stability. The second subsystem consists of a bearing-based distributed position observer relying on the attitude estimates provided by the rotational observer. This leads to an overall pose

estimation scheme with local exponential stability guarantees. It is worth pointing out that our proposed distributed pose estimation scheme, contrary to most existing schemes in the literature, relies on local bearing measurements that are also time-varying in the inertial frame.

The bearing-based distributed attitude observers proposed in both parts are interesting contributions in their own right, as they are stand-alone (*i.e.*, do not depend on the position estimation) and could be used in other applications involving rotating multi-agent rigid-body systems. Numerical simulation results are provided to illustrate the performance of the proposed bearing-based distributed pose estimation schemes introduced in both parts. The results presented in this chapter are based on our work in (Boughellaba and Tayebi, 2022; Boughellaba and Tayebi, 2023b; Boughellaba and Tayebi, 2023a).

3.2 Bearing-Based Distributed Pose Observer Design: Fixed Positions and Time-Varying Orientations

In this section, we consider the problem of distributed pose estimation for multi-agent rigid-body systems where the agents have static positions and time-varying orientations. First, we design two AGAS stand-alone bearing-based distributed attitude observers that evolve on $SO(3)$ and $SO(3) \times \mathbb{R}^3$, respectively. Then, relying on the attitude estimates provided by one of these rotational observers together with local relative (time-varying) bearing measurements, we design an input-to-state stable distributed position observer. This leads to an overall AGAS distributed localization scheme.

3.2.1 Problem Formulation

Consider a network of n rigid-body agents, where the motion of each agent $i \in \mathcal{V}$ is governed by the following rotational kinematic equation:

$$\dot{R}_i = R_i[\omega_i]^\times, \tag{3.1}$$

where $R_i \in SO(3)$ represents the orientation of the body-attached frame of agent i with respect to the inertial frame, and $\omega_i \in \mathbb{R}^3$ is the angular velocity of agent i measured in the body-attached frame of the same agent. Let $p_i \in \mathbb{R}^3$ denote the position of agent i with respect to the inertial frame. We assume that the positions of the agents are fixed and do not change with time, *i.e.*, $\dot{p}_i = 0$, for all $i \in \mathcal{V}$. The measurement of the local relative bearing between agent i and agent j is given by

$$b_{ij}^i := R_i^T b_{ij}, \tag{3.2}$$

where $b_{ij} := \frac{p_j - p_i}{||p_j - p_i||}$ and b_{ij}^i are the relative bearing measurements between agent i and agent j expressed in the inertial frame and the body-attached frame of agent i, respectively. Note that the relative bearing measurements expressed in the inertial frame (*i.e.*,

b_{ij} for every $(i, j) \in \mathcal{E}$) do not change with time since the agents' positions are assumed to be constant. Next, let us introduce the following assumptions that will be needed in our design:

Assumption 3.1 *The angular velocity of each agent is available for measurement and bounded.*

Assumption 3.2 *By assigning a number to each agent, we assume that agents 1 and 2 are the leaders and the other agents are the followers. We also assume that*

a) *The leaders know their pose, and have no neighbors, i.e., $\mathcal{N}_k = \{\varnothing\}$ $k = 1, 2$.*

b) *Each agent $i \in \mathcal{V}_f$, where $\mathcal{V}_f := \mathcal{V} \setminus \{1, 2\}$ denotes the set of followers, measures b_{ij}^i and receives $(\hat{R}_j, \hat{p}_j, b_{ji}^j)$ from its neighbors $j \in \mathcal{N}_i$.*

c) *No two agents are collocated, and the set of neighbors of each agent $i \in \mathcal{V}_f$ satisfies $\mathcal{N}_i \subseteq \{1, 2, 3, ..., i-1\}$ with $|\mathcal{N}_i| \geq 2$, and each agent measures at least two non-collinear bearing vectors.*

Assumption 3.2 defines the cascaded structure of the inter-agent interaction graph topology $\mathcal{G}$, which is instrumental in establishing our stability results via mathematical induction. This cascaded structure stems from the fact that each agent i only needs the information (relative bearing measurements and estimated poses) about the preceding agents that belong to its neighbor set $\mathcal{N}_i \subseteq \{1, 2, \ldots, i-1\}$, for instance, see Figure 3.1 and Figure 3.2. The black circles denote the leaders and the white ones denote the followers.
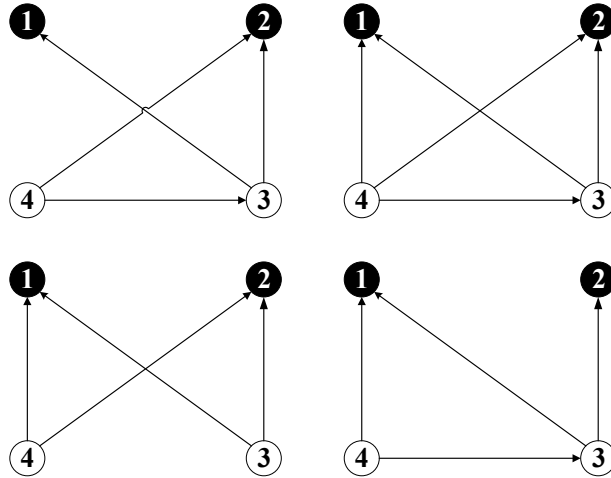
Figure 3.1: All possible interaction graphs for a four-agent system.
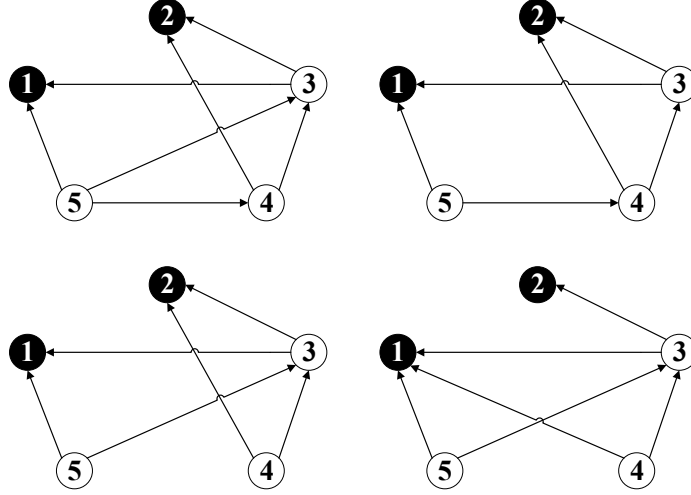
Figure 3.2: Four possible interaction graphs for a five-agent system.

Suppose Assumptions 3.1-3.2 are satisfied. Our objective is to design an AGAS bearing-based distributed pose (position and orientation) estimation scheme using the available measurements.

Remark 3.1 *The multi-agent system defined in* (3.1)*, under Assumption 3.2, could be practically related to a motion capture system consisting of a network of cameras with fixed positions and time-varying orientations.*

3.2.2 Bearing-Based Distributed Attitude Estimation on $SO(3)$

We propose the following distributed attitude observer on $SO(3)$:

$$\dot{\hat{R}}_i = \hat{R}_i \left[\omega_i - k_R \hat{R}_i^T \sum_{j \in \mathcal{N}_i} k_{ij} (\hat{R}_j b_{ij}^j \times \hat{R}_i b_{ij}^i) \right]^\times, \tag{3.3}$$

for $i \in \mathcal{V}_f$, where $k_R, k_{ij} > 0$, $\hat{R}_i \in SO(3)$ is the estimate of R_i, and $\hat{R}_l = R_l$, $l \in \{1, 2\}$. Under Assumption 3.2, one has $||p_i - p_j|| \neq 0$ and consequently the bearing measurement $b_{ij}^i(t)$, $i \in \mathcal{V}$, $j \in \mathcal{N}_i$, is well defined $\forall t \geq 0$.

The intuition behind the design of the observer correcting term, $\sum_{j \in \mathcal{N}_i} k_{ij} (\hat{R}_j b_{ij}^j \times \hat{R}_i b_{ij}^i)$, is to align the local relative bearings measured by each agent with the same relative bearings measured by the agent's neighbors using the attitude estimates. Once this alignment is achieved, the correcting term vanishes and the attitude estimates converge (almost globally) to the actual ones.

Now, by defining the attitude estimation error $\tilde{R}_i := R_i \hat{R}_i^T$, the last term of (3.3) can be rewritten as follows:

$$\sum_{j \in \mathcal{N}_i} k_{ij} (\hat{R}_j b_{ij}^j \times \hat{R}_i b_{ij}^i) = \sum_{j \in \mathcal{N}_i} k_{ij} (b_{ij} \times \tilde{R}_i^T b_{ij}) + \sum_{j \in \mathcal{N}_i} k_{ij} \left((\tilde{R}_j^T - I_3) b_{ij} \times \tilde{R}_i^T b_{ij} \right)$$

$$= -2\psi(M_i\tilde{R}_i) + \sum_{j \in \mathcal{N}_i} k_{ij}\left((\tilde{R}_j^T - I_3)b_{ij} \times \tilde{R}_i^T b_{ij}\right), \qquad (3.4)$$

where $M_i := \sum_{j \in \mathcal{N}_i} k_{ij}b_{ij}b_{ij}^T$. The last equation was obtained using identity (2.32). Note that since the positions of the agents are fixed, one can verify that the relative bearings expressed in the inertial frame are static, and consequently the matrix M_i is time-invariant. It is always possible to choose $k_{ij} > 0$ such that the matrix M_i is positive semi-definite with three distinct eigenvalues. From (3.1) and (3.3), it follows that the time derivative of the attitude estimation error, for every $i \in \mathcal{V}_f$, is given by

$$\dot{\hat{R}}_i = -R_i\left[\omega_i - k_R\hat{R}_i^T \sum_{j \in \mathcal{N}_i} k_{ij}(\hat{R}_j b_{ij}^j \times \hat{R}_i b_{ij}^i)\right]^\times \hat{R}_i^T + R_i[\omega_i]^\times \hat{R}_i^T$$

$$= k_R\tilde{R}_i\left[\sum_{j \in \mathcal{N}_i} k_{ij}(\hat{R}_j b_{ij}^j \times \hat{R}_i b_{ij}^i)\right]^\times. \qquad (3.5)$$

Using identities (2.20) and (2.26), and in view of (3.4), one can simplify the last equation as follows:

$$\dot{\tilde{R}}_i = -2k_R\tilde{R}_i\left[\psi(M_i\tilde{R}_i)\right]^\times + k_R\tilde{R}_i\left[\sum_{j \in \mathcal{N}_i} k_{ij}g_{ij}(\tilde{R}_j)\right]^\times, \qquad (3.6)$$

where $g_{ij}(\tilde{R}_j) := (\tilde{R}_j^T - I_3)b_{ij} \times \tilde{R}_i^T b_{ij}$. Note that the term $g_{ij}(\tilde{R}_j)$ is bounded and vanishes when $\tilde{R}_j = I_3$. Furthermore, system (3.6) can be viewed as a cascaded system, where the attitude estimation errors of the neighbors are considered as inputs to the following unforced system:

$$\dot{\tilde{R}}_i = -2k_R\tilde{R}_i\left[\psi(M_i\tilde{R}_i)\right]^\times. \qquad (3.7)$$

Since the matrix M_i is time-invariant, we are able to derive the set of isolated equilibria of system (3.7) and study their stability properties. The following lemma provides the stability properties of the unforced system (3.7).

Lemma 3.1 *Let $k_{ij} > 0$ such that M_i is positive semi-definite with three distinct eigenvalues. Then, the following statements hold for all $i \in \mathcal{V}_f$:*

  i) All solutions of (3.7) converge to the following set of isolated equilibria: $\Upsilon := \{I_3\} \cup \{\tilde{R}_i = \mathcal{R}_\alpha(\pi, v_i) | v_i \in \mathcal{E}(M_i)\}$, where $\mathcal{E}(M_i) \subset \mathbb{S}^2$ is the set of unit eigenvectors of matrix M_i.

  ii) The desired equilibrium $\tilde{R}_i = I_3$ is locally exponentially stable.

  iii) The linearized system of (3.7), at each undesired equilibrium $\Upsilon/\{I_3\}$, has at least one positive eigenvalue.

  iv) The undesired equilibria $\Upsilon/\{I_3\}$ are unstable and the desired equilibrium $\tilde{R}_i = I_3$ is AGAS.

Proof See Appendix A.1

Remark 3.2 *Lemma 3.1 provides local exponential stability and AGAS of the desired equilibrium $\tilde{R}_i = I_3$ of the unforced system (3.7). The AGAS result is the strongest result one can achieve with smooth time-invariant vector fields on $SO(3)$ (Koditschek, 1989).*

In the next lemma, we will study the ISS property of the forced attitude error dynamics (3.6), with respect to its inputs (*i.e.*, $\tilde{R}_j$ with $j \in \mathcal{N}_i$), using the notion of *almost global ISS* introduced in Section 2.7.

Lemma 3.2 *Let M_i be positive semi-definite with three distinct eigenvalues. Then, system (3.6) is almost globally ISS, for every $i \in \mathcal{V}_f$, with respect to I_3 and inputs $\tilde{R}_j$ where $j \in \mathcal{N}_i$.*

Proof See Appendix A.2

Remark 3.3 *As shown in the proof of Lemma 3.2, the knowledge of the isolated equilibria of system (3.7) and their stability properties were instrumental in deriving the result of Lemma 3.2.*

When dealing with nonlinear systems on $\mathbb{R}^n$, it is common to consider the origin (*i.e.*, zero) as an equilibrium point, and the ISS is implicitly stated with respect to this equilibrium point. On the special orthogonal group $SO(3)$ the desired equilibrium is the identity $\tilde{R}_i = I_3$. The statement "almost global ISS with respect to I_3" indicates that the equilibrium I_3 is AGAS for the unperturbed system, *i.e.*, unforced system (3.7). Therefore, as commonly used in the literature dealing with ISS on manifolds, we explicitly mention the equilibrium I_3 in the statement of Lemma 3.2 to emphasise that the system's equilibrium is not the origin since we are working on $SO(3)$. Now, relying on the results presented in Lemmas 3.1 and 3.2, one can state the following theorem about the stability properties of the n-agent cascaded system given in (3.6).

Theorem 3.1 *Under Assumption 3.2, the equilibrium point $(\tilde{R}_3 = I_3, \tilde{R}_4 = I_3, \ldots, \tilde{R}_n = I_3)$ of the n-agent cascaded system (3.6) is AGAS.*

Proof See Appendix A.3

Remark 3.4 *Showing that the desired equilibrium $\tilde{R}_i = I$ of the unforced system (3.7) is AGAS, while treating the neighbors' states as inputs to the agent's unforced dynamics, i.e., system (3.7), and analyzing the ISS of these dynamics with respect to these inputs, we were able to derive the result in Theorem 3.1. This theorem provides the strongest possible stability result one can achieve with smooth vector fields on $SO(3)$ (Koditschek, 1989).*

3.2.3 Bearing-Based Distributed Attitude Estimation with Filtered Measurements

For $i \in \mathcal{V}_f$, we propose the following distributed attitude estimation law on $SO(3) \times \mathbb{R}^3$

$$\dot{\hat{R}}_i = \hat{R}_i \left[\omega_i - \hat{R}_i^T \Omega_i \right]^\times \tag{3.8}$$

$$\dot{\Omega}_i = -k_\Omega \Omega_i + \sum_{j \in \mathcal{N}_i} k_{ij} (\hat{R}_j b_{ij}^j \times \hat{R}_i b_{ij}^i), \tag{3.9}$$

with $k_\Omega, k_{i,j} > 0$, $\Omega_i \in \mathbb{R}^3$ and $\hat{R}_i \in SO(3)$ is the estimate of R_i, and $\hat{R}_l = R_l$, $l \in \{1, 2\}$. The main difference between this distributed attitude observer and the previous one, given in (3.3), lies in the introduction of the auxiliary time-varying vector Ω_i. This vector is used to relocate the correcting term $\sum_{j \in \mathcal{N}_i} k_{ij} (\hat{R}_j b_{ij}^j \times \hat{R}_i b_{ij}^i)$ one integrator away from the attitude dynamics. This distributed attitude estimation scheme is more practical than the one in the previous section, since it relies on filtered bearing measurements. Now, let the attitude estimation error be $\tilde{R}_i := R_i \hat{R}_i^T$. In view of (3.8)-(3.9) and (3.4), one can derive the following error dynamics, for $i \in \mathcal{V}_f$:

$$\dot{\tilde{R}}_i = \tilde{R}_i [\Omega_i]^\times \tag{3.10}$$

$$\dot{\Omega}_i = -k_\Omega \Omega_i - 2\psi(M_i \tilde{R}_i) + \sum_{j \in \mathcal{N}_i} k_{ij} g_{ij}(\tilde{R}_j). \tag{3.11}$$

Recall that the matrix $M_i = \sum_{j \in \mathcal{N}_i} k_{ij} b_{ij} b_{ij}^T$ is time-invariant because the relative bearings expressed in the inertial frame are static, and it is always possible to choose $k_{ij} > 0$ such that the matrix M_i is positive semi-definite with three distinct eigenvalues. The above system can also be viewed as a cascaded system, where the attitude estimation errors of the neighbors are considered as inputs to the following unforced system:

$$\dot{\tilde{R}}_i = \tilde{R}_i [\Omega_i]^\times \tag{3.12}$$

$$\dot{\Omega}_i = -k_\Omega \Omega_i - 2\psi(M_i \tilde{R}_i). \tag{3.13}$$

Similar to Lemma 3.1, in the next lemma, we will study the stability properties of the unforced system (3.12)-(3.13).

Lemma 3.3 *Consider system (3.12)-(3.13). Let $k_{ij} > 0$ such that M_i is positive semi-definite with three distinct eigenvalues. Then, $\forall i \in \mathcal{V}_f$, the following statements hold:*

i) All solutions of (3.12)-(3.13) converge to the following set of isolated equilibria:
$$\Upsilon_1 := \{(I_3, 0)\} \cup \{(\tilde{R}_i, \Omega_i) \in SO(3) \times \mathbb{R}^3 : \tilde{R}_i = \mathcal{R}_\alpha(\pi, v_i), v_i \in \mathcal{E}(M_i), \Omega_i = 0\}.$$

ii) The desired equilibrium $(I_3, 0)$ is locally exponentially stable.

iii) The linearized system of (3.12)-(3.13), at each undesired equilibrium $\Upsilon_1/\{(I_3, 0)\}$, has at least one positive eigenvalue.

iv) The undesired equilibria $\Upsilon_1/\{(I_3, 0)\}$ are unstable and the desired equilibrium $(\tilde{R}_i = I_3, \Omega_i = 0)$ is AGAS.

Proof See Appendix A.4

Remark 3.5 *From Lemmas 3.1 and 3.3, one can observe that both bearing-based distributed attitude observers (3.3) and (3.8)-(3.9) are AGAS. This is the strongest achievable stability result with smooth time-invariant vector fields on $SO(3)$ as discussed in (Koditschek, 1989).*

In the following lemma, we will use the notion of almost global ISS to study the ISS property of the forced attitude error dynamics (3.10)-(3.11), with respect to its inputs $\tilde{R}_j$, $j \in \mathcal{N}_i$.

Lemma 3.4 *Let M_i be positive semi-definite with three distinct eigenvalues. System (3.10)-(3.11) is almost globally ISS, for every $i \in \mathcal{V}_f$, with respect to the equilibrium $(I_3, 0)$ and inputs $\tilde{R}_j$, $j \in \mathcal{N}_i$.*

Proof See Appendix A.5

In what follows, we will establish the stability properties of the n-agent cascaded system given in (3.10)-(3.11).

Theorem 3.2 *Under Assumption 3.2, the equilibrium point $(\tilde{R}_3 = I_3, \Omega_3 = 0, \tilde{R}_4 = I_3, \Omega_4 = 0, \ldots, \tilde{R}_n = I_3, \Omega_n = 0)$ of the n-agent cascaded system (3.10)-(3.11) is AGAS.*

Proof See Appendix A.6

Next, we will rely on the attitude estimates provided by either observer (3.3) or observer (3.8)-(3.9) to propose a bearing-based distributed position estimation scheme. These attitude estimates, along with local relative bearing measurements, will be fed to the proposed position estimation scheme.

3.2.4 Bearing-Based Distributed Pose Estimation

Consider the distributed attitude observer (3.3) (or (3.8)-(3.9)) together with the following distributed position estimation law:

$$\dot{\hat{p}}_i = -[\sigma_i]^\times \hat{p}_i - k_p \sum_{j \in \mathcal{N}_i} \hat{R}_i P_{b_{ij}^i} \hat{R}_i^T (\hat{p}_i - \hat{p}_j), \tag{3.14}$$

for every $i \in \mathcal{V}_f$, where $k_p, k_R, k_{ij} > 0$, $\hat{p}_i \in \mathbb{R}^3$ is the estimate of p_i, $\hat{R}_i \in SO(3)$ is the estimate of R_i obtained from the distributed attitude observer (3.3) (or (3.8)-(3.9)), and $(\hat{R}_l, \hat{p}_l) = (R_l, p_l)$, $l \in \{1, 2\}$. Note that, considering the distributed attitude observer (3.3), one has $\sigma_i = k_R \left(\sum_{j \in \mathcal{N}_i} k_{ij} \left(\hat{R}_j b_{ij}^j \times \hat{R}_i b_{ij}^i \right) \right)$, and considering the distributed attitude observer (3.8)-(3.9), one has $\sigma_i = \Omega_i$. Define the position estimation error as $\tilde{p}_i := p_i - \tilde{R}_i \hat{p}_i$. The time derivative of $\tilde{p}_i$ is given by

$$\dot{\tilde{p}}_i = -k_p \sum_{j \in \mathcal{N}_i} P_{b_{ij}} \tilde{p}_i + k_p \sum_{j \in \mathcal{N}_i} P_{b_{ij}} (p_j - \tilde{R}_i \hat{p}_j), \tag{3.15}$$

with $i \in \mathcal{V}_f$. We have used the fact that $P_{b_{ij}}(p_i - p_j) = 0$ and $P_{b_{ij}^i} = R_i^T P_{b_{ij}} R_i$ to obtain the last equality. It follows from (3.15) that

$$\dot{\tilde{p}}_i = -k_p \sum_{j \in \mathcal{N}_i} P_{b_{ij}} \tilde{p}_i + k_p \sum_{j \in \mathcal{N}_i} P_{b_{ij}} f_j(\tilde{p}_j, \tilde{R}_j, \tilde{R}_i), \tag{3.16}$$

where $f_j(\tilde{p}_j, \tilde{R}_j, \tilde{R}_i) := \left((\tilde{R}_j - I_3) - (\tilde{R}_i - I_3) \right) \tilde{R}_j^T (p_j - \tilde{p}_j) + \tilde{p}_j$. It is clear that, for $\tilde{p}_j = 0$ and $\tilde{R}_j = \tilde{R}_i = I_3$, one has $f_i(\tilde{p}_j, \tilde{R}_j, \tilde{R}_i) = 0$. System (3.16) can be seen as a cascaded system, where the attitude and position estimation errors of the neighbors as well as the attitude estimation error of agent i are considered as inputs to the following unforced system:

$$\dot{\tilde{p}}_i = -k_p \sum_{j \in \mathcal{N}_i} P_{b_{ij}} \tilde{p}_i. \tag{3.17}$$

Since the relative bearing measurements expressed in the inertial frame are constant, it is clear that that system (3.17) is a simple linear time-invariant system. Now, we study the stability of the equilibrium point $\tilde{p}_i = 0$ of system (3.17) and the ISS property of system (3.16).

Proposition 3.1 *Consider system* (3.17) *under Assumption 3.2. The equilibrium point* $\tilde{p}_i = 0$, $i \in \mathcal{V}_f$, *is globally exponentially stable (GES).*

Proof Under the assumption that at least two bearing vectors are non-collinear (Assumption 3.2), for every $i \in \mathcal{V}_f$, the matrix $\sum_{j \in \mathcal{N}_i} P_{b_{ij}}$ is positive definite, and hence, the equilibrium $\tilde{p}_i = 0$ of the unforced position error dynamics (3.17) is GES.

Lemma 3.5 *Suppose Assumption 3.2 is satisfied. Then, for every* $i \in \mathcal{V}_f$, *system* (3.16) *is ISS with respect to its inputs* $\tilde{p}_j$, $\tilde{R}_j$ *and* $\tilde{R}_i$.

Proof See Appendix A.7

Theorem 3.3 *Under Assumption 3.2, the following statements hold:*

1) *The equilibrium point* $(\tilde{R}_3 = I_3, \tilde{R}_4 = I_3, \ldots, \tilde{R}_n = I_3, \tilde{p}_3 = 0, \tilde{p}_4 = 0, \ldots, \tilde{p}_n = 0)$ *of the cascaded attitude and position estimation schemes given by* (3.3) *and* (3.14) *is AGAS.*

2) *The equilibrium point* $(\tilde{R}_3 = I_3, \Omega_3 = 0, \tilde{R}_4 = I_3, \Omega_4 = 0, \ldots, \tilde{R}_n = I_3, \Omega_n = 0, \tilde{p}_3 = 0, \tilde{p}_4 = 0, \ldots, \tilde{p}_n = 0)$ *of the cascaded attitude and position estimation schemes given by* (3.8) $-$ (3.9) *and* (3.14) *is AGAS.*

Proof See Appendix A.8

Remark 3.6 *The result of Theorem 3.3 (AGAS) is also valid in the particular situation where the agents' positions are time-varying and the relative bearings are kept constant (e.g., a motion that keeps the bearings constant through a collective translation and scaling of the entire network).*

The proposed bearing-based distributed pose estimation scheme (3.3) and (3.14) (or (3.8)-(3.9) and (3.14)) can be used to address some of the well-known practical problems of self-localization for sensor networks. For instance, consider a motion capture system consisting of a network of n static cameras with time-varying orientation looking at a

given scene, and the objective is to estimate the motion of a given object with respect to a reference frame. In this case, one needs to know the pose (position and orientation) of each camera with respect to the reference frame, which can be done through a calibration procedure every time we change the network configuration. Our proposed localization algorithm (3.3) and (3.14) (or (3.8)-(3.9) and (3.14)) could automatically handle this calibration procedure, making the deployment of large sensor networks much easier.

3.2.5 Simulation Results

In this section, we present some numerical simulation results to illustrate the performance of both proposed bearing-based localization schemes (3.3), (3.14) and (3.8)-(3.9), (3.14).

In these simulations, we consider an eight-agent rigid-body system in a 3-dimensional space with the following fixed positions: $p_1 = [0\ 0\ 0]^T$, $p_2 = [2\ 0\ 1]^T$, $p_3 = [2\ 2\ 2]^T$, $p_4 = [0\ 2\ 3]^T$, $p_5 = [0\ 0\ 4]^T$, $p_6 = [2\ 0\ 5]^T$, $p_7 = [2\ 2\ 6]^T$ and $p_8 = [0\ 2\ 7]^T$. The rotational subsystem is driven by the following angular velocities: $\omega_1 = [1\ -2\ 1]^T$, $\omega_2(t) = [-\cos 3t\ 1\ \sin 2t]^T$, $\omega_3(t) = [-\cos t\ 1\ \sin 2t]^T$, $\omega_4(t) = [-\cos 2t\ 1\ \sin 5t]^T$, $\omega_5(t) = [-\cos 5t\ 1\ \sin 9t]^T$, $\omega_6(t) = [-\cos 2t\ \sin 9t\ 1]^T$, $\omega_7(t) = [-\cos 4t\ 1\ 2]^T$ and $\omega_8(t) = [-2\ 1\ \sin 9t]^T$. The initial rotations of all agents are chosen to be the identity. Based on Assumption 3.2, we use a directed graph topology to model the interaction between the agent in the network as it is shown in Figure 3.3. Accordingly, the neighbors sets are given as $\mathcal{N}_1 = \mathcal{N}_2 = \{\varnothing\}$, $\mathcal{N}_3 = \{1, 2\}$, $\mathcal{N}_4 = \{2, 3\}$, $\mathcal{N}_5 = \{1, 4\}$, $\mathcal{N}_6 = \{2, 4, 5\}$, $\mathcal{N}_7 = \{3, 4, 6\}$ and $\mathcal{N}_8 = \{1, 7\}$.
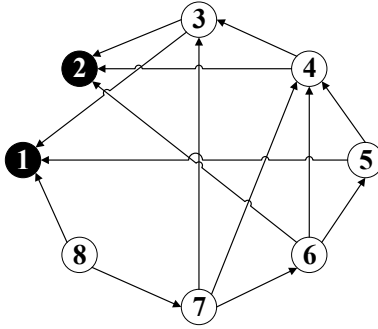
Figure 3.3: The interaction graph (the black circles represent the leaders).

For both observers, we consider the following initial conditions: $\hat{p}_3(0) = [-2\ 0\ -1]^T$, $\hat{p}_4(0) = [-1\ 2\ 2]^T$, $\hat{p}_5(0) = [-2\ 2\ 4]^T$, $\hat{p}_6(0) = [0\ 0\ 0]^T$, $\hat{p}_7(0) = [-4\ 0\ 1]^T$, $\hat{p}_8(0) = [-3\ \frac{1}{2}\ 2]^T$, $\hat{R}_3(0) = \mathcal{R}_\alpha(0.1\pi, v)$, $\hat{R}_4(0) = \mathcal{R}_\alpha(0.2\pi, v)$, $\hat{R}_5(0) = \mathcal{R}_\alpha(0.3\pi, v)$, $\hat{R}_6(0) = \mathcal{R}_\alpha(0.9\pi, v)$, $\hat{R}_7(0) = \mathcal{R}_\alpha(0.4\pi, v)$ and $\hat{R}_8(0) = \mathcal{R}_\alpha(0.5\pi, v)$ with $v = [1\ 0\ 0]^T$. The gain parameters are taken as follows: $k_p = 1$, $k_R = 1$ and $k_{ij} = 1$ for each $(i, j) \in \mathcal{E}$. Figures 3.4 and 3.5 show the time evolution of the individual attitude and position estimation error norms for each agent and the average attitude and position estimation error norms of all agents in the network, respectively. These results are obtained by considering the proposed distributed pose observer given by equations (3.3) and (3.14).
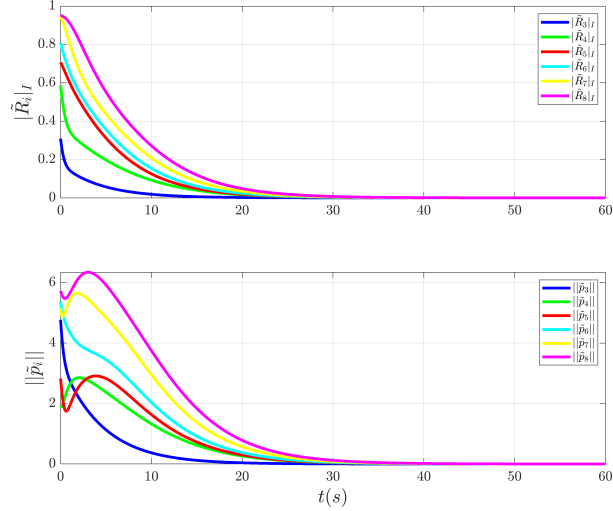
Figure 3.4: Time evolution of the individual estimation error norms for the observer (3.3), (3.14).

Figure 3.5: Time evolution of the average estimation error norms for the observer (3.3), (3.14).

Additionally, to simulate the bearing-based distributed pose estimation scheme (3.8)-(3.9), (3.14), we assume that $\Omega_i(0) = 0$, for every $i \in \mathcal{V}_f$, and we pick $k_\Omega = 1$. The time evolution of the individual attitude and position estimation error norms for each agent as well as the average attitude and position estimation error norms of all agents in the network considering the observer (3.8)-(3.9), (3.14) are provided in Figures 3.6 and 3.7, respectively.

To further validate the performance of the two proposed localization schemes, we performed additional simulations with biased and noisy measurements. To do this, we add the following constant biases to the angular velocity measurements: $b_{\omega_1} = [0.1\ 0.07\ 0.01]^T, b_{\omega_2} = [0.001\ 0\ 0.01]^T, b_{\omega_3} = [0.02\ 0.07\ 0.01]^T, b_{\omega_4} = [0.1\ 0.02\ 0.01]^T, b_{\omega_5} =$
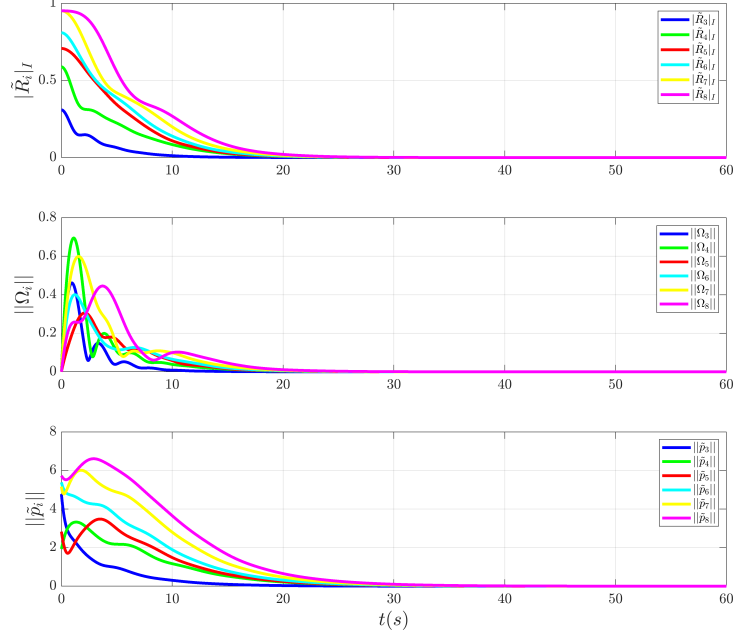
Figure 3.6: Time evolution of the individual estimation error norms considering the observer (3.8)-(3.9), (3.14).

$[0.09\ 0.07\ 0.01]^T, b_{\omega_6} = [0.1\ 0.04\ 0.03]^T, b_{\omega_7} = [0.1\ 0.07\ 0]^T$ and $b_{\omega_8} = [0\ 0.07\ 0.01]^T$. We also assume that each angular velocity measurement is corrupted by additive white Gaussian noise with zero mean and 0.01 variance. Similar to (Hamel and Samson, 2018), the noises are added to the bearing measurements according to the following equation:

$$b_{ij}^i = \frac{\text{sign}(b_{ij,3}^i)}{d_{b_{ij}^i}} \left(b_{ij,1}^i/b_{ij,3}^i + n_{ij,1}^i,\ b_{ij,2}^i/b_{ij,3}^i + n_{ij,2}^i,\ 1 \right) \tag{3.18}$$

$$d_{b_{ij}^i} = || \left(b_{ij,1}^i/b_{ij,3}^i + n_{ij,1}^i,\ b_{ij,2}^i/b_{ij,3}^i + n_{ij,2}^i,\ 1 \right) ||, \tag{3.19}$$

where $n_{ij,1}^i$ and $n_{ij,2}^i$ are additive white Gaussian noise with zero mean and a variance of 0.001. Figures 3.8 and 3.9 depict the time evolution of the individual attitude and position estimation error norms for each agent and the average attitude and position estimation error norms of all agents in the network, respectively, under noisy and biased measurements, considering the observers (3.3), (3.14).
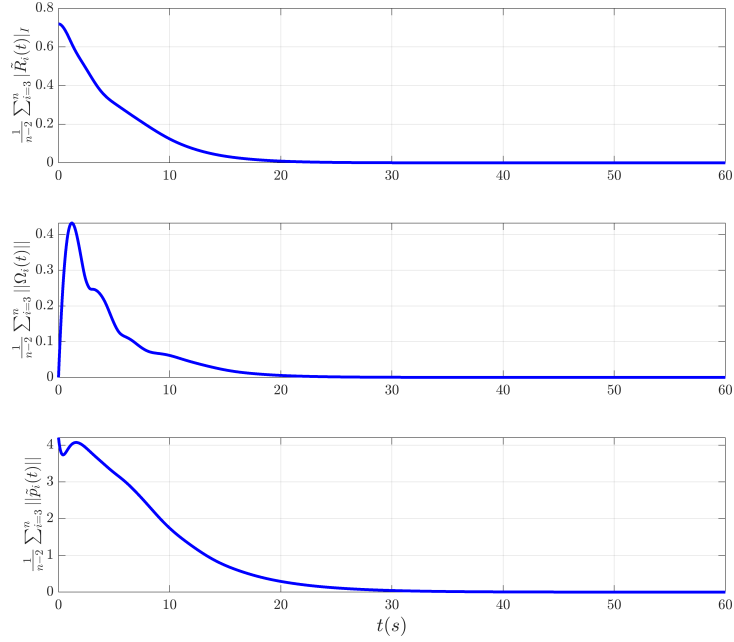
Figure 3.7: Time evolution of the average estimation error norms considering the observer (3.8)-(3.9), (3.14).
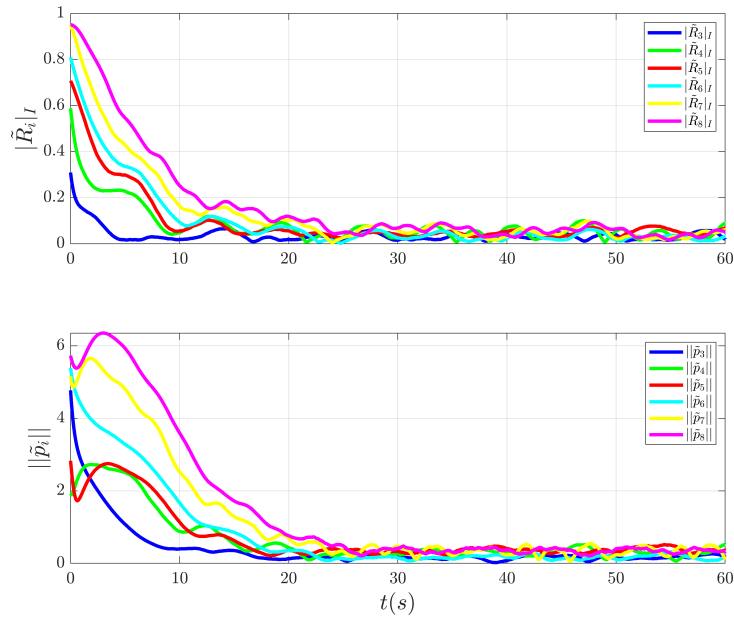
Figure 3.8: Time evolution of the individual estimation error norms, with noisy and biased measurements, for observer (3.3), (3.14).

For the pose observer (3.8)-(3.9), (3.14), Figures 3.10 and 3.11 illustrate the time evolution of the individual attitude and position estimation error norms and the average attitude and position estimation error norms of all agents in the network, under noisy and biased measurements.
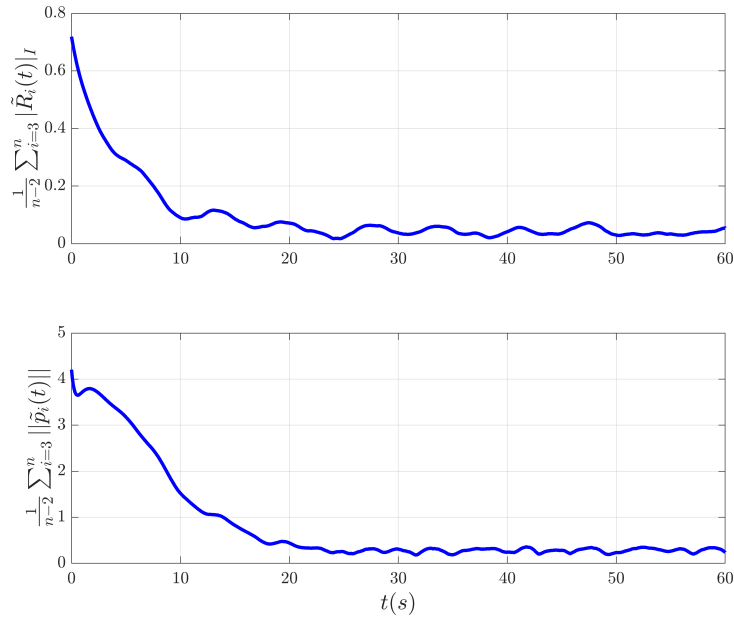
Figure 3.9: Time evolution of the average estimation error norms, with noisy and biased measurements, for observer (3.3), (3.14).

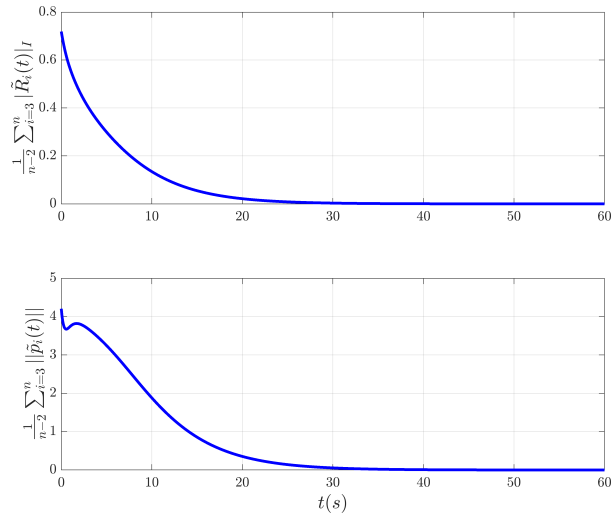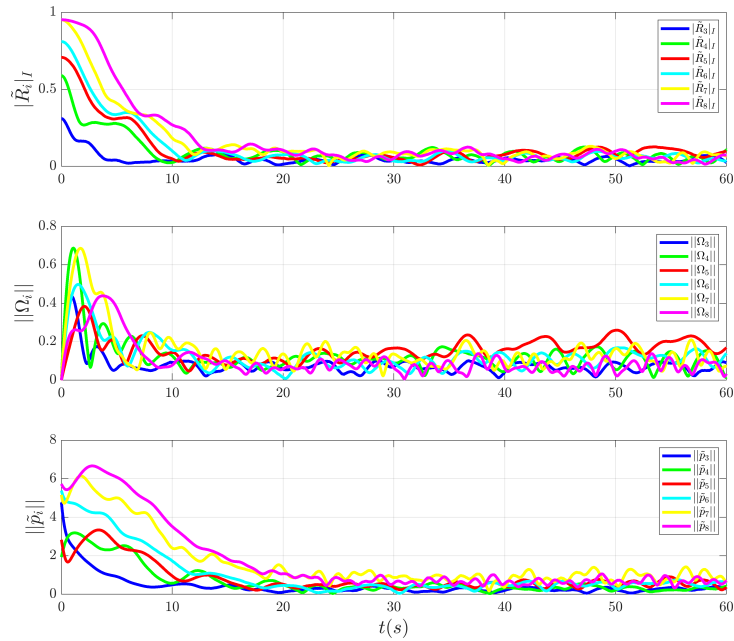Figure 3.10: Time evolution of the individual estimation error norms for the observer(3.8)-(3.9), (3.14).
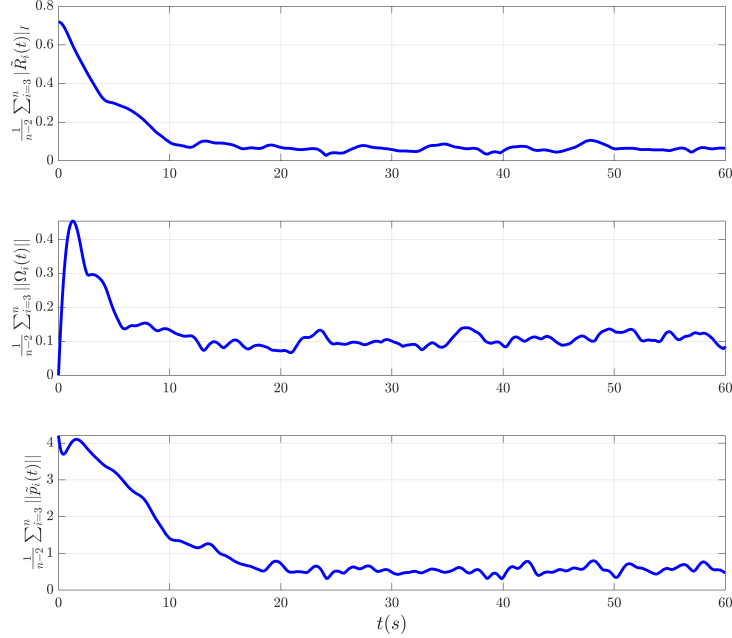
Figure 3.11: Time evolution of the average estimation error norms for the observer (3.8)-(3.9), (3.14).

3.3 Bearing-Based Distributed Pose Observer Design: Time-Varying Positions and Orientations

In this section, we address the problem of distributed pose estimation for multi-agent rigid-body systems where the agents are allowed to have simultaneous translational and rotational motion. We propose an exponentially stable bearing-based distributed nonlinear pose estimation scheme on $SO(3) \times \mathbb{R}^3$. Similar to the previous pose observer design, the overall bearing-based distributed pose estimation scheme is a cascade of two subsystems. The first subsystem is a standalone bearing-based distributed attitude observer endowed with local exponential stability. The second subsystem consists of a bearing-based distributed position observer that relies on the attitude estimates provided by the rotational observer.

3.3.1 Problem Formulation

Consider an n-agent system, where each agent is modeled as a rigid body governed by the following rotational and translational kinematic equations:

$$\dot{R}_i = R_i[\omega_i]^\times \tag{3.20}$$

$$\dot{p}_i = v_i, \tag{3.21}$$

where $p_i \in \mathbb{R}^3$, $v_i \in \mathbb{R}^3$ are the position and velocity of agent i expressed in the inertial frame, the matrix $R_i \in SO(3)$ represents the orientation of the body-attached frame of

agent i with respect to the inertial frame, and $\omega_i \in \mathbb{R}^3$ is the angular velocity of agent i measured in the body-attached frame of the same agent. The measurement of the local relative bearing between agent i and agent j is given by

$$b_{ij}^i := R_i^T b_{ij}, \tag{3.22}$$

where $b_{ij} := \frac{p_j - p_i}{||p_j - p_i||}$ and b_{ij}^i are the relative bearing measurements between the agents i and j expressed in the inertial frame and the body-attached frame of agent i, respectively. Note that both vectors b_{ij}^i and b_{ij} are time-varying, since the agents are allowed to have translational motion as per the dynamics (3.21). However, in the expression of both vectors b_{ij}^i and b_{ij}, the time argument t is omitted for simplicity. To proceed with the observer design, we introduce the following assumptions which are similar to Assumptions 3.1 and 3.2 with slight differences:

Assumption 3.3 *The linear and angular velocities of each agent are available for measurement and bounded.*

Assumption 3.4 *By assigning a number to each agent, we assume that agents* 1 *and* 2 *are the leaders and the other agents are the followers. We also assume that*

a. *The leaders know their pose, and have no neighbors, i.e., $\mathcal{N}_k = \{\varnothing\} \; \forall k = 1, 2$. We also assume that the leaders' positions are bounded.*

b. *Each agent $i \in \mathcal{V}_f$ measures b_{ij}^i and receives $(\hat{R}_j, \hat{p}_j, b_{ji}^j)$ from its neighbors $j \in \mathcal{N}_i$.*

c. *The set of neighbors of each agent $i \in \mathcal{V}_f$ satisfies $\mathcal{N}_i \subseteq \{1, 2, 3, ..., i-1\}$ with $|\mathcal{N}_i| \geq 2$, and each agent measures at least two uniformly non-collinear bearing vectors.*

Assumption 3.5 *As time evolves, no inter-agent collision occurs.*

From Assumption 3.5 one verifies that $||p_i - p_j|| \neq 0$. Consequently, the bearing measurement $b_{ij}^i(t)$, for each $i \in \mathcal{V}$ and $j \in \mathcal{N}_i$, is well defined $\forall t \geq 0$.

Consider system (3.20)-(3.21) with measurements (3.22). Under Assumptions 3.3-3.5. Our objective is to design a distributed pose (position and orientation) estimation scheme on $SO(3) \times \mathbb{R}^3$ endowed with exponential stability guarantees.

3.3.2 Bearing-Based Distributed Attitude Estimation on $SO(3)$

For every $i \in \mathcal{V}_f$, we propose the following attitude observer on $SO(3)$:

$$\dot{\hat{R}}_i = \hat{R}_i \left[\omega_i - k_i^R \sum_{j \in \mathcal{N}_i} (\hat{R}_i^T \hat{R}_j b_{ij}^j) \times b_{ij}^i \right]^\times, \tag{3.23}$$

where $k_i^R > 0$, $\hat{R}_i \in SO(3)$ is the estimate of R_i, and $\hat{R}_l = R_l$, $l \in \{1, 2\}$ according to Assumption 3.4. Define the attitude estimation error as $\tilde{R}_i := R_i \hat{R}_i^T$, for every $i \in \mathcal{V}$. In

view of (3.20) and (3.23), the time derivative of the attitude estimation error for each follower $i \in \mathcal{V}_f$ is given by

$$\dot{\hat{R}}_i = R_i[\omega_i]^\times \hat{R}_i^T - R_i \left[\omega_i - k_i^R \sum_{j \in \mathcal{N}_i} (\hat{R}_i^T \hat{R}_j b_{ij}^j) \times b_{ij}^i\right]^\times \hat{R}_i^T.$$

Considering properties (2.20) and (2.26), the last equation can be simplified as follows:

$$\dot{\tilde{R}}_i = -k_i^R \tilde{R}_i \left[2\psi(M_i \tilde{R}_i) - \sum_{j \in \mathcal{N}_i} (\tilde{R}_j^T - I)b_{ij} \times \hat{R}_i b_{ij}^i\right]^\times, \tag{3.24}$$

where $M_i = \sum_{j \in \mathcal{N}_i} b_{ij} b_{ij}^T$. Identity (2.32) was used to obtain the last equality. Since the positions of the agents are not fixed, the relative bearings measured in the inertial frame are not static. Consequently, the matrix M_i is time-varying for every $i \in \mathcal{V}$. The stability properties of the attitude observer (3.23) are established in the next theorem.

Theorem 3.4 *Consider the attitude kinematics (3.20) with measurements (3.22) and observer (3.23), where Assumptions 3.3-3.5 are satisfied. Define the state vector $x(t) := [|\tilde{R}_3(t)|_I, |\tilde{R}_4(t)|_I, \ldots, |\tilde{R}_n(t)|_I]^T$. Then, for any $0 < \varepsilon < 1$, there exists a sufficiently large $k_i^R > 0, i \in \mathcal{V}_f$, such that the equilibrium $x = 0$ is exponentially stable (ES) for all initial conditions satisfying $||x(0)|| \leq \varepsilon$.*

Proof See Appendix A.9

Theorem 3.4 shows that the proposed distributed attitude observer is endowed only with local exponential stability guarantees and the basin of attraction shrinks as the number of agents in the network increases. This result is not as strong as the AGAS result in Theorem 3.1. This is the price one has to pay for allowing the agents' positions to be time-varying, which adds extra difficulties to the analysis of the distributed attitude estimation scheme. The difficulties arise mainly from the fact that the matrix M_i is time-varying which does not allow the characterization of the set of isolated equilibria of the unforced system $\dot{\tilde{R}}_i = -k_i^R \tilde{R}_i[2\psi(M_i \tilde{R}_i)]^\times$.

In the following section, we will design a bearing-based distributed pose estimation scheme on $SO(3) \times \mathbb{R}^3$ that relies on the attitude estimates provided by the observer dynamics (3.23) and the local relative bearing measurements.

3.3.3 Bearing-Based Distributed Pose Estimation on $SO(3) \times \mathbb{R}^3$

Consider the distributed attitude observer (3.23) with the following distributed position estimation law:

$$\dot{\hat{p}}_i = v_i - \left[k_i^R \hat{R}_i \sum_{j \in \mathcal{N}_i} (\hat{R}_i^T \hat{R}_j b_{ij}^j) \times b_{ij}^i\right]^\times \hat{p}_i - k_p \sum_{j \in \mathcal{N}_i} \hat{R}_i P_{b_{ij}^i} \hat{R}_i^T (\hat{p}_i - \hat{p}_j), \tag{3.25}$$

for every $i \in \mathcal{V}_f$, where $k_p, k_i^R > 0$, $\hat{p}_i \in \mathbb{R}^3$ is the estimate of p_i, $\hat{R}_i \in SO(3)$ is the estimate of R_i obtained from (3.23), and $(\hat{R}_l, \hat{p}_l) = (R_l, p_l)$, $l \in \{1, 2\}$. In view of (3.21), (3.24), and (3.25), the time derivative of the position estimation error $\tilde{p}_i := p_i - \tilde{R}_i \hat{p}_i$, for every $i \in \mathcal{V}_f$, is given by

$$\dot{\tilde{p}}_i = -k_p \sum_{j \in \mathcal{N}_i} P_{b_{ij}} \tilde{p}_i + k_p \sum_{j \in \mathcal{N}_i} P_{b_{ij}} (p_j - \tilde{R}_i \hat{p}_j) + (I - \tilde{R}_i) v_i. \tag{3.26}$$

We have used the fact that $P_{b_{ij}}(p_i - p_j) = 0$ and $P_{b_{ij}^i} = R_i^T P_{b_{ij}} R_i$ to obtain the last equality. Furthermore, one has

$$\dot{\tilde{p}}_i = -k_p \sum_{j \in \mathcal{N}_i} P_{b_{ij}} \tilde{p}_i + k_p \sum_{j \in \mathcal{N}_i} P_{b_{ij}} \left(\tilde{p}_j - (\tilde{R}_i - \tilde{R}_j)\hat{p}_j \right) + (I - \tilde{R}_i) v_i$$

$$= -k_p \sum_{j \in \mathcal{N}_i} P_{b_{ij}} \tilde{p}_i + k_p \sum_{j \in \mathcal{N}_i} h_{ij}(t, \tilde{p}_j, \tilde{R}_j, \tilde{R}_i), \tag{3.27}$$

where $h_{ij}(t, \tilde{p}_j, \tilde{R}_j, \tilde{R}_i) = P_{b_{ij}} \left(\tilde{p}_j - (\tilde{R}_i - \tilde{R}_j)\hat{p}_j \right) + (I - \tilde{R}_i) v_i$. One can verify that $h_{ij}(t, \tilde{p}_j, \tilde{R}_j, \tilde{R}_i) = 0$ for $\tilde{p}_j = 0$ and $\tilde{R}_j = \tilde{R}_i = I_3$. Therefore, one can consider the estimation errors, namely $\tilde{p}_j$, $\tilde{R}j$ and $\tilde{R}_i$, as inputs to $\tilde{p}_i$−system (3.27). Additionally, under Assumption 3.4, one can verify that the matrix $\sum_{j \in \mathcal{N}_i} P_{b_{ij}}$ is uniformly positive definite, and hence, the equilibrium $\tilde{p}_i = 0$ of (3.27), with $\tilde{p}_j = 0$ and $\tilde{R}_j = \tilde{R}_i = I_3$, is UGES. Now, let us study the ISS properties of system (3.27).

Lemma 3.6 *Suppose Assumption 3.4 is satisfied. Then, for every $i \in \mathcal{V}_f$, system (3.27) is ISS with respect to its inputs $\tilde{p}_j$, $\tilde{R}_j$ and $\tilde{R}_i$.*

Proof See Appendix A.10

Theorem 3.5 *Consider the kinematics (3.20)-(3.21) with measurements (3.22) and the cascaded observer (3.23), (3.25), where Assumptions 3.3-3.5 are satisfied. Assume that the result in Theorem 3.4 holds. Then, The equilibrium $(\tilde{R}_3 = I_3, \tilde{R}_4 = I_3, \ldots, \tilde{R}_n = I_3, \tilde{p}_3 = 0, \tilde{p}_4 = 0, \ldots, \tilde{p}_n = 0)$ is exponentially stable for the overall cascaded system (3.24), (3.27).*

Proof See Appendix A.11

Theorem 3.5 provides local exponential stability of the overall cascaded distributed bearing-based pose estimation scheme (3.23), (3.25). The local result is mainly due to the local exponential stability of the attitude observer of the rotational subsystem.

3.3.4 Simulation Results

In this section, we perform some numerical simulations to illustrate the performance of the proposed bearing-based localization scheme (3.23), (3.25).

In these simulations, we consider a network of five agents forming a pentagon shape in

$\mathbb{R}^3$, rotating around the x-axis (see Figure 3.12), with the following time-varying positions: $p_i(t) = R^T(t)p_i(0)$ where $R(t) = [1 \ 0 \ 0; 0 \ \cos\frac{\pi}{6}t \ -\sin\frac{\pi}{6}t; 0 \ \sin\frac{\pi}{6}t \ \cos\frac{\pi}{6}t]$, $p_1(0) = [2 \ -1 \ 1]^T$, $p_2(0) = [2 \ 1 \ 2]^T$, $p_3(0) = [2 \ 1 \ 0]^T$, $p_4(0) = [2 \ 1 \ -2]^T$ and $p_5(0) = [2 \ -1 \ -1]^T$. The rotation subsystem is driven by the following angular velocities: $\omega_1 = [1 \ -2 \ 1]^T$, $\omega_2(t) = [-\cos 3t \ 1 \ \sin 2t]^T$, $\omega_3(t) = [-\cos t \ 1 \ \sin 2t]^T$, $\omega_4(t) = [-\cos 2t \ 1 \ \sin 5t]^T$ and $\omega_5(t) = [-\cos t \ 1 \ \sin 9t]^T$. The agents initial rotations are chosen to be the identity.
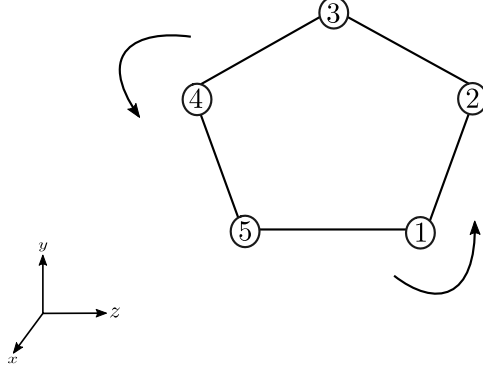
Figure 3.12: The five-agent network in $\mathbb{R}^3$.

The interactions between the agents in the network are described by the directed graph shown in Figure 3.13. It follows that the neighbors sets of the agents are $\mathcal{N}_1 = \mathcal{N}_2 = \{\varnothing\}$, $\mathcal{N}_3 = \{1, 2\}$, $\mathcal{N}_4 = \{2, 3\}$ and $\mathcal{N}_5 = \{3, 4\}$.
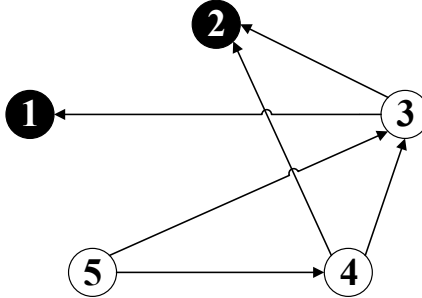
Figure 3.13: The interaction graph (the black circles represent the leaders).

The initial conditions of the observer (3.23), (3.25) are chosen to be: $\hat{p}_3(0) = [-2 \ 0 \ -1]^T$, $\hat{p}_4(0) = [-1 \ 2 \ 2]^T$, $\hat{p}_5(0) = [-2 \ 2 \ 4]^T$, $\hat{R}_3(0) = \mathcal{R}_a(0.1\pi, v_0)$, $\hat{R}_4(0) = \mathcal{R}_a(0.2\pi, v_0)$ and $\hat{R}_5(0) = \mathcal{R}_a(0.3\pi, v_0)$ with $v_0 = [1 \ 0 \ 0]^T$. The gain parameters are taken as follows: $k_p = 1$, $k_3^R = 10$, $k_4^R = 5$ and $k_5^R = 3$. Figures 3.14 and 3.15 depict the time evolution of the individual attitude and position estimation error norms for each agent and the average attitude and position estimation error norms of all agents in the network, respectively.
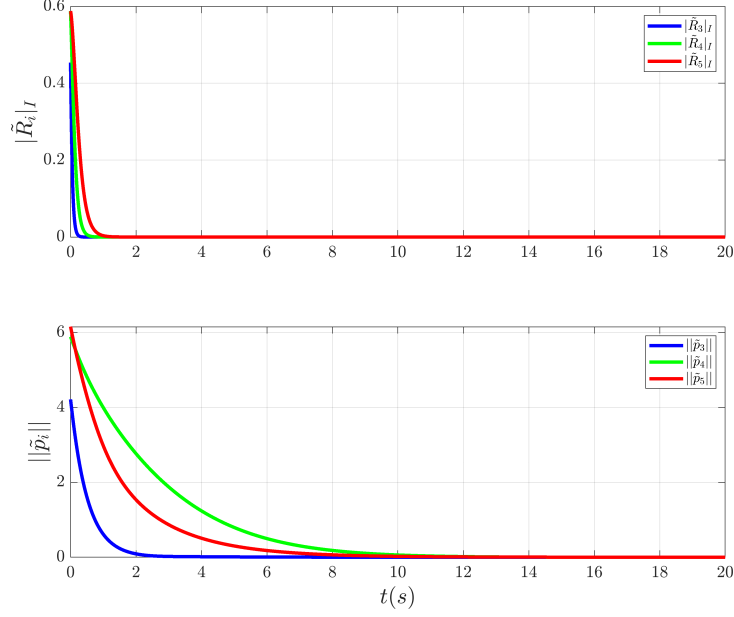
Figure 3.14: Time evolution of the individual estimation error norms.
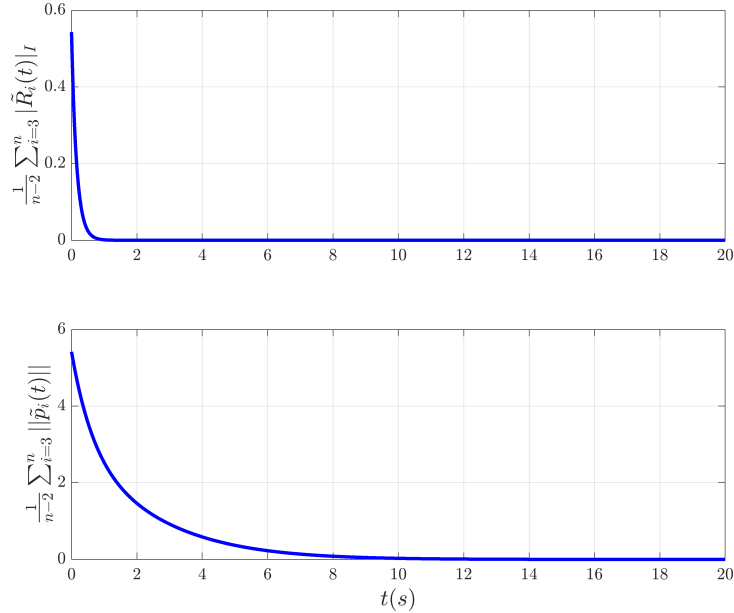
Figure 3.15: Time evolution of the average estimation error norms.

To further illustrate the performance of the localization scheme (3.23), (3.25), as in the previous section, we introduce noise and biases into the measurements. We assume that the linear and angular velocity measurements are affected by additive white Gaussian noise with a mean of zero and a variance of 0.1. We also assume that the bearing measurements are subject to additive white Gaussian noise with zero mean and 0.01 variance, according to the expressions (3.18)-(3.19). The following constant biases are added to the angular velocity measurements: $b_{\omega_3} = [0.02\ 0.07\ 0.01]^T$, $b_{\omega_4} = [0.1\ 0.02\ 0.01]^T$ and $b_{\omega_5} =$

$[0.09\ 0.07\ 0.01]^T$. Figures 3.16 and 3.17 show the time evolution of the individual attitude and position estimation error norms and the average attitude and position estimation error norms of all agents in the network, with noisy and biased measurements.
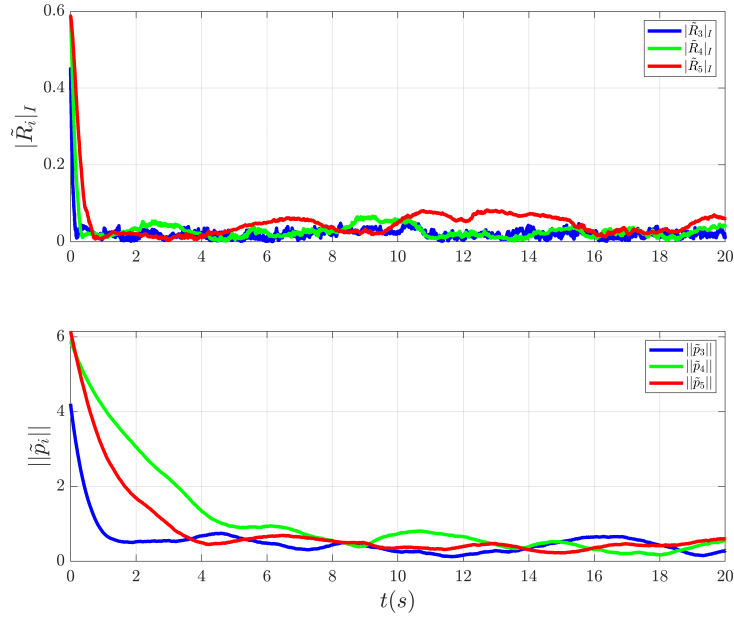
Figure 3.16: Time evolution of the individual estimation error norms with noisy and biased measurements.
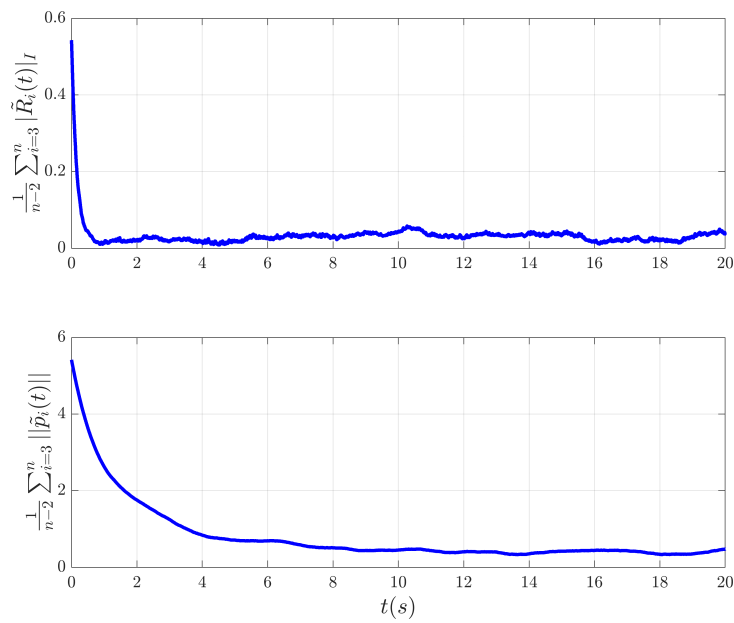
Figure 3.17: Time evolution of the average estimation error norms with noisy and biased measurements.

3.4 Conclusion

In this chapter, we proposed bearing-based localization schemes to address the problem of distributed pose estimation for multi-agent rigid-body systems, where two agents have access to their respective poses. The proposed schemes rely solely on individual angular velocity measurements and local information exchange between neighboring agents (relative time-varying bearing measurements and estimated poses), available according to a directed graph topology defined in Assumptions 3.2 and 3.4.

As a first contribution, we proposed two AGAS bearing-based distributed pose estimation schemes for multi-agent rigid-body networks in which the agents have fixed positions and time-varying orientations. As a second contribution, we explored the case where the agents are allowed to have simultaneous translational and rotational motion. Accordingly, we proposed an exponential bearing-based distributed pose estimation scheme. However, the proposed observer has a domain of attraction that shrinks as the number of agents increases. Therefore, designing a bearing-based distributed pose estimation scheme with strong stability guarantees independent of the number of agents would be an interesting extension to this contribution.

Chapter 4

Relative Attitude Measurements Based Distributed Attitude Estimation for Multi-Agent Rigid-Body Systems on $SO(3)$ with Application to Distributed Pose Estimation

4.1 Introduction

In this chapter, we first consider the problem of distributed attitude estimation of multi-agent rigid-body systems, evolving on $SO(3)$, with global asymptotic stability guarantees, relying on individual angular velocity and relative attitude information. Thereafter, we deal with the design of a distributed pose estimation scheme, for multi-agent rigid-body systems, via a cascade of a distributed attitude observer and a distributed position observer.

Motivated by the classical (Euclidean) consensus algorithms (Ren and Beard, 2007; Mesbahi and Egerstedt, 2010), some distributed attitude estimation schemes have been proposed in the literature (Lee and Ahn, 2016a; Lee and Ahn, 2016b; Van Tran et al., 2018; Lee et al., 2019; Van Tran et al., 2019; Van Tran and Ahn, 2020). These approaches rely on the orthogonalization of some auxiliary matrices using the Gram-Schmidt procedure which is not always viable as the auxiliary matrices may be singular at some time instances. The distributed attitude estimation schemes proposed in the above references are shown to be AGAS.

We first propose a continuous nonlinear distributed attitude estimation scheme on $SO(3)$, with AGAS guarantees, without using the Gram-Schmidt orthogonalization procedure. Thereafter, we proceed with the *hybridization* of the proposed continuous estimation scheme to derive a new hybrid nonlinear distributed attitude estimation scheme, with global asymptotic stability guarantees, allowing the attitude estimation errors to

converge to an unknown common constant orientation which can be determined in the presence of a leader in the group (knowing its absolute orientation). To the best of our knowledge, there are no results in the literature achieving such strong stability properties for the estimation problem at hand. The proposed hybrid estimation scheme relies on time-varying scalar auxiliary variables, inspired from (Wang and Tayebi, 2022), which are governed by some appropriately designed hybrid dynamics. These auxiliary variables enable the estimation scheme to keep the relative attitude errors away from the undesired equilibria through continuous flow and discrete jumps. In both designs, we assume that the interaction graph topology is an undirected tree, and each agent measures its own angular velocity in the respective body-frame, measures the relative orientation with respect to its neighbours, and receives information from its neighbors.

Finally, we design a distributed position estimation law that uses the estimated attitudes, provided by the hybrid distributed attitude observer, the local relative (time-varying) bearing information, and the individual linear velocities. This design guarantees global pose estimation of the n-agent rigid-body system up to a constant translation and orientation. Finally, some numerical simulation results are presented to illustrate the performance of the proposed observers. The results presented in this chapter are based on our work in (Boughellaba and Tayebi, 2023c; Boughellaba and Tayebi, 2023d).

4.2   Problem Formulation

Consider an n-agent rigid-body system governed by the following rotational kinematic equation:

$$\dot{R}_i = R_i[\omega_i]^\times, \tag{4.1}$$

where $R_i \in SO(3)$ represents the orientation of the body-attached frame of agent i with respect to the inertial frame, and $\omega_i \in \mathbb{R}^3$ is the angular velocity of agent i measured in the body-attached frame. The measurement of the relative orientation between agent i and agent j is given by

$$R_{ij} := R_i^T R_j, \tag{4.2}$$

where $(i,j) \in \mathcal{E}$. Note that, according to the kinematic equation (4.1), the orientations of the agents are time-varying. However, for the sake of simplicity, the time argument t has been omitted from the above expression. Let the graph $\mathcal{G}$ describe the interaction between agents (the relative measurements and communication). To derive our results, the following assumptions are needed:

Assumption 4.1 *Each agent $i \in \mathcal{V}$ measures the relative orientations R_{ij} with respect to its neighboring agents $j \in \mathcal{N}_i$. In addition, each agent can also share information, through communication, with its neighbors.*

Assumption 4.2 *The interaction graph $\mathcal{G}$ is assumed to be an undirected tree.*

Assumption 4.3 *The body-frame angular velocity of each agent is bounded and available.*

Consider a network of n agents governed by the kinematic equation (4.1). Suppose Assumptions 4.1-4.3 are satisfied. Our objective consists in designing a distributed attitude estimation scheme endowed with global asymptotic stability guarantees. Since only relative attitude measurements are available, it should be understood that the goal is to globally estimate the orientation of each agent up to a common constant orientation. This common constant orientation can be determined if at least one agent has access to its own orientation, in which case, all the estimated orientations will converge to the actual orientations.

4.3 Distributed Attitude Estimation Using Relative Attitude Measurements

For $i \in \mathcal{V}$, we propose the following attitude observer on $SO(3)$:

$$\dot{\hat{R}}_i = \hat{R}_i \left[\omega_i - k_R \hat{R}_i^T \sigma_i \right]^\times , \tag{4.3}$$

where $k_R > 0$, $\hat{R}_i \in SO(3)$ is the estimate of R_i, and $\sigma_i \in \mathbb{R}^3$ is the correcting term that will be designated later. Let $\tilde{R}_i := R_i \hat{R}_i^T$ denote the absolute attitude error of agent i. In view of (4.1) and (4.3), one has

$$\dot{\tilde{R}}_i = k_R \tilde{R}_i [\sigma_i]^\times. \tag{4.4}$$

Consider an arbitrary orientation of the interaction graph $\mathcal{G}$. For every $(i, j) \in \mathcal{E}$, suppose that agent i and agent j are the head and tail, respectively, of the oriented edge connecting them, indexed by k. One can define the relative attitude error between them as $\bar{R}_k := \tilde{R}_j^T \tilde{R}_i$, where $\{k\} = \mathcal{M}_i^+ \cap \mathcal{M}_j^- \in \mathcal{M}$. From (4.4), one can derive the following dynamics for the relative attitude errors:

$$\dot{\bar{R}}_k = k_R \bar{R}_k [\bar{\sigma}_k]^\times, \tag{4.5}$$

where $\bar{\sigma}_k := \sigma_i - \bar{R}_k^T \sigma_j$. Note that, for every $i \in \mathcal{V}$ and $j \in \mathcal{N}_i$, the intersection between the sets $\mathcal{M}_i^+$ and $\mathcal{M}_j^-$ is either a set with a single element (if agent i and agent j are the head and tail, respectively, of the oriented edge connecting them) or an empty set otherwise. Let $\bar{\sigma} = [\bar{\sigma}_1^T, \bar{\sigma}_2^T, \ldots, \bar{\sigma}_m^T]^T \in \mathbb{R}^{3m}$ and $\sigma = [\sigma_1^T, \sigma_2^T, \ldots, \sigma_n^T]^T \in \mathbb{R}^{3n}$. One can verify that (Bai et al., 2008)

$$\bar{\sigma} = \boldsymbol{H}(t)^T \sigma, \tag{4.6}$$

where

$$\boldsymbol{H}(t) := [H_{ik}]_{3n \times 3m} \quad \text{with} \quad H_{ik} = \begin{cases} I_3 & k \in \mathcal{M}_i^+ \\ -\bar{R}_k & k \in \mathcal{M}_i^- \\ 0 & \text{otherwise} \end{cases}. \tag{4.7}$$

Note that the matrix $\boldsymbol{H}$ inherits some properties from the incidence matrix H such as the adjacency relationships in the graph and also the orientation that the graph enjoys. Note also that the arbitrary orientation assigned to the graph $\mathcal{G}$ is only a dummy orientation

introduced to simplify the process of the design and analysis of our proposed schemes and does not change the nature of the interaction graph $\mathcal{G}$ from being an undirected graph. It is clear that the matrix $\boldsymbol{H}$ depends on the interaction graph $\mathcal{G}$ and its orientation. Therefore, in the following lemma, we present an important property that $\boldsymbol{H}$ enjoys when the interaction graph $\mathcal{G}$ satisfies Assumption 4.2.

Lemma 4.1 *Consider the matrix $\boldsymbol{H}(t)$ obtained from the graph $\mathcal{G}$ with an arbitrary orientation of the edges, satisfying Assumption 4.2. Then, $\forall t \geq 0$, $\boldsymbol{H}(t)x = 0$ implies $x = 0$.*

Proof See Appendix B.1

Since the graph $\mathcal{G}$ is assumed to be an undirected tree, one can verify that the matrix $\boldsymbol{H}(t)$ is not a square matrix ($m = n-1$). Moreover, from Lemma 4.1, one can deduce that the matrix $\boldsymbol{H}(t)$ has a full column rank for all $t \geq 0$. This is instrumental in establishing the stability properties of our proposed distributed attitude observers.

In the sequel, we propose two attitude estimation schemes through an appropriate design of the correcting term σ_i. We will start with the continuous version of the observer in the next section.

4.3.1 Continuous Distributed Attitude Estimation Design

Consider the observer given in (4.3), with the following correcting term:

$$\sigma_i = - \sum_{j \in \mathcal{N}_i} \psi(A\hat{R}_j R_{ij}^T \hat{R}_i^T), \tag{4.8}$$

where $i \in \mathcal{V}$ and $A \in \mathbb{R}^{3 \times 3}$. Let $x := (\bar{R}_1, \bar{R}_2, \ldots, \bar{R}_m) \in \mathcal{S}$, with $\mathcal{S} := (SO(3))^m$. From (4.5)-(4.8), one can derive the following multi-agent closed-loop dynamics:

$$\dot{x} = f(x) \qquad x \in \mathcal{S}, \tag{4.9}$$

where

$$f(x) = \begin{bmatrix} f_1(x) \\ \vdots \\ f_m(x) \end{bmatrix} \quad \text{with} \quad f_k(x) = k_R \bar{R}_k [\bar{\sigma}_k]^\times.$$

The following assumption is needed for our developments:

Assumption 4.4 *A is a symmetric and positive definite matrix with three distinct eigenvalues.*

The following theorem provides the stability properties of the equilibrium points of (4.9):

Theorem 4.1 *Consider the attitude kinematics (4.1) with measurements (4.2) and observer (4.3) together with the correcting term (4.8), where Assumptions 4.1-4.4 are satisfied. Then, the following statements hold:*

i) *All solutions of (4.9) converge to the following set of equilibria:* $\Upsilon := \{x \in \mathcal{S} : \forall k \in \mathcal{M}, \ \psi(A\bar{R}_k) = 0\} = \mathcal{A} \cup \{x \in \mathcal{S} : \bar{R}_{\bar{m}} = I_3, \bar{R}_{\bar{n}} = UD_\beta U^T, \ \bar{m} \in \mathcal{M}^I, \ \bar{n} \in \mathcal{M}^\pi, \ \beta \in \{1,2,3\}\}$, *where* $\mathcal{A} := \{x \in \mathcal{S} : \forall k \in \mathcal{M}, \ \bar{R}_k = I_3\}$, $\mathcal{M}^I \cup \mathcal{M}^\pi = \mathcal{M}$, $|\mathcal{M}^\pi| > 0$, $|\mathcal{M}^I| \geq 0$, $D_1 = diag(1,-1,-1)$, $D_2 = diag(-1,1,-1)$, $D_3 = diag(-1,-1,1)$, *and* $U \in O(3)$ *such that* $A = U\Lambda U^T$ *with* $\Lambda = diag(\lambda_1, \lambda_2, \lambda_3)$ *and* $\lambda_1, \lambda_2, \lambda_3$ *are the distinct eigenvalues of* A.

ii) *The desired equilibrium set* $\mathcal{A}$, *for the closed-loop system (4.9), is locally asymptotically stable.*

iii) *The set of all undesired equilibrium points* $\Upsilon \setminus \mathcal{A}$ *is unstable and the desired equilibrium set* $\mathcal{A}$ *is AGAS for the closed-loop system (4.9).*

Proof See Appendix B.2

In contrast to (Lee and Ahn, 2016a; Lee and Ahn, 2016b; Van Tran et al., 2018; Lee et al., 2019; Li et al., 2020), our proposed continuous attitude observer, given in (4.3) and (4.8), can estimate time-varying orientations. Moreover, the estimated orientations provided by our proposed scheme are well-defined for any instant of time, which is not the case in (Van Tran et al., 2019; Lee et al., 2019; Li et al., 2020), since reliable attitude estimates are obtained only at the steady state. This makes our proposed distributed attitude estimation scheme a strong candidate for use in applications that require instantaneous orientations for feedback. However, as shown in the proof of Theorem 4.1, the trajectories of the closed-loop system (4.9) may converge to a level set containing the undesired equilibrium set $\Upsilon \setminus \mathcal{A}$. Unfortunately, due to the topological obstruction on $SO(3)$, there is no continuous time-invariant distributed attitude estimation scheme that guarantees global asymptotic stability of the desired equilibrium set $\mathcal{A}$ (Koditschek, 1989). Therefore, in the sequel, we will propose a hybrid distributed attitude estimation scheme endowed with global asymptotic stability.

4.3.2 Hybrid Distributed Attitude Estimation Design

The design of the correcting term (4.8) was based on the gradient of the smooth potential function $V_T(x)$ (see the proof of Theorem 4.1). However, this design does not guarantee global asymptotic stability of the desired equilibrium set $\mathcal{A}$, since the potential function $V_T(x)$ has more than one critical set ($\mathcal{A}$ and $\Upsilon \setminus \mathcal{A}$). It is well known that the design of gradient-based laws using smooth potential functions on $SO(3)$ leads to the aforementioned problem (Morse, 1934). This has motivated many authors to propose hybrid gradient-based solutions that ensure the existence of a unique global attractor (Mayhew and Teel, 2011b; Mayhew and Teel, 2011a; Mayhew and Teel, 2013; Berkane and Tayebi, 2017). The key idea in these solutions is to switch between a family of smooth potential functions via an appropriate switching mechanism, which leads to generating a non-smooth gradient with only one global attractor. Note that the construction of this family of smooth potential functions relies on the compactness assumption of the manifold. Therefore, the hybrid gradient-based solutions proposed in (Mayhew and Teel, 2011b; Mayhew and Teel, 2011a; Mayhew and Teel, 2013; Berkane and Tayebi, 2017)

are not applicable to non-compact manifolds such as $SE(3)$. Recently, the authors of (Wang and Tayebi, 2022) proposed a new hybrid scheme that relies only on one potential function parameterized by a scalar variable governed by an appropriately designed hybrid dynamics guaranteeing that the closed-loop dynamics a unique desired global attractor. In contrast to (Mayhew and Teel, 2011b; Mayhew and Teel, 2011a; Mayhew and Teel, 2013; Berkane and Tayebi, 2017), the hybrid scheme, given in (Wang and Tayebi, 2022), is easy to design and does not require any assumption about the compactness of the manifold.

4.3.2.1 Switching Mechanism Design for Multi-Agent Systems

Let $\mathcal{A}_h := \{x_h \in \mathcal{S}_h : \forall k \in \mathcal{M}, \ \bar{R}_k = I_3, \xi_k = 0\}$, where $x_h := (\bar{R}_1, \ldots, \bar{R}_m, \xi_1, \ldots, \xi_m) \in \mathcal{S}_h$ with $\mathcal{S}_h := SO(3)^m \times \mathbb{R}^m$. Consider the following potential function, inspired from (Wang and Tayebi, 2022), on $\mathcal{S}_h$, with respect to $\mathcal{A}_h$:

$$U_R(x_h) = \sum_{k=1}^{m} U(\bar{R}_k, \xi_k), \tag{4.10}$$

where $U : SO(3) \times \mathbb{R} \to \mathbb{R}_{\geq 0}$ is a potential function with respect to $(I_3, 0)$. The following set represents the set of all critical points of U_R:

$$\Upsilon_h := \{x_h \in \mathcal{S}_h : \forall k \in \mathcal{M}, \nabla_{\bar{R}_k} U_R = 0 \text{ and } \nabla_{\xi_k} U_R = 0\}, \tag{4.11}$$

where $\nabla_{\bar{R}_k} U_R$ and $\nabla_{\xi_k} U_R$ are the gradients of U_R with respect to $\bar{R}_k$ and ξ_k, respectively. The potential function U_R is chosen such that $\mathcal{A}_h \subset \Upsilon_h$. In what follows, inspired by (Wang and Tayebi, 2022), we will introduce an essential condition for our hybrid scheme design related to the potential function U_R.

Condition 4.1 *Consider the potential function* (4.10). *There exist a scalar $\delta > 0$ and a nonempty finite set $\Xi \subset \mathbb{R}$ such that for every $x_h \in \Upsilon_h \setminus \mathcal{A}_h$*

$$U(\bar{R}_k, \xi_k) - \min_{\bar{\xi}_k \in \Xi} U(\bar{R}_k, \bar{\xi}_k) > \delta, \tag{4.12}$$

for every $k \in \mathcal{M}$ such that $\bar{R}_k \neq I_3$.

Note that the set $\Upsilon_h \setminus \mathcal{A}_h$ denotes the set of all undesired critical points of U_R. Condition 4.1 plays a key role in the design of the hybrid scheme to be introduced shortly, since it implies that, at the undesired critical set $\Upsilon_h \setminus \mathcal{A}_h$, there will always exist $\bar{\xi}_k \in \Xi$, for every $k \in \mathcal{M}$, where $\bar{R}_k \neq I_3$, such that $U(\bar{R}_k, \bar{\xi}_k)$ is lower than $U(\bar{R}_k, \xi_k)$ by a constant gap δ. Thus, resetting the value of ξ_k to $\bar{\xi}_k$ will effectively steer the state away from the undesired critical set $\Upsilon_h \setminus \mathcal{A}_h$. This, together with an appropriate design of the vector field that ensures that U_R is non-increasing during the flows, will ensure global asymptotic stability of the desired equilibrium set $\mathcal{A}_h$.

Now, for every $i \in \mathcal{V}$ and $k \in \mathcal{M}_i^+$, we propose the following hybrid dynamics for ξ_k:

$$\underbrace{\dot{\xi}_k = - k_\xi \nabla_{\xi_k} U_R}_{x_h \in \mathcal{F}_i} \tag{4.13}$$

$$\underbrace{\xi_k^+ \in \begin{cases} \xi_k \text{ if } U(\bar{R}_k, \xi_k) - U(\bar{R}_k, \xi_k^*) \leq \delta \\ \xi_k^* \text{ if } U(\bar{R}_k, \xi_k) - U(\bar{R}_k, \xi_k^*) \geq \delta, \end{cases}}_{x_h \in \mathcal{J}_i} \tag{4.14}$$

where $k_\xi > 0$ and $\xi_k^* := \arg \min\limits_{\bar{\xi}_k \in \Xi} U(\bar{R}_k, \bar{\xi}_k)$. The flow set $\mathcal{F}_i$ and the jump set $\mathcal{J}_i$, for agent i, are defined as follows:

$$\mathcal{F}_i := \{x_h \in \mathcal{S}_h : \forall k \in \mathcal{M}_i^+, U(\bar{R}_k, \xi_k) - \min_{\bar{\xi}_k \in \Xi} U(\bar{R}_k, \bar{\xi}_k) \leq \delta\} \tag{4.15}$$

$$\mathcal{J}_i := \{x_h \in \mathcal{S}_h : \exists k \in \mathcal{M}_i^+, U(\bar{R}_k, \xi_k) - \min_{\bar{\xi}_k \in \Xi} U(\bar{R}_k, \bar{\xi}_k) \geq \delta\}. \tag{4.16}$$

It is important to note that for each $i \in \mathcal{V}$, both the flow set $\mathcal{F}_i$ and the jump set $\mathcal{J}_i$ are distributed. In other words, for each $i \in \mathcal{V}$, the definition of both sets, namely $\mathcal{F}_i$ and $\mathcal{J}_i$, considers only the edges connecting agent i, where i is the head of these oriented edges, with its neighbors $j \in \mathcal{N}_i$. Now, let $\xi := [\xi_1, \xi_2, \ldots, \xi_m]^T \in \mathbb{R}^m$, from (4.13)-(4.14), one obtains the following hybrid dynamics:

$$\mathcal{H}_\xi : \begin{cases} \dot{\xi} = F_\xi(x_h) & x_h \in \mathcal{F} \\ \xi^+ \in G_\xi(x_h) & x_h \in \mathcal{J} \end{cases} \tag{4.17}$$

where

$$\mathcal{F} := \bigcap_{i=1}^n \mathcal{F}_i, \qquad \mathcal{J} := \bigcup_{i=1}^n \mathcal{J}_i, \tag{4.18}$$

and

$$F_\xi(x_h) = \begin{bmatrix} -k_\xi \nabla_{\xi_1} U_R \\ \vdots \\ -k_\xi \nabla_{\xi_m} U_R \end{bmatrix}, \; G_\xi(x_h) = \begin{bmatrix} \{\xi_1, \xi_1^*\} \\ \vdots \\ \{\xi_m, \xi_m^*\} \end{bmatrix}.$$

Based on the definition of the jump set $\mathcal{J}$, one can verify that the set of all undesired critical points belongs to the jump set $\mathcal{J}$, i.e., $\Upsilon_h \setminus \mathcal{A}_h \subset \mathcal{J}$. Also, in view of the jump map $G_\xi(x_h)$, one can check that, if $x_h \in \mathcal{J}$, there exits $k \in \mathcal{M}$ such that $U(\bar{R}_k, \xi_k) - U(\bar{R}_k, \xi_k^*) \geq \delta$, which ensures that U_R decreases at least by δ after each jump.

4.3.2.2 Generic Hybrid Distributed Attitude Observer Design

For every $i \in \mathcal{V}$, we propose the following distributed non-smooth gradient-based correcting scheme:

$$\sigma_i = \sum_{l \in \mathcal{M}_i^-} \bar{R}_l \psi \left(\bar{R}_l^T \nabla_{\bar{R}_l} U_R \right) - \sum_{p \in \mathcal{M}_i^+} \psi \left(\bar{R}_p^T \nabla_{\bar{R}_p} U_R \right) \tag{4.19}$$

$$\underbrace{\dot{\xi}_k = - k_\xi \nabla_{\xi_k} U_R}_{x_h \in \mathcal{F}_i}$$

$$\underbrace{\xi_k^+ \in \begin{cases} \xi_k & \text{if } U(\bar{R}_k, \xi_k) - U(\bar{R}_k, \xi_k^*) \leq \delta \\ \xi_k^* & \text{if } U(\bar{R}_k, \xi_k) - U(\bar{R}_k, \xi_k^*) \geq \delta, \end{cases}}_{x_h \in \mathcal{J}_i} \tag{4.20}$$

where $k \in \mathcal{M}_i^+$. Moreover, given the above expression of σ_i, for every $i \in \mathcal{V}$, together with equation (4.6), one can verify that

$$\bar{\sigma} = -\boldsymbol{H}^T \boldsymbol{H} \, \Psi_{\nabla}^{\bar{R}}, \tag{4.21}$$

where

$$\Psi_{\nabla}^{\bar{R}} := \left[\psi \left(\bar{R}_1^T \nabla_{\bar{R}_1} U_R \right)^T, \psi \left(\bar{R}_2^T \nabla_{\bar{R}_2} U_R \right)^T, \ldots, \psi \left(\bar{R}_m^T \nabla_{\bar{R}_m} U_R \right)^T \right]^T \in \mathbb{R}^{3m},$$

and the block matrix $\boldsymbol{H}$ is given in (4.7). The matrix $\boldsymbol{H}^T \boldsymbol{H}$ is positive definite according to Lemma 4.1. Next, we will establish the stability property of the desired equilibrium set $\mathcal{A}_h$ under the distributed non-smooth gradient-based correcting term (4.19)-(4.20). In view of (4.4)-(4.6) and (4.19)-(4.21), one can derive the following multi-agent hybrid closed-loop dynamics:

$$\mathcal{H} : \begin{cases} \dot{x}_h = F(x_h) & x_h \in \mathcal{F} \\ x_h^+ \in G(x_h) & x_h \in \mathcal{J} \end{cases} \tag{4.22}$$

where

$$F(x_h) = \begin{bmatrix} k_R \bar{R}_1 [\bar{\sigma}_1]^{\times} \\ \vdots \\ k_R \bar{R}_m [\bar{\sigma}_m]^{\times} \\ -k_{\xi} \nabla_{\xi_1} U_R \\ \vdots \\ -k_{\xi} \nabla_{\xi_m} U_R \end{bmatrix}, \quad G(x_h) = \begin{bmatrix} \bar{R}_1 \\ \vdots \\ \bar{R}_m \\ \{\xi_1, \xi_1^*\} \\ \vdots \\ \{\xi_m, \xi_m^*\} \end{bmatrix}.$$

The flow map $\mathcal{F}$ and the jump map $\mathcal{J}$ are defined in (4.18). It is worth noting that the hybrid closed-loop system (4.22) is autonomous.

Remark 4.1 *According to the flow map $F(x_h)$, the dynamics of the state x_h flow along a negative direction of the gradient of U_R, driving the state x_h towards the critical points of U_R during the flow. However, the jump map $G(x_h)$ pushes the state x_h away from the undesired critical set $\Upsilon_h \setminus \mathcal{A}_h$, which leaves the desired critical set $\mathcal{A}_h$ as a global attractor to our proposed distributed hybrid correcting scheme.*

Before proceeding with the stability analysis, it is important to verify that system (4.22) is well-posed[1]. This involves showing that the hybrid closed-loop system (4.22) satisfies the hybrid basic conditions (Goebel et al., 2012, Assumption 6.5).

Lemma 4.2 *The hybrid closed-loop system (4.22) satisfies the hybrid basic conditions introduced in Section 2.6.2.*

---

[1]See (Goebel et al., 2012, Definition 6.2) for the definition of well-posedness.

Proof See Appendix B.3

In the following theorem, we will establish the stability properties of the multi-agent hybrid closed-loop system (4.22).

Theorem 4.2 *Let $k_R, k_\xi > 0$ and suppose that Assumptions 4.1, 4.2 and Condition 4.1 hold. Then, the set $\mathcal{A}_h$ is globally asymptotically stable for the multi-agent hybrid closed-loop system (4.22) and the number of jumps is finite.*

Proof See Appendix B.4

Remark 4.2 *Note that the design of our proposed hybrid distributed attitude observer (4.3), (4.19)-(4.20) is based on a generic potential function U_R, defined on $\mathcal{S}_h$, with respect to $\mathcal{A}_h$. It is also important to note that the flow set $\mathcal{F}$ and the jump set $\mathcal{J}$, given in (4.18), depend on the parameters δ and Ξ. These parameters, along with the potential function U_R, must be carefully designed to satisfy Condition 4.1.*

In the next section, we will provide the explicit structure of our proposed hybrid estimation scheme by first introducing the potential function and specifying the set of parameters $\mathcal{P}$ such as Condition 4.1 is satisfied. We then provide the explicit form of our proposed hybrid distributed attitude observer in terms of relative attitude measurements and attitude estimates.

4.3.2.3 Explicit Hybrid Distributed Attitude Observer Design Using Relative Attitude Measurements

Let us begin this section by introducing the potential function U_R and some useful related properties. Consider the potential function $U_R(x_h)$, given in (4.10), where $U(\bar{R}_k, \xi_k)$ is defined as follows:

$$U(\bar{R}_k, \xi_k) := \text{tr}\Big(A \left(I_3 - \bar{R}_k \mathcal{R}_\alpha(\xi_k, u) \right) \Big) + \frac{\gamma}{2}\xi_k^2, \tag{4.23}$$

with $A \in \mathbb{R}^{3 \times 3}$ is a positive definite matrix with three distinct eigenvalues, $u \in \mathbb{S}^2$ is a constant unit vector and γ is a positive scalar. Note that U_T is an extension of the potential function $U(R_e, \theta)$ proposed in (Wang and Tayebi, 2022) for a single agent attitude control design. In the following proposition, we will derive the gradient of U_R with respect to $\bar{R}_k$ and ξ_k and give the set of all its critical points.

Proposition 4.1 *Consider the potential function $U_R(x_h) = \sum_{k=1}^{m} U(\bar{R}_k, \xi_k)$, where U given in (4.23) and Assumption 4.4 is satisfied. Then, the following statements hold:*

- $\psi\left(\bar{R}_k^T \nabla_{\bar{R}_k} U_R\right) = \mathcal{R}_\alpha(\xi_k, u)\psi(A\bar{R}_k\mathcal{R}_\alpha(\xi_k, u))$ *for all $k \in \mathcal{M}$.*

- $\nabla_{\xi_k} U_R = \gamma\xi_k + 2u^T\psi(A\bar{R}_k\mathcal{R}_\alpha(\xi_k, u))$ *for all $k \in \mathcal{M}$.*

- $\Upsilon_h = \{x_h \in \mathcal{S}_h : \forall k \in \mathcal{M}, \ \mathbb{P}_a(A\bar{R}_k) = 0, \xi_k = 0\}$.

- $\mathcal{A}_h \subset \Upsilon_h$.

Proof See Appendix B.5

Remark 4.3 *Note that the expressions for the gradients of U_R with respect to $\bar{R}_k$ and ξ_k, given in Proposition 4.1, are derived in terms of the relative attitude errors $\bar{R}_k$ which can be constructed from the relative orientation measurements (4.2) and the estimated orientations as follows: $\bar{R}_k = \hat{R}_j R_{ij}^T \hat{R}_i^T$, with $(i,j) \in \mathcal{E}$ and $\mathcal{M}_i^+ \cap \mathcal{M}_j^- = \{k\}$.*

Consider the set of parameters $\mathcal{P} := \{\Xi, A, u, \gamma, \delta\}$. The next proposition gives the possible choices for the parameters in the set $\mathcal{P}$ such that Condition 4.1 is satisfied.

Proposition 4.2 *Consider the potential function U_R. Then, Condition 4.1 holds under the following set of parameters $\mathcal{P}$:*

$$\mathcal{P} : \begin{cases} \Xi = \{|\xi_i| \in (0, \pi], i = 1, \cdots, l\} \\ A : 0 < \lambda_1 \leq \lambda_2 < \lambda_3 \\ u = \alpha_1 q_1 + \alpha_2 q_2 + \alpha_3 q_2 \\ \gamma < \frac{4\Delta^*}{\pi^2} \\ 0 < \delta < \left(\frac{4\Delta^*}{\pi^2} - \gamma\right) \frac{\xi_L^2}{2}, \xi_L := \max_{\xi \in \Xi} |\xi| \end{cases} \tag{4.24}$$

where $\alpha_1^2 + \alpha_2^2 + \alpha_3^2 = 1$ and $\Delta^* > 0$ are given as follows:

- *If $\lambda_1 = \lambda_2$, $\alpha_3^2 = 1 - \frac{\lambda_2}{\lambda_3}$ and $\Delta^* = \lambda_1(1 - \frac{\lambda_2}{\lambda_3})$.*

- *If $\lambda_2 \geq \frac{\lambda_1 \lambda_3}{\lambda_3 - \lambda_1}$, $\alpha_i^2 = \frac{\lambda_i^A}{\lambda_2 + \lambda_3}, i \in \{2, 3\}$ and $\Delta^* = \lambda_1$.*

- *If $\lambda_1 < \lambda_2 < \frac{\lambda_1 \lambda_3}{\lambda_3 - \lambda_1}$, $\alpha_i^2 = 1 - \frac{4 \prod_{l \neq i} \lambda_l}{\sum_{l=1}^3 \sum_{k \neq l}^3 \lambda_l \lambda_k}, \forall i \in \{1, 2, 3\}$, and $\Delta^* = \frac{4 \prod_l \lambda_l}{\sum_{l=1}^3 \sum_{k \neq l}^3 \lambda_l \lambda_k}$.*

where (λ_i, q_i) denotes the i-th pair of eigenvalue-eigenvector of matrix A.

Proof The proof is omitted as it can be easily established following the same arguments of the proof of (Wang and Tayebi, 2022, Proposition 2).

Let us conclude this section by giving the explicit form of our proposed hybrid distributed attitude estimation scheme. From Proposition 4.1, Proposition 4.2, and the fact in Remark 4.3, one can explicitly express the hybrid distributed attitude observer, given in (4.3) and (4.19)-(4.20), in terms of the relative attitude measurements and the attitude estimates as follows:

$$\begin{aligned} \dot{\hat{R}}_i &= \hat{R}_i[\omega_i - k_R \hat{R}_i^T \sigma_i]^\times \\ \dot{\xi}_k &= -k_\xi \left(\gamma \xi_k + 2u^T \psi\left(A\bar{R}_k \mathcal{R}_a(\xi_k, u)\right)\right) \\ \sigma_i &= -\underbrace{\left(\sum_{j \in \mathcal{I}_i} \mathcal{R}_a(\xi_p, u)\psi(A\hat{R}_j R_{ij}^T \hat{R}_i^T \mathcal{R}_a(\xi_p, u)) + \sum_{j \in \mathcal{O}_i} \psi(A\mathcal{R}_a(\xi_l, u)^T \hat{R}_j R_{ij}^T \hat{R}_i^T)\right)}_{x_h \in \mathcal{F}_i} \end{aligned} \tag{4.25}$$

$$\hat{R}_i^+ = \hat{R}_i$$

$$\xi_k^+ \in \underbrace{\begin{cases} \xi_k & \text{if} \quad U(\bar{R}_k, \xi_k) - U(\bar{R}_k, \xi_k^*) \leq \delta \\ \xi_k^* & \text{if} \quad U(\bar{R}_k, \xi_k) - U(\bar{R}_k, \xi_k^*) \geq \delta \end{cases}}_{x_h \in \mathcal{J}_i} \tag{4.26}$$

where $i \in \mathcal{V}$, $k \in \mathcal{M}_i^+$, $\{p\} = \mathcal{M}_i^+ \cap \mathcal{M}_j^- \in \mathcal{M}$, $\{l\} = \mathcal{M}_i^- \cap \mathcal{M}_j^+ \in \mathcal{M}$. Note that $\mathcal{N}_i = \mathcal{I}_i \cup \mathcal{O}_i$, with $\mathcal{I}_i := \{j \in \mathcal{N}_i : j \text{ is the tail of the edge } (i,j) \in \mathcal{E}\}$ and $\mathcal{O}_i := \{j \in \mathcal{N}_i : j \text{ is the head of the edge } (i,j) \in \mathcal{E}\}$. Recall that the flow set $\mathcal{F}_i$ and the jump set $\mathcal{J}_i$, for every $i \in \mathcal{V}$, are given in (4.15) and (4.16), respectively.

Remark 4.4 *For the implementation of our proposed hybrid distributed attitude observer* (4.25)-(4.26)*, we assume that the dynamics of ξ_k are implemented at agent i, and agent j receives the information about ξ_k from agent i, according to Assumption 4.1, for every* $(i,j) \in \mathcal{E}$ *such that $\{k\} = \mathcal{M}_i^+ \cap \mathcal{M}_j^-$.*

In the following section, we will leverage the proposed hybrid distributed attitude estimation scheme (4.25)-(4.26) for the design a distributed pose estimation using relative attitude and bearing Measurements. The key idea consists in expressing the local relative (time-varying) bearing measurements in the inertial frame, using the estimated attitudes obtained from (4.25)-(4.26), so they can be used, together with linear velocity measurements, in the position estimation scheme.

4.4 Distributed Pose Estimation Using Relative Attitude and Bearing Measurements

In this section, we consider the problem of distributed pose estimation for multi-agent rigid-body systems where the agents are allowed to have simultaneous translational and rotational motion. Using the hybrid distributed attitude observer (4.25)-(4.26), we propose a hybrid distributed position estimation scheme that relies on the relative attitude and bearing measurements as well as the individual angular and linear velocity measurements. In contrast to Section 3.3, the resulting overall hybrid distributed pose estimation scheme globally estimates the poses of the agents up to a constant translation and orientation which can be determined if there is at least one agent that measures its absolute orientation and position. Before presenting our proposed observer, let us first formally state the problem at hand.

Consider a group of rigid body systems governed by the rotational kinematic equation (4.1) and the following translational kinematic equation:

$$\dot{p}_i = v_i, \tag{4.27}$$

where $p_i \in \mathbb{R}^3$ and $v_i \in \mathbb{R}^3$ are the position and velocity of agent i, respectively, expressed in the inertial frame and $i \in \mathcal{V}$. Let $p := \begin{bmatrix} p_1^T, p_2^T, \ldots, p_n^T \end{bmatrix}^T \in \mathbb{R}^{3n}$. The graph $\mathcal{G}$ together with the stack position vector p define the formation $\mathcal{G}(p(t))$.

The measurement of the local relative bearing between agent i and agent j is given by

$$b_{ij}^i(t) := R_i^T b_{ij}(t), \tag{4.28}$$

where $b_{ij}(t) := \frac{p_j(t)-p_i(t)}{||p_j(t)-p_i(t)||}$ and $b_{ij}^i(t)$ are the relative bearing measurements between agent i and agent j expressed in the inertial frame and the body-attached frame of agent i, respectively. Recall that the agents orientations are time-varying, but for the sake of simplicity, the time argument t is omitted in the expression of R_i in (4.28). Next, we will introduce some important definitions and assumptions.

Definition 4.1 *(Tang et al., 2020b) Consider the formation $\mathcal{G}(p(t))$ with an arbitrary orientation of the graph $\mathcal{G}$. Define the matrix $\boldsymbol{L}$ and bearing Laplacian matrix $\boldsymbol{L}_B$ as $\boldsymbol{L} := L \otimes I_3$ and $\boldsymbol{L}_B(t) := \boldsymbol{H}diag(P_{b_k(t)})\boldsymbol{H}^T$, respectively, where b_k is the bearing vector corresponding to the edge k, and $\boldsymbol{H} = H \otimes I_3$ $\big(H$ and L are the incidence and the Laplacian matrices, respectively, corresponding to the graph $\mathcal{G}\big)$. The bearing Laplacian matrix is called persistently exciting (PE) if there exists $T > 0$ and $\mu > 0$ such that:*

$$\int_t^{t+T} \boldsymbol{L}_B(\tau)d\tau \geq \mu\boldsymbol{L}, \tag{4.29}$$

for all $t \geq 0$.

Definition 4.2 *(Tang et al., 2020b) The formation $\mathcal{G}(p(t))$ is BPE if the graph $\mathcal{G}$ is connected and its bearing Laplacian matrix is PE.*

Assumption 4.5 *Each agent i in the formation measures the local relative bearings b_{ij}^i with respect to its neighboring agents $j \in \mathcal{N}_i$.*

Assumption 4.6 *The formation $\mathcal{G}(p(t))$ is bearing persistently exciting.*

Assumption 4.7 *As the formation evolves over time, there is no collision between agents.*

Assumption 4.8 *The body-frame linear velocity of each agent is bounded and available for measurement by the agent.*

Consider a network of n rigid-body agents governed by the pose kinematic equations (4.1) and (4.27), where Assumptions 4.1-4.8 are satisfied. Our objective is to design a distributed position observer cascaded with the hybrid distributed attitude observer (4.25)-(4.26) such that the resulting distributed pose estimation scheme is endowed with global asymptotic stability guarantees.

Remark 4.5 *Note that, unlike Section 3.3, the proposed observer will estimate the agents' poses up to a constant translation and orientation which can be determined if at least one agent has access to its absolute pose.*

Now, let us proceed with the observer design. Considering the hybrid distributed attitude observer (4.25)-(4.26), we propose the following hybrid distributed position estimation law:

$$\dot{\hat{p}}_i = \underbrace{\hat{R}_i v_i^i - k_p \sum_{j \in \mathcal{N}_i} \hat{R}_i \left(P_{b_{ij}^i(t)} \hat{R}_i^T \hat{p}_i - R_{ij} P_{b_{ji}^j(t)} \hat{R}_j^T \hat{p}_j \right) - k_R [\sigma_i]^\times \hat{p}_i}_{x_h \in \mathcal{F}_i} \tag{4.30}$$

$$\underbrace{\hat{p}_i^+ = \hat{p}_i}_{x_h \in \mathcal{J}_i} \tag{4.31}$$

where $i \in \mathcal{V}$, $k_p > 0$, $\hat{p}_i \in \mathbb{R}^3$ is the estimate of p_i and v_i^i is the body-frame linear velocity of agent i. Under Assumption 4.7, one has $||p_i - p_j|| \neq 0$ and consequently the bearing measurement $b_{ij}^i(t)$, for every $(i,j) \in \mathcal{E}$, is well defined for all $t \geq 0$. Using the facts that $v_i^i = R_i^T v_i$ and $P_{b_{ij}^i(t)} = R_i^T P_{b_{ij}(t)} R_i$, it follows from (4.30) that the position estimate $\hat{p}_i$ of each agent $i \in \mathcal{V}$, during the flows, can be rewritten as follows:

$$\dot{\hat{p}}_i = \tilde{R}_i^T v_i - k_p \tilde{R}_i^T \sum_{j \in \mathcal{N}_i} P_{b_{ij}(t)} \left(\tilde{R}_i \hat{p}_i - \tilde{R}_j \hat{p}_j \right) - k_R [\sigma_i]^\times \hat{p}_i. \tag{4.32}$$

Define the position estimation error as $\tilde{p}_i := \tilde{R}_i \hat{p}_i - p_i$, for every $i \in \mathcal{V}$. In view of (4.27), (4.4) and (4.32), the time derivative of $\tilde{p}_i$ is given by the following hybrid dynamics:

$$\underbrace{\dot{\tilde{p}}_i = k_p \sum_{j \in \mathcal{N}_i} P_{b_{ij}(t)} (\tilde{p}_j - \tilde{p}_i)}_{x_h \in \mathcal{F}_i} \tag{4.33}$$

$$\underbrace{\tilde{p}_i^+ = \tilde{p}_i}_{x_h \in \mathcal{J}_i} \tag{4.34}$$

for every $i \in \mathcal{V}$. Equations (4.33) and (4.34) were obtained using the fact that $P_{b_{ij}}(p_j - p_i) = 0$ and $\tilde{p}^+ = \tilde{R}_i^+ \hat{p}_i^+ - p_i = \tilde{R}_i \hat{p}_i - p_i = \tilde{p}_i$, respectively. In view of the definition of the position estimation error $\tilde{p}_i$, we were able to derive the above hybrid distributed estimation error dynamics independent of the attitude estimates provided by the hybrid attitude observer (4.25)-(4.26). Now, let $e_i := \tilde{p}_i - \frac{1}{n} \sum_{q=1}^n \tilde{p}_q(0)$, it follows from (4.33)-(4.34) that

$$\underbrace{\dot{e}_i = k_p \sum_{j \in \mathcal{N}_i} P_{b_{ij}(t)} (e_j - e_i)}_{x_h \in \mathcal{F}_i} \tag{4.35}$$

$$\underbrace{e_i^+ = e_i}_{x_h \in \mathcal{J}_i} \tag{4.36}$$

Define the new state space $\bar{\mathcal{S}}_h := SO(3)^m \times \mathbb{R}^m \times \mathbb{R}^{3n} \times \mathbb{R}$ and the new state $\bar{x}_h := \left(\bar{R}_1, \ldots, \bar{R}_m, \xi_1, \ldots, \xi_m, e_1, \ldots, e_n, t \right) \in \bar{\mathcal{S}}_h$. From (4.22), (4.25)-(4.26) and (4.35)-(4.36),

one obtains the following extended hybrid multi-agent closed-loop system:

$$\bar{\mathcal{H}} : \begin{cases} \dot{\bar{x}}_h = \bar{F}(\bar{x}_h) & \bar{x}_h \in \bar{\mathcal{F}} \\ \bar{x}_h^+ \in \bar{G}(\bar{x}_h) & \bar{x}_h \in \bar{\mathcal{J}} \end{cases} \tag{4.37}$$

where $\bar{\mathcal{F}} := \{\bar{x}_h \in \bar{\mathcal{S}}_h : \ x_h \in \mathcal{F}\}$ and where $\bar{\mathcal{J}} := \{\bar{x}_h \in \bar{\mathcal{S}}_h : \ x_h \in \mathcal{J}\}$, and the flow and jump maps are given by

$$\bar{F}(\bar{x}_h) := \begin{bmatrix} k_R \bar{R}_1 [\bar{\sigma}_1]^\times \\ \vdots \\ k_R \bar{R}_m [\bar{\sigma}_m]^\times \\ -k_\xi \left(\gamma \xi_1 + 2u^T \psi \left(A \bar{R}_1 \mathcal{R}_a(\xi_1, u)\right)\right) \\ \vdots \\ -k_\xi \left(\gamma \xi_m + 2u^T \psi \left(A \bar{R}_m \mathcal{R}_a(\xi_m, u)\right)\right) \\ k_p \sum_{j \in \mathcal{N}_1} P_{b_{1j}(t)}(e_j - e_1) \\ \vdots \\ k_p \sum_{j \in \mathcal{N}_n} P_{b_{nj}(t)}(e_j - e_n) \\ 1 \end{bmatrix} \quad \text{and} \quad \bar{G}(\bar{x}_h) := \begin{bmatrix} \bar{R}_1 \\ \vdots \\ \bar{R}_m \\ \{\xi_1, \xi_1^*\} \\ \vdots \\ \{\xi_m, \xi_m^*\} \\ e_1 \\ \vdots \\ e_n \\ t \end{bmatrix}.$$

Recall that $\bar{\sigma} = \boldsymbol{H}^T \sigma$ where σ_i, for every $i \in \mathcal{V}$, is given in (4.25), $\xi_k^* := \operatorname*{argmin}_{\bar{\xi}_k \in \Xi} U(\bar{R}_k, \bar{\xi}_k)$, and the maps $\mathcal{F}$ and $\mathcal{J}$ are defined in (4.18). Note that, since the relative bearings are time-varying, we consider the time t as an additional state variable to make the overall system (4.37) autonomous. Note also that $\bar{\mathcal{F}} \cup \bar{\mathcal{J}} = \bar{\mathcal{S}}_h$.

Lemma 4.3 *The hybrid closed-loop system* (4.37) *satisfies the hybrid basic conditions introduced in Section 2.6.2.*

Proof The proof is established using the same arguments as in the proof of Lemma 4.2 and hence omitted here.

Now, let us state the main result of this section.

Theorem 4.3 *Consider the hybrid closed-loop system* (4.37) *with* $k_R, k_\xi, k_p > 0$. *Let Assumptions 4.1-4.8 and Condition 4.1 hold. Then, the set* $\bar{\mathcal{A}}_h := \{\bar{x}_h \in \bar{\mathcal{S}}_h : \ \bar{R}_1 = I_3, \ldots, \bar{R}_m = I_3, \xi_1 = 0, \ldots, \xi_m = 0, e_1 = 0, \ldots, e_n = 0\}$ *is globally asymptotically stable and the number of jumps is finite.*

Proof See Appendix B.6

Remark 4.6 *Note that the result in Theorem 4.3 implies that the poses of the n agents can be estimated up to a constant translation and orientation. This constant translation and orientation can be determined if at least one agent in the formation has access to its absolute attitude and position (i.e., having a leader in the group), in which case the poses of the agents can be estimated without ambiguity.*

Unlike most existing works (*e.g.*, (Li et al., 2020; Lee et al., 2019; Zhao and Zelazo, 2016)), our proposed bearing-based hybrid distributed position estimation scheme can globally estimate the individual poses of the multi-agent rigid-body system subjected to time-varying translational and rotational motion. Furthermore, in contrast to (Tang et al., 2020b; Tang et al., 2020a), our scheme relies on local time-varying bearing measurements. This is made possible by the hybrid distributed attitude observer (4.25)-(4.26), which was instrumental in designing this scheme with a global stability result.

4.5 Simulation Results

In this section, we will present some numerical simulations to investigate the performance of the continuous attitude observer (4.3), (4.8), the hybrid attitude observer (4.25)-(4.26), as well as the hybrid distributed position estimation law (4.30)-(4.31).

In these simulations, we consider a five-agent rigid-body system in a three-dimensional space that forms a square pyramid rotating around the z-axis (see Figure 4.1) with the following positions: $p_i(t) = R^T(t)p_i(0)$ where $R(t) = [\cos\frac{\pi}{6}t \ -\sin\frac{\pi}{6}t \ 0; \ \sin\frac{\pi}{6}t \ \cos\frac{\pi}{6}t \ 0; \ 0\ 0\ 1]$, $p_1(0) = [-2 \ -2 \ -2]^T$, $p_2(0) = [2 \ -2 \ -2]^T$, $p_3(0) = [-2\ 2\ -2]^T$, $p_4(0) = [2\ 2\ -2]^T$ and $p_5(0) = [0\ 0\ 0]^T$. The agents rotational motions are driven by the following angular velocities: $\omega_1 = [1 \ -2 \ 1]^T$, $\omega_2(t) = [-\cos 3t \ 1 \ \sin 2t]^T$, $\omega_3(t) = [-\cos t \ 1 \ \sin 2t]^T$, $\omega_4(t) = [-\cos 2t \ 1 \ \sin 5t]^T$ and $\omega_5 = [1.5\ 4\ 5]^T$, where the initial agents rotations are chosen to be the identity, *i.e.*, $R_i(0) = I_3$, for every $i \in \mathcal{V}$.
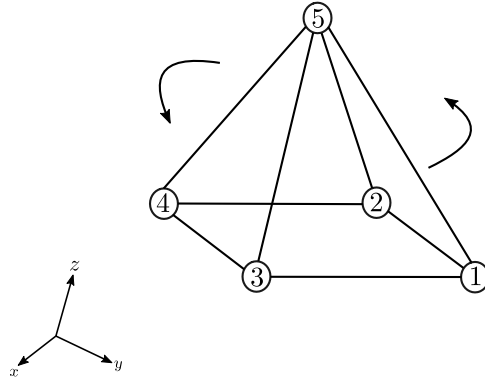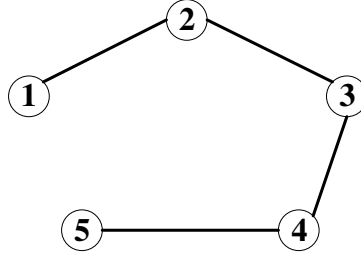

Figure 4.1: Five-agent network in $\mathbb{R}^3$.

We use an undirected graph topology to describe the interactions between the agents (see Figure 4.2). Accordingly, the neighbors sets are given as $\mathcal{N}_1 = \{2\}$, $\mathcal{N}_2 = \{1,3\}$, $\mathcal{N}_3 = \{2,4\}$, $\mathcal{N}_4 = \{3,5\}$ and $\mathcal{N}_5 = \{4\}$.

Figure 4.2: The interaction graph $\mathcal{G}$.

We assign an arbitrary orientation to the graph $\mathcal{G}$ and we index each oriented edge with a number as it is shown in Figure 4.3. The attitude initial conditions, for both observers (4.3), (4.8) and (4.25)-(4.26), are chosen as $\hat{R}_1(0) = \mathcal{R}_\alpha(-\frac{\pi}{2}, v)$, $\hat{R}_2(0) = \mathcal{R}_\alpha(\frac{\pi}{2}, v)$, $\hat{R}_3(0) = \mathcal{R}_\alpha(-\frac{\pi}{2}, v)$, $\hat{R}_4(0) = \mathcal{R}_\alpha(\frac{\pi}{2}, v)$ and $\hat{R}_5(0) = \mathcal{R}_\alpha(-\frac{\pi}{2}, v)$, with $v = [0\ 0\ 1]^T$. In addition, for the *Hybrid observer*, we choose the following initial conditions for the auxiliary variables: $\xi_k(0) = 0$, $k \in \{1, 2, 3, 4\}$. Note that, according to these initial conditions, one has $\bar{R}_k(0) = \mathcal{R}_\alpha(\pi, v)$ and $\xi_k(0) = 0$, $k = \{1, 2, 3, 4\}$, which implies that $x(0) \in \Upsilon \setminus \mathcal{A}$ and $x_h(0) \in \Upsilon_h \setminus \mathcal{A}_h$. The parameters of the set $\mathcal{P}$ are selected as follows: $\Xi = \{0.08\pi\}$, $A = \text{diag}([5, 8.57, 12])$, $\gamma = 1.9251$, $\delta = 0.0030$, $u = [0\ 0.6455\ 0.7638]^T$ and $\Delta^* = 5$. For the gain parameters, we pick: $k_R = 1.1$ and $k_\xi = 3.5$. To simulate the *Hybrid observer*, we have used the HyEQ Toolbox (Sanfelice et al., 2013). Figure 4.4 and Figure 4.5 depict
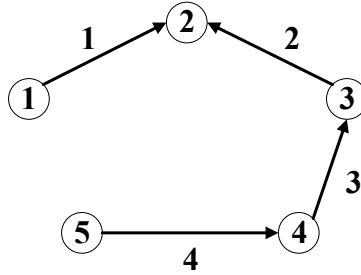
Figure 4.3: The interaction graph $\mathcal{G}$ with an orientation.

the time evolution of the relative attitude error norms $|\bar{R}_k(t)|_I$, for both observers (4.3), (4.8) and (4.25)-(4.26), and the auxiliary variables $\xi_k(t)$, $k = \{1, 2, 3, 4\}$, respectively, associated with each edge. Notice that, at $t = 0$, the variables $\xi_k(t)$, $k = \{1, 2, 3, 4\}$, jump from 0 to 0.08π and then converge to zero as $t \to \infty$. Also, the relative attitude error norms $|\bar{R}_k(t)|_I$, for both observers, converge to zero as $t \to \infty$.

Figure 4.4: Time evolution of the relative attitude error norm, associated with each edge, for the *Continuous observer* and the *Hybrid observer*.
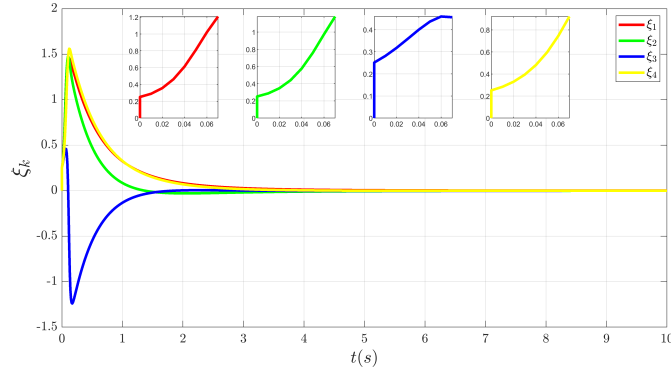
Figure 4.5: Time evolution of the hybrid variable ξ_k associated with each edge.

Remark 4.7 *To study the relationship between the choice of the matrix A and the convergence rate of our proposed schemes, we conducted a series of simulations with different choices of A in Matlab. It is observed that the convergence rates increase when the eigenvalues of A are increased.*

In the second simulation, we assume that the measurements are subjected to noise. The noisy measurements of the attitude and the angular velocity are given as $R_{ij}^n = R_{ij}\exp([n_R]^\times)$ and $\omega_i^n = \omega_i + n_\omega$, respectively, for every $i \in \mathcal{V}$ and $j \in \mathcal{N}_i$, where n_R and n_ω are additive white Gaussian noise with zero mean and a variance of 0.01. We consider the same initial conditions and observer parameters as in the previous simulation. Figure 4.6 and Figure 4.7 illustrate the time evolution of the relative attitude error norms

$|\bar{R}_k(t)|_I$, for both schemes, and the auxiliary variables $\xi_k(t)$, $k = \{1, 2, 3, 4\}$, respectively, associated with each edge.
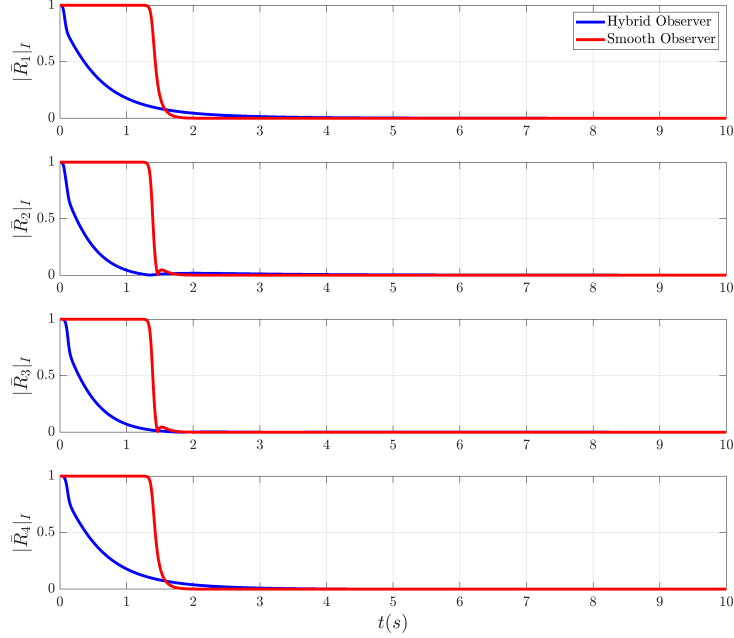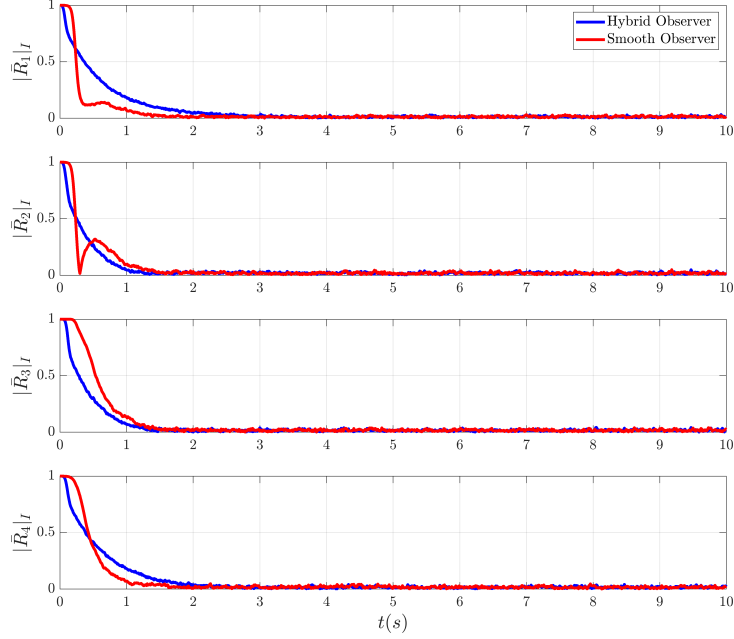

Figure 4.6: Time evolution of the relative attitude error norm, associated with each edge, for the *Continuous observer* and the *Hybrid observer* using noisy measurements.
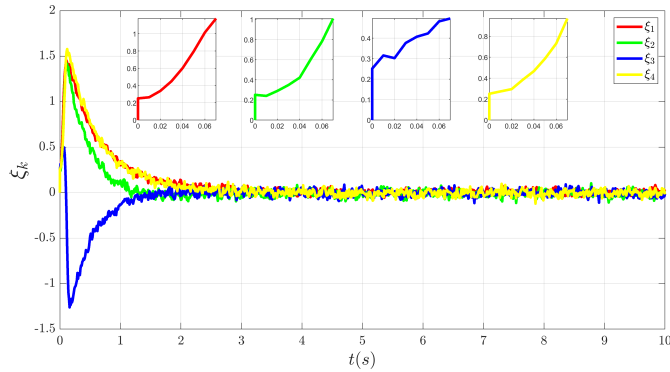
Figure 4.7: Time evolution of the hybrid variable ξ_k associated with each edge, using noisy measurements.

Next, we simulate the proposed hybrid distributed position estimation scheme (4.30)-(4.31) together with the hybrid distributed attitude observer (4.25)-(4.26). We consider the following initial conditions for the estimated positions: $\hat{p}_1(0) = [1\ 1\ 0]^T$, $\hat{p}_2(0) = [-1\ 2\ 1]^T$, $\hat{p}_3(0) = [-2\ 0\ -1]^T$, $\hat{p}_4(0) = [-1\ 2\ 2]^T$ and $\hat{p}_5(0) = [-1\ 1\ 1]^T$. We pick $k_p = 1$. For the attitude observer (4.25)-(4.26), we consider the same initial conditions and observer parameters as in the first simulation. The time evolution of the position and the relative position estimation error norms are shown in Figure 4.8 and Figure 4.9, respectively.
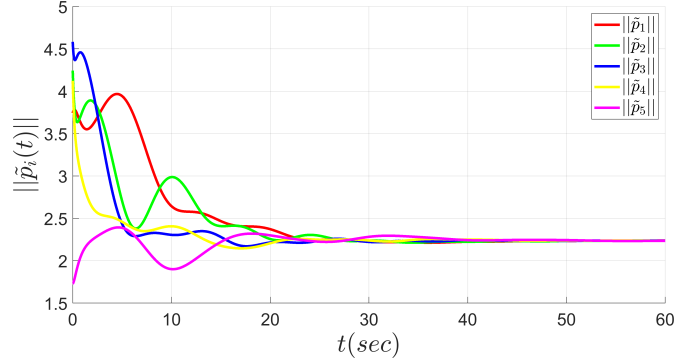
Figure 4.8: Time evolution of the position estimation error norm.
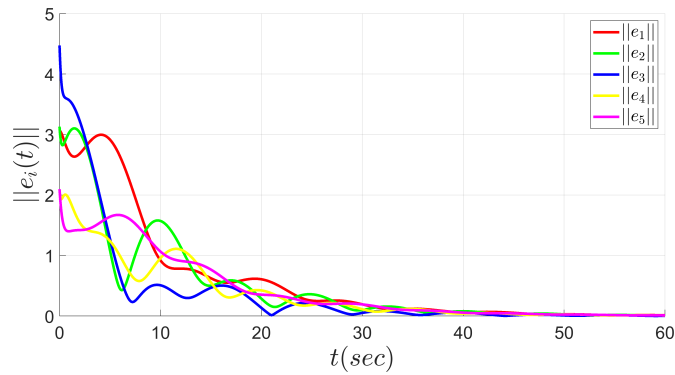
Figure 4.9: Time evolution of the relative position estimation error norm.

4.6 Conclusion

In this chapter, we addressed the problem of distributed attitude estimation of multi-agent rigid-body systems, evolving on $SO(3)$, relying on individual angular velocity and relative attitude information. Two nonlinear distributed attitude estimation schemes evolving on $SO(3)$ have been proposed. The first AGAS continuous observer is used as a baseline for the derivation of a hybrid version enjoying global asymptotic stability of the desired equilibrium set $\mathcal{A}_h$, which implies that the attitude of each agent can be estimated (globally) up to a common constant orientation which can be uniquely determined if at least one agent has access to its absolute attitude. This hybrid distributed attitude estimation scheme relies on auxiliary time-varying scalar variables associated to each edge k, namely ξ_k, which are governed by the hybrid dynamics (4.13)-(4.14). These auxiliary variables are appropriately designed to keep the relative attitude errors away from the undesired equilibrium set $\Upsilon_h \backslash \mathcal{A}_h$. Furthermore, the hybrid distributed attitude estimation scheme has been used with a hybrid distributed position estimation scheme to globally asymptotically estimate the pose of n rigid body systems, up to a constant translation and orientation, relying on local relative time-varying bearing measurements and individual linear velocity measurements.

Chapter 5

Global Attitude Synchronization on $SO(3)$

5.1 Introduction

In this chapter, we consider the attitude alignment problem for a group of rigid body systems evolving on $SO(3)$ under an undirected, acyclic and connected graph topology. Addressing such a problem using local information exchange is an interesting problem, from a theoretical and practical point of views, that has attracted the attention of the research community in the last few decades. Despite the literature abundance with regards to the control of multi-agent systems in the Euclidean space, the literature is relatively limited when it comes to multi-agent rigid-body systems evolving on smooth manifolds. Nevertheless, inspired by the classical consensus techniques, some attitude alignment schemes on $SO(3)$ have been proposed in the literature (Maadani et al., 2020; Van Tran et al., 2022; Tron et al., 2012; Tron et al., 2013; Markdahl, 2021; Sarlette et al., 2009; Sarlette et al., 2007; Sarlette and Sepulchre, 2009a; Wei et al., 2018). The above mentioned references achieve, at best, almost global asymptotic stability due to the well-known topological obstruction to global asymptotic stability via smooth vector fields on $SO(3)$ (Koditschek, 1989). On the other hand, some quaternion-based hybrid attitude alignment schemes, with global stability results, have been proposed in the literature (Mayhew et al., 2012; Gui and de Ruiter, 2018). Unfortunately, the quaternion representation double-covers $SO(3)$, which means that quaternions do not provide unique attitude representations. This lack of uniqueness can further affect quaternion-based feedback laws and may lead to undesirable phenomena, such as unwinding. Therefore, using the multi-agent switching mechanism introduced in chapter 4, we propose a new distributed hybrid feedback control scheme on $SO(3)$ for global attitude synchronization of a group of rigid body systems to a common orientation. The proposed hybrid feedback scheme relies on the individual angular velocity measurements as well as the relative attitude information.

Eliminating the need for velocity measurements in a network with a large number of agents can significantly reduce the costs associated with sensors and the communication flow between agents. Additionally, it ensures a certain level of immunity against angular

velocity sensor failures. Therefore, as a second contribution of this chapter, we propose a velocity-free distributed hybrid feedback control law for attitude synchronization that relies solely on relative orientation information, with global asymptotic stability guarantees. This velocity-free law uses the outputs of some auxiliary dynamical systems to generate the necessary damping to compensate for the lack of angular velocity information. To the best of the author's knowledge, these are the first results in the literature dealing with global attitude synchronization on $SO(3)$ with and without angular velocity measurements.

At the end of this chapter, we will present some numerical simulations to illustrate the performance of the two proposed distributed hybrid feedback control laws. The results presented in this chapter have been published in (Boughellaba and Tayebi, 2024).

5.2   Problem Formulation

Consider the n-agent rigid-body system governed by the following rotational dynamics:

$$\begin{cases} \dot{R}_i & = R_i[\omega_i]^\times \\ J_i\dot{\omega}_i & = -[\omega_i]^\times J_i\omega_i + \tau_i, \end{cases} \tag{5.1}$$

where $R_i \in SO(3)$ represents the orientation of the body-attached frame of agent i with respect to the inertial frame, $\omega_i \in \mathbb{R}^3$ is the body-frame angular velocity of agent i, and $\tau_i \in \mathbb{R}^3$ is the control torque that will be designed later. The inertia matrix $J_i \in \mathbb{R}^{3\times3}$ is constant and known.

Let the graph $\mathcal{G}$ be undirected tree describing the interaction between agents, which implies that if two agents are neighbors, their relative orientation is available to each of them, either by measurement if the agents are equipped with a relative attitude sensor, or by construction if they share their absolute orientations through communication. The relative orientation between agent i and agent j is defined as follows:

$$R_{ij} := R_i^T R_j, \tag{5.2}$$

where $(i,j) \in \mathcal{E}$. Considering an arbitrary orientation to the graph $\mathcal{G}$, if two agents i and j are connected by an oriented edge k, one can define the relative attitude as $\bar{R}_k := R_j^T R_i$, where $\{k\} = \mathcal{M}_i^+ \cap \mathcal{M}_j^- \in \mathcal{M}$. It follows from (5.1) that

$$\dot{\bar{R}}_k = \bar{R}_k[\bar{\omega}_k]^\times \tag{5.3}$$

$$J_i\dot{\omega}_i = -[\omega_i]^\times J_i\omega_i + \tau_i, \tag{5.4}$$

where $\bar{\omega}_k := \omega_i - \bar{R}_k^T\omega_j$. Recall that, for every $i \in \mathcal{V}$ and $j \in \mathcal{N}_i$, the intersection between the sets $\mathcal{M}_i^+$ and $\mathcal{M}_j^-$ is either a single-element set (if agent i and agent j are the head and tail, respectively, of the directed edge connecting them) or an empty set otherwise. Let $\bar{\omega} = [\bar{\omega}_1^T, \bar{\omega}_2^T, \ldots, \bar{\omega}_m^T]^T \in \mathbb{R}^{3m}$ and $\omega = [\omega_1^T, \omega_2^T, \ldots, \omega_n^T]^T \in \mathbb{R}^{3n}$. One can verify that (Bai et al., 2008)

$$\bar{\omega} = \boldsymbol{H}(t)^T\omega, \tag{5.5}$$

where the time-varying matrix $\boldsymbol{H}(t)$ is given in (4.7).

Our objective is to design a distributed hybrid feedback law τ_i such that the equilibrium $(\bar{R}_1 = I_3, \ldots, \bar{R}_m = I_3, \omega_1 = 0, \ldots, \omega_n = 0)$ is globally asymptotically stable. To achieve this objective, we propose two distributed hybrid feedback laws (one with angular velocity measurements and one without). Both feedback laws rely on a generic potential function on $SO(3)^m \times \mathbb{R}^m$. The design of the two distributed hybrid feedback laws relies on the multi-agent switching mechanism introduced in Section 4.3.2.1.

5.3 Distributed Hybrid Feedback Design

For every $i \in \mathcal{V}$, we propose the following distributed hybrid feedback control scheme

$$
\underbrace{\begin{aligned}
\tau_i = & -k_\omega \omega_i + k_R \left(\sum_{l \in \mathcal{M}_i^-} \bar{R}_l \psi \left(\bar{R}_l^T \nabla_{\bar{R}_l} U_R \right) - \sum_{p \in \mathcal{M}_i^+} \psi \left(\bar{R}_p^T \nabla_{\bar{R}_p} U_R \right) \right) \\
\dot{\xi}_k = & -k_\xi \nabla_{\xi_k} U_R
\end{aligned}}_{x \in \mathcal{F}_i}
\tag{5.6}
$$

$$
\underbrace{\xi_k^+ \in \begin{cases} \xi_k & \text{if} \quad U(\bar{R}_k, \xi_k) - U(\bar{R}_k, \xi_k^*) \leq \delta_{\bar{R}} \\ \xi_k^* & \text{if} \quad U(\bar{R}_k, \xi_k) - U(\bar{R}_k, \xi_k^*) \geq \delta_{\bar{R}} \end{cases}}_{x \in \mathcal{J}_i}
\tag{5.7}
$$

where $k_\xi, k_R, k_\omega > 0$, $\xi_k^* := \underset{\bar{\xi}_k \in \Xi}{\arg\min}\, U(\bar{R}_k, \bar{\xi}_k)$ and $k \in \mathcal{M}_i^+$. The flow set $\mathcal{F}_i$ and the jump set $\mathcal{J}_i$, for agent i, are defined as follows:

$$
\mathcal{F}_i := \{ x \in \mathcal{S} : \forall k \in \mathcal{M}_i^+, U(\bar{R}_k, \xi_k) - \underset{\bar{\xi}_k \in \Xi}{\min} U(\bar{R}_k, \bar{\xi}_k) \leq \delta_{\bar{R}} \},
$$

$$
\mathcal{J}_i := \{ x \in \mathcal{S} : \exists k \in \mathcal{M}_i^+, U(\bar{R}_k, \xi_k) - \underset{\bar{\xi}_k \in \Xi}{\min} U(\bar{R}_k, \bar{\xi}_k) \geq \delta_{\bar{R}} \}.
$$

Define the new state $\bar{x} := (x, \omega_1, \ldots, \omega_n) \in \bar{\mathcal{S}}$, where $\bar{\mathcal{S}} := SO(3)^m \times \mathbb{R}^m \times \mathbb{R}^{3n}$. In view of (5.3)-(5.4) and (5.6)-(5.7), one can derive the following multi-agent hybrid closed-loop dynamics:

$$
\bar{\mathcal{H}} : \begin{cases} \dot{\bar{x}} = \bar{F}(\bar{x}), & \bar{x} \in \bar{\mathcal{F}} := \{ \bar{x} \in \bar{\mathcal{S}} : x \in \mathcal{F} \} \\ \bar{x}^+ \in \bar{G}(\bar{x}), & \bar{x} \in \bar{\mathcal{J}} := \{ \bar{x} \in \bar{\mathcal{S}} : x \in \mathcal{J} \} \end{cases}
\tag{5.8}
$$

where

$$
\mathcal{F} := \bigcap_{i=1}^n \mathcal{F}_i, \qquad \mathcal{J} := \bigcup_{i=1}^n \mathcal{J}_i,
\tag{5.9}
$$

and

$$
\bar{F}(\bar{x}) := \begin{bmatrix} \bar{R}_1[\bar{\omega}_1]^\times \\ \vdots \\ \bar{R}_M[\bar{\omega}_m]^\times \\ -k_\xi \nabla_{\xi_1} U_R \\ \vdots \\ -k_\xi \nabla_{\xi_m} U_R \\ J_1^{-1} f_1(x) - k_\omega J_1^{-1}\omega_1 \\ \vdots \\ J_n^{-1} f_n(x) - k_\omega J_n^{-1}\omega_n \end{bmatrix}, \quad \bar{G}(\bar{x}) := \begin{bmatrix} \bar{R}_1 \\ \vdots \\ \bar{R}_m \\ \{\xi_1, \xi_1^*\} \\ \vdots \\ \{\xi_m, \xi_m^*\} \\ \omega_1 \\ \vdots \\ \omega_n \end{bmatrix},
$$

where $f_i(x)$ is given by

$$
f_i(x) := k_R \left[\sum_{l \in \mathcal{M}_i^-} \bar{R}_l \psi \left(\bar{R}_l^T \nabla_{\bar{R}_l} U_R \right) - \sum_{p \in \mathcal{M}_i^+} \psi \left(\bar{R}_p^T \nabla_{\bar{R}_p} U_R \right) \right] \tag{5.10}
$$

From equations (5.8)-(5.9), one can deduce that $\bar{\mathcal{F}} \cup \bar{\mathcal{J}} = \bar{\mathcal{S}}$. Furthermore, one can note that $\bar{\mathcal{F}}$ and $\bar{\mathcal{J}}$ are closed sets, and the hybrid closed-loop system (5.8) is autonomous.

Lemma 5.1 *The hybrid closed-loop system* (5.8) *satisfies the hybrid basic conditions introduced in Section 2.6.2.*

Proof The proof is established using the same arguments as in the proof of Lemma 4.2.

Remark 5.1 *Condition 4.1, introduced in the previous chapter, implies that the set of all undesired critical points belongs to the jump set $\mathcal{J}$, i.e., $\bar{\Upsilon} \setminus \mathcal{A} \subset \mathcal{J}$. The jump map $\bar{G}$ will reset the states to values that result in a decrease of $U_R(x)$.*

Now, we will present our first result in this chapter, which is related to the stability properties of the multi-agent hybrid closed-loop system (5.8).

Theorem 5.1 *Let $k_R, k_\xi, k_\omega > 0$ and suppose that Condition 4.1 is satisfied. Then, the set $\bar{\mathcal{A}} := \{\bar{x} \in \bar{\mathcal{S}} : x \in \mathcal{A}, \ \omega = 0\}$ is globally asymptotically stable for the multi-agent hybrid closed-loop system (5.8) and the number of jumps is finite.*

Proof See Appendix C.1

Note that the implementation of the proposed distributed hybrid feedback law (5.6)-(5.7) requires that each agent should have access to its angular velocity. This can be costly, especially in the case of a network with a large number of agents. Therefore, in the next section, inspired by (Tayebi, 2008) and (Wang and Tayebi, 2022), we introduce an auxiliary dynamical system for each agent to generate the necessary damping that compensates for the lack of angular velocity information.

5.4 Distributed Hybrid Feedback Design without Velocity Measurements

For every $i \in \mathcal{V}$, we introduce the auxiliary state $(Q_i, \zeta_i) \in SO(3) \times \mathbb{R}$ with the following hybrid dynamics:

$$
\begin{aligned}
\dot{Q}_i =& k_Q Q_i \left[\tilde{Q}_i \psi \left(\tilde{Q}_i^T \nabla_{\tilde{Q}_i} U(\tilde{Q}_i, \zeta_i) \right) \right]^\times \\
\underbrace{\dot{\zeta}_i =& - k_\zeta \nabla_{\zeta_i} U(\tilde{Q}_i, \zeta_i)}_{(Q_i, \zeta_i) \in \mathcal{F}_i^{\tilde{Q}}}
\end{aligned}
\tag{5.11}
$$

$$
\begin{aligned}
Q_i^+ =& Q_i \\
\zeta_i^+ \in& \begin{cases} \zeta_i & \text{if} \quad U(\tilde{Q}_i, \zeta_i) - U(\tilde{Q}_i, \zeta_i^*) \le \delta_{\tilde{Q}} \\ \zeta_i^* & \text{if} \quad U(\tilde{Q}_i, \zeta_i) - U(\tilde{Q}_i, \zeta_i^*) \ge \delta_{\tilde{Q}} \end{cases}
\end{aligned}
\tag{5.12}
$$
$$
\underbrace{}_{(Q_i, \zeta_i) \in \mathcal{J}_i^{\tilde{Q}}}
$$

where $k_Q, k_\zeta > 0$, $Q_i(0) \in SO(3)$, $\zeta_i(0) \in \mathbb{R}$, $\tilde{Q}_i := Q_i^T R_i$ and $\zeta_i^* := \underset{\bar{\zeta}_i \in \Pi}{\operatorname{argmin}} \, U(\tilde{Q}_i, \bar{\zeta}_i)$.

Before defining the flow set $\mathcal{F}_i^{\tilde{Q}}$ and the jump set $\mathcal{J}_i^{\tilde{Q}}$, it is important to first introduce the following condition, which is adopted from (Wang and Tayebi, 2022).

Condition 5.1 *Let U be a potential function on $SO(3) \times \mathbb{R}$, with respect to $(I_3, 0)$. Let $(I_3, 0) \in \Upsilon$, where $\Upsilon := \{ (\tilde{Q}_i, \zeta_i) \in SO(3) \times \mathbb{R} : \nabla_{\tilde{Q}_i} U(\tilde{Q}_i, \zeta_i) = 0, \nabla_{\zeta_i} U(\tilde{Q}_i, \zeta_i) = 0 \}$ is the set of all critical points of $U(\tilde{Q}_i, \zeta_i)$. There exist a scalar $\delta_{\tilde{Q}} > 0$ and a nonempty finite set Π such that, for every $(\tilde{Q}_i, \zeta_i) \in \Upsilon \setminus \{ (I_3, 0) \}$, one has*

$$
U(\tilde{Q}_i, \zeta_i) - \underset{\bar{\zeta}_i \in \Pi}{min} \, U(\tilde{Q}_i, \bar{\zeta}_i) > \delta_{\tilde{Q}}.
\tag{5.13}
$$

The motivation behind Condition 5.1 is similar to that of Condition 4.1. Condition 5.1 implies that all undesired critical points in $\Upsilon \setminus \{ (I_3, 0) \}$ are inside the jump set $\mathcal{J}_i^{\tilde{Q}}$, and as such, the jump map in (5.12) will take care of steering the state away from the undesired critical points $\Upsilon \setminus \{ (I_3, 0) \}$.

Remark 5.2 *Consider the potential function U defined in (4.23). Proposition 2 in (Wang and Tayebi, 2022) gives the possible choices of parameters $\{ \Pi, A, u, \gamma, \delta_{\tilde{Q}} \}$ for which Condition 5.1 is satisfied.*

According to Condition 5.1, one defines the flow set $\mathcal{F}_i^{\tilde{Q}}$ and the jump set $\mathcal{J}_i^{\tilde{Q}}$ as follows:

$$
\mathcal{F}_i^{\tilde{Q}} := \{ (\tilde{Q}_i, \zeta_i) \in SO(3) \times \mathbb{R} : U(\tilde{Q}_i, \zeta_i) - \underset{\bar{\zeta}_i \in \Xi}{min} U(\tilde{Q}_i, \bar{\zeta}_i) \le \delta_{\tilde{Q}} \},
$$

$$
\mathcal{J}_i^{\tilde{Q}} := \{ (\tilde{Q}_i, \zeta_i) \in SO(3) \times \mathbb{R} : U(\tilde{Q}_i, \zeta_i) - \underset{\bar{\zeta}_i \in \Xi}{min} U(\tilde{Q}_i, \bar{\zeta}_i) \ge \delta_{\tilde{Q}} \}.
$$

It follows from (5.11)-(5.12) that

$$\dot{\tilde{Q}}_i = \tilde{Q}_i \left[\omega_i - k_Q \psi \left(\tilde{Q}_i^T \nabla_{\tilde{Q}_i} U(\tilde{Q}_i, \zeta_i) \right) \right]^\times$$
$$\underbrace{\dot{\zeta}_i = - k_\zeta \nabla_{\zeta_i} U(\tilde{Q}_i, \zeta_i)}_{(Q_i, \zeta_i) \in \mathcal{F}_i^{\tilde{Q}}} \tag{5.14}$$

$$\tilde{Q}_i^+ = \tilde{Q}_i$$
$$\underbrace{\zeta_i^+ \in \begin{cases} \zeta_i & \text{if} \quad U(\tilde{Q}_i, \zeta_i) - U(\tilde{Q}_i, \zeta_i^*) \le \delta_{\tilde{Q}} \\ \zeta_i^* & \text{if} \quad U(\tilde{Q}_i, \zeta_i) - U(\tilde{Q}_i, \zeta_i^*) \ge \delta_{\tilde{Q}} \end{cases}}_{(Q_i, \zeta_i) \in \mathcal{J}_i^{\tilde{Q}}} \tag{5.15}$$

For every $i \in \mathcal{V}$, we propose the following distributed hybrid velocity-free feedback control law

$$\tau_i = k_R \left(\sum_{l \in \mathcal{M}_i^-} \bar{R}_l \psi \left(\bar{R}_l^T \nabla_{\bar{R}_l} U_R \right) - \sum_{p \in \mathcal{M}_i^+} \psi \left(\bar{R}_p^T \nabla_{\bar{R}_p} U_R \right) \right) - k_{\tilde{Q}} \psi \left(\tilde{Q}_i^T \nabla_{\tilde{Q}_i} U(\tilde{Q}_i, \zeta_i) \right)$$
$$\underbrace{\dot{\xi}_k = - k_\xi \nabla_{\xi_k} U_R}_{x \in \mathcal{F}_i} \tag{5.16}$$

$$\underbrace{\xi_k^+ \in \begin{cases} \xi_k & \text{if} \quad U(\bar{R}_k, \xi_k) - U(\bar{R}_k, \xi_k^*) \le \delta_{\bar{R}} \\ \xi_k^* & \text{if} \quad U(\bar{R}_k, \xi_k) - U(\bar{R}_k, \xi_k^*) \ge \delta_{\bar{R}} \end{cases}}_{x \in \mathcal{J}_i} \tag{5.17}$$

Note that the feedback control law presented above, is obtained by replacing, in (5.6)-(5.7), the angular velocity ω_i with the term $\psi \left(\tilde{Q}_i^T \nabla_{\tilde{Q}_i} U(\tilde{Q}_i, \zeta_i) \right)$ which can be constructed from the outputs of the auxiliary system (5.11)-(5.12).

Now, let $\hat{x} := (\bar{x}, \tilde{Q}_i, \ldots, \tilde{Q}_n, \zeta_1, \ldots, \zeta_n) \in \hat{\mathcal{S}} := \bar{\mathcal{S}} \times SO(3)^n \times \mathbb{R}^n$. One can derive the following hybrid dynamics:

$$\hat{\mathcal{H}} : \begin{cases} \dot{\hat{x}} = \hat{F}(\hat{x}), & \hat{x} \in \hat{\mathcal{F}} \\ \hat{x}^+ \in \hat{G}(\hat{x}), & \hat{x} \in \hat{\mathcal{J}} \end{cases} \tag{5.18}$$

where

$$\hat{\mathcal{F}} := \{ \hat{x} \in \hat{\mathcal{S}} : \bar{x} \in \bar{\mathcal{F}} \text{ and } \forall i \in \mathcal{V}, (\tilde{Q}_i, \zeta_i) \in \mathcal{F}_i^{\tilde{Q}} \}$$
$$\hat{\mathcal{J}} := \{ \hat{x} \in \hat{\mathcal{S}} : \bar{x} \in \bar{\mathcal{J}} \text{ or } \exists i \in \mathcal{V}, (\tilde{Q}_i, \zeta_i) \in \mathcal{J}_i^{\tilde{Q}} \}$$

and

$$\hat{F}(\hat{x}) := \begin{bmatrix} \bar{R}_1[\bar{\omega}_1]^\times \\ \vdots \\ \bar{R}_m[\bar{\omega}_m]^\times \\ -k_\xi \nabla_{\xi_1} U_R \\ \vdots \\ -k_\xi \nabla_{\xi_m} U_R \\ J_1^- \left(-[\omega_1]^\times J_1 \omega_1 + \tau_1 \right) \\ \vdots \\ J_n^- \left(-[\omega_n]^\times J_n \omega_n + \tau_n \right) \\ \tilde{Q}_1 \left[\omega_1 - k_Q \psi \left(\tilde{Q}_1^T \nabla_{\tilde{Q}_1} U(\tilde{Q}_1, \zeta_1) \right) \right]^\times \\ \vdots \\ \tilde{Q}_n \left[\omega_n - k_Q \psi \left(\tilde{Q}_n^T \nabla_{\tilde{Q}_n} U(\tilde{Q}_n, \zeta_n) \right) \right]^\times \\ k_\zeta \nabla_{\zeta_1} U(\tilde{Q}_1, \zeta_1) \\ \vdots \\ k_\zeta \nabla_{\zeta_n} U(\tilde{Q}_n, \zeta_n) \end{bmatrix}, \quad \hat{G}(\hat{x}) := \begin{bmatrix} \bar{R}_1 \\ \vdots \\ \bar{R}_m \\ \{\xi_1, \xi_1^*\} \\ \vdots \\ \{\xi_m, \xi_m^*\} \\ \omega_1 \\ \vdots \\ \omega_n \\ \tilde{Q}_1 \\ \vdots \\ \tilde{Q}_n \\ \{\zeta_1, \zeta_1^*\} \\ \vdots \\ \{\zeta_n, \zeta_n^*\} \end{bmatrix}.$$

It follows from (5.18) that $\hat{\mathcal{F}} \cup \hat{\mathcal{J}} = \hat{\mathcal{S}}$. In addition, $\hat{\mathcal{F}}$ and $\hat{\mathcal{J}}$ are closed sets, and the hybrid closed-loop system (5.18) is autonomous and satisfies the hybrid basic conditions introduced in Section 2.6.2. Our second result in this chapter can be stated as follows:

Theorem 5.2 *Let $k_{\tilde{Q}}, k_Q, k_\zeta, k_R, k_\xi > 0$ and suppose Conditions 4.1 and 5.1 are satisfied. Then, the set $\hat{\mathcal{A}} := \{\hat{x} \in \hat{\mathcal{S}} : \bar{x} \in \bar{\mathcal{A}}, \forall i \in \mathcal{V}, (\tilde{Q}_i, \zeta_i) = (I_3, 0)\}$ is globally asymptotically stable for the multi-agent hybrid closed-loop system (5.18) and the number of jumps is finite.*

Proof See Appendix C.2

5.5 Explicit Distributed Hybrid Feedback Control Design

The two proposed distributed hybrid feedback control laws (5.6)-(5.7) and (5.16)-(5.17) are designed based on a generic potential function U_R, defined on $\mathcal{S}_h$, with respect to $\mathcal{A}_h$. In this section we will derive an explicit form of the two proposed distributed hybrid feedback control laws. Consider the potential function given in (4.23). The distributed hybrid feedback law (5.6) can be explicitly rewritten as follows:

$$\tau_i = -k_\omega \omega_i - k_R \left(\sum_{j \in \mathcal{O}_i} \psi \left(A \mathcal{R}_a(\xi_l, u)^T R_j^T R_i \right) + \sum_{j \in \mathcal{I}_i} \mathcal{R}_a(\xi_p, u) \psi \left(A R_j^T R_i \mathcal{R}_a(\xi_p, u) \right) \right), \tag{5.19}$$

where $i \in \mathcal{V}$, $\{p\} = \mathcal{M}_i^+ \cap \mathcal{M}_j^- \in \mathcal{M}$, $\{l\} = \mathcal{M}_i^- \cap \mathcal{M}_j^+ \in \mathcal{M}$, $\mathcal{I}_i := \{j \in \mathcal{N}_i : j$ is the tail of the edge $(i,j) \in \mathcal{E}\}$ and $\mathcal{O}_i := \{j \in \mathcal{N}_i : j$ is the head of the edge $(i,j) \in \mathcal{E}\}$. Furthermore, the following explicit form can also be obtained for the velocity-free distributed hybrid feedback control law (5.16):

$$\tau_i = -k_R \left(\sum_{j \in \mathcal{O}_i} \psi \left(A\mathcal{R}_a(\xi_l, u)^T R_j^T R_i \right) + \sum_{j \in \mathcal{I}_i} \mathcal{R}_a(\xi_p, u) \psi \left(AR_j^T R_i \mathcal{R}_a(\xi_p, u) \right) \right)$$
$$- k_{\tilde{Q}} \mathcal{R}_a(\zeta_i, u) \psi \left(AQ_i^T R_i \mathcal{R}_a(\zeta_i, u) \right). \tag{5.20}$$

The dynamics of ξ_k, during the flows, for both control laws (5.19) and (5.20) are given by

$$\dot{\xi}_k = -k_\xi \left(\gamma \xi_k + 2u^T \psi \left(A\bar{R}_k \mathcal{R}_a(\xi_k, u) \right) \right), \tag{5.21}$$

for every $k \in \mathcal{M}_i^+$ where $i \in \mathcal{V}$. Again, for the practical implementation of our proposed distributed hybrid feedback laws, we assume that the dynamics of ξ_k are implemented at agent i, and agent j receives the information about ξ_k from agent i through communication, for every $(i,j) \in \mathcal{E}$ such that $\{k\} = \mathcal{M}_i^+ \cap \mathcal{M}_j^-$. In addition, the dynamics of the auxiliary state (Q_i, ζ_i), during the flows, are also given explicitly as follows:

$$\dot{Q}_i = k_Q Q_i \left[Q_i^T R_i \mathcal{R}_a(\zeta_i, u) \psi \left(AQ_i^T R_i \mathcal{R}_a(\zeta_i, u) \right) \right]^\times \tag{5.22}$$
$$\dot{\zeta}_i = -k_\zeta \left(\gamma \zeta_i + 2u^T \psi \left(AQ_i^T R_i \mathcal{R}_a(\zeta_i, u) \right) \right). \tag{5.23}$$

Remark 5.3 *Note that $\mathcal{N}_i = \mathcal{I}_i \cup \mathcal{O}_i$. Therefore, both hybrid feedback control laws (5.19) and (5.20) are distributed since they rely only on the neighboring agents. The control law (5.19) requires the individual angular velocities ω_i, while the control law (5.20) does not.*

5.6 Simulation Results

In this section, we provide some numerical simulation results to illustrate the performance of the two proposed distributed hybrid feedback control laws (5.19) and (5.20), referred to as *Hybrid Controller* and *Velocity-free Hybrid Controller*, respectively. For comparison purposes, we also consider the following continuous feedback control law:

$$\tau_i = -k_\omega \omega_i - k_R \sum_{j \in \mathcal{N}_i} \psi(AR_j^T R_i), \tag{5.24}$$

which is derived from the proposed distributed hybrid feedback control law (5.19) by letting $\xi_i = 0$. This control law is referred to as *Continuous Controller*. We consider a seven-agent rigid-body system under the undirected graph topology depicted in Figure 5.1. The neighbor sets are given as $\mathcal{N}_1 = \{2\}$, $\mathcal{N}_2 = \{1,3\}$, $\mathcal{N}_3 = \{2,4,6\}$, $\mathcal{N}_4 = \{3,5\}$, $\mathcal{N}_5 = \{4\}$, $\mathcal{N}_6 = \{3,7\}$ and $\mathcal{N}_7 = \{6\}$.
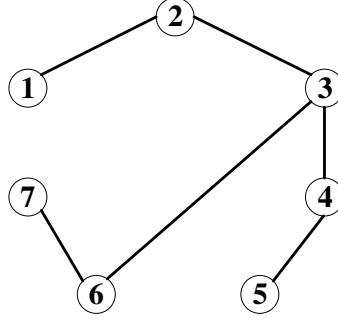
Figure 5.1: The interaction graph $\mathcal{G}$.

We assign an arbitrary orientation to the graph $\mathcal{G}$ and we index each oriented edge with a number as shown in Figure 5.2. We consider the following initial conditions: $\omega(0) = 0$, $\xi(0) = 0$, $\zeta(0) = 0$, $R_1(0) = \mathcal{R}_\alpha(-\frac{\pi}{2}, v)$, $R_2(0) = \mathcal{R}_\alpha(\frac{\pi}{2}, v)$, $R_3(0) = \mathcal{R}_\alpha(-\frac{\pi}{2}, v)$, $R_4(0) = \mathcal{R}_\alpha(\frac{\pi}{2}, v)$, $R_5(0) = \mathcal{R}_\alpha(-\frac{\pi}{2}, v)$, $R_6(0) = \mathcal{R}_\alpha(\frac{\pi}{2}, v)$, $R_7(0) = \mathcal{R}_\alpha(-\frac{\pi}{2}, v)$, $Q_1(0) = \mathcal{R}_\alpha(\frac{\pi}{2}, v)$, $Q_2(0) = \mathcal{R}_\alpha(-\frac{\pi}{2}, v)$, $Q_3(0) = \mathcal{R}_\alpha(\frac{\pi}{2}, v)$, $Q_4(0) = \mathcal{R}_\alpha(-\frac{\pi}{2}, v)$, $Q_5(0) = \mathcal{R}_\alpha(\frac{\pi}{2}, v)$, $Q_6(0) = \mathcal{R}_\alpha(-\frac{\pi}{2}, v)$ and $Q_7(0) = \mathcal{R}_\alpha(\frac{\pi}{2}, v)$, with $v = [0\ 0\ 1]^T$. Note that these initial conditions are chosen such that the state belongs to the set of undesired equilibria. In addition, the gains and hybrid scheme parameters are set to $k_R = 0.4$, $k_\omega = 0.1$, $k_Q = 30$, $k_{\tilde{Q}} = 3$, $k_\xi = k_\zeta = 20$, $\delta_{\bar{R}} = \delta_{\tilde{Q}} = 0.3848$, $\gamma = 1.9251$, $\Xi = \Pi = \{0.9\pi\}$, $u = [0\ 0.6455\ 0.7638]^T$ and $A = \mathrm{diag}([5, 8.57, 12])$. To simulate the *Hybrid Controller* and the *Velocity-free Hybrid Controller*, we used the HyEQ Toolbox (Sanfelice et al., 2013).
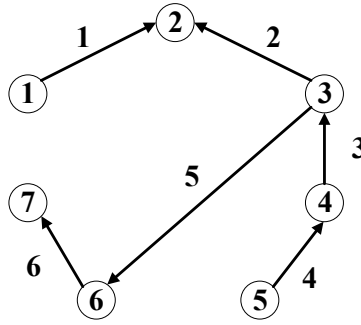
Figure 5.2: The interaction graph $\mathcal{G}$ with orientation.

Figures 5.3-5.7 present the simulation results of our proposed distributed hybrid feedback control laws (5.19) and (5.20), as well as the continuous feedback law given in (5.24). Since the initial conditions belong to the jump set $\hat{\mathcal{J}}$, the variables ξ_k and ζ_i, for every $k \in \mathcal{M}$ and $i \in \mathcal{V}$, at $t = 0$, jump from 0 to 0.9π and then converge to zero as $t \to \infty$. Furthermore, the states $\bar{R}_k$ and ω_i, for every $k \in \mathcal{M}$ and $i \in \mathcal{V}$, also converge to zero as $t \to \infty$ for both controllers. It is worth noting that the two proposed controllers improve convergence rate of the relative attitudes compared to the *Continuous Controller*.
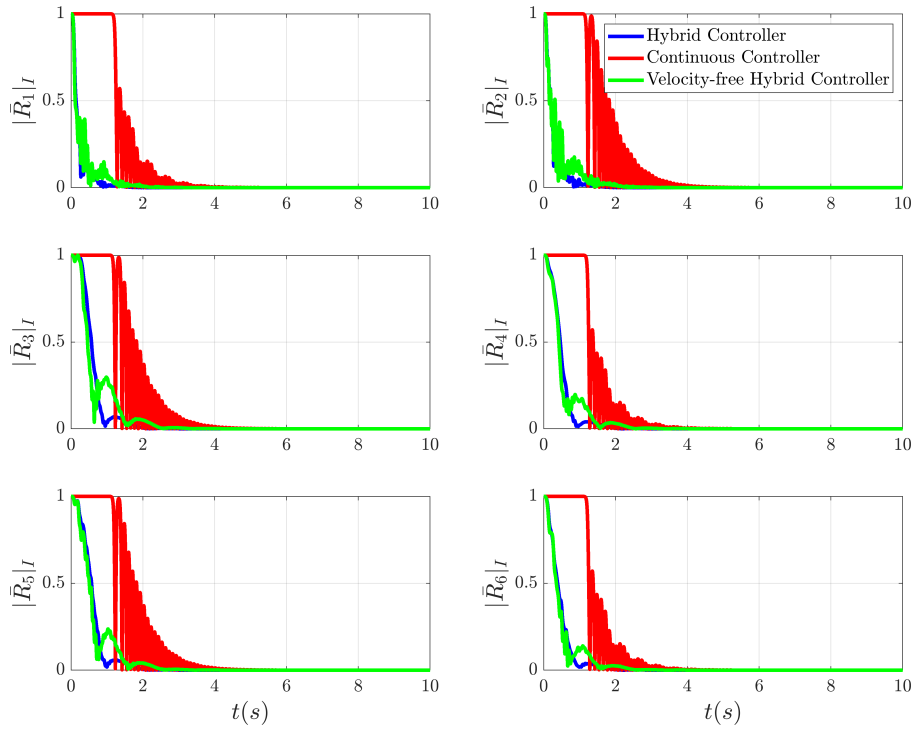
Figure 5.3: Time evolution of the relative attitude associated with each edge.
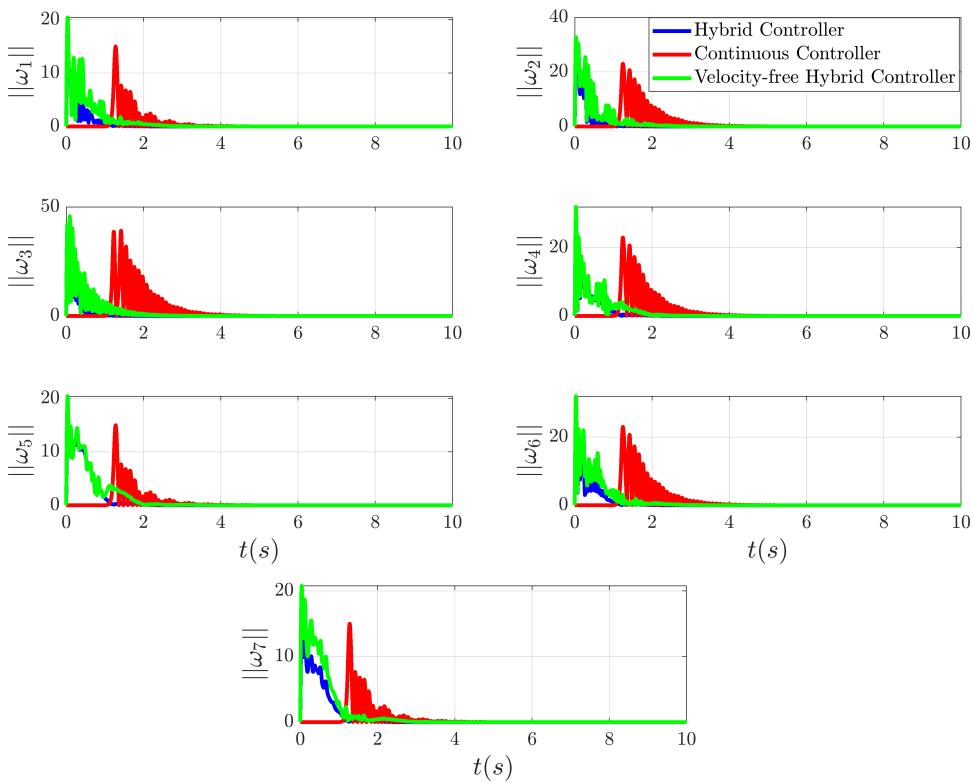
Figure 5.4: Time evolution of the angular velocity of each agent.
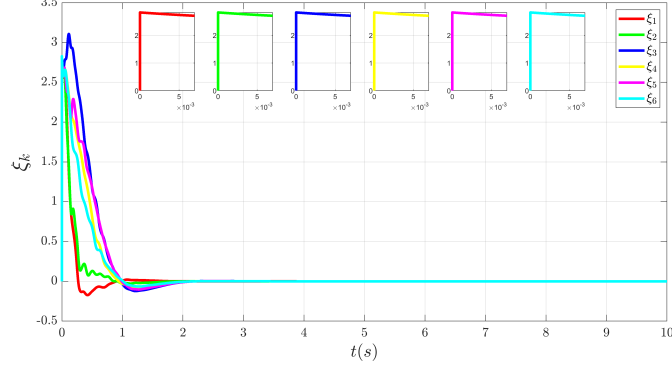
Figure 5.5: Time evolution of the hybrid variable ξ_k associated with each edge.
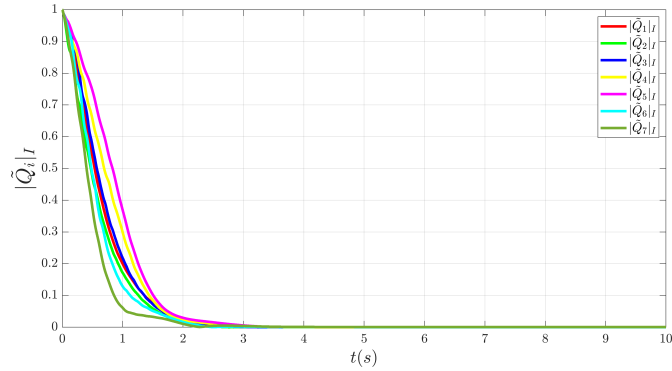
Figure 5.6: Time evolution of the auxiliary state $\tilde{Q}_i$ associated with each agent.
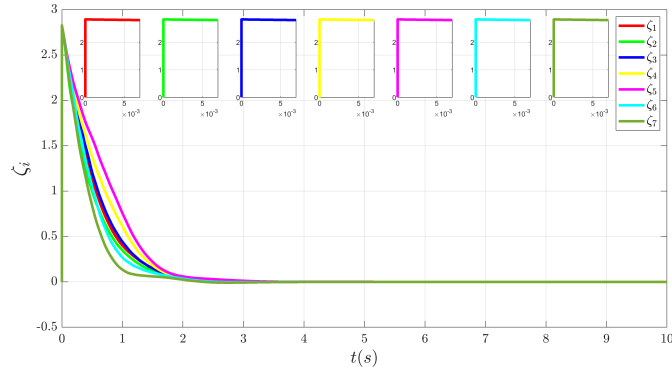
Figure 5.7: Time evolution of the hybrid variable ζ_i associated with each agent.

In the following simulation, we assume that the measurements are subjected to noise. The noisy measurements of the attitude and angular velocity are given as $R_i^n = R_i \exp([n_R]^\times)$ and $\omega_i^n = \omega_i + n_\omega$, respectively, for every $i \in \mathcal{V}$, where n_R and n_ω are additive white Gaussian noise with zero mean and a variance of 0.01. We consider the same initial conditions and observer parameters as in the previous simulation. Figures 5.8-5.12 illustrate the performance of the distributed hybrid feedback control laws (5.19) and (5.20) with noisy measurements.
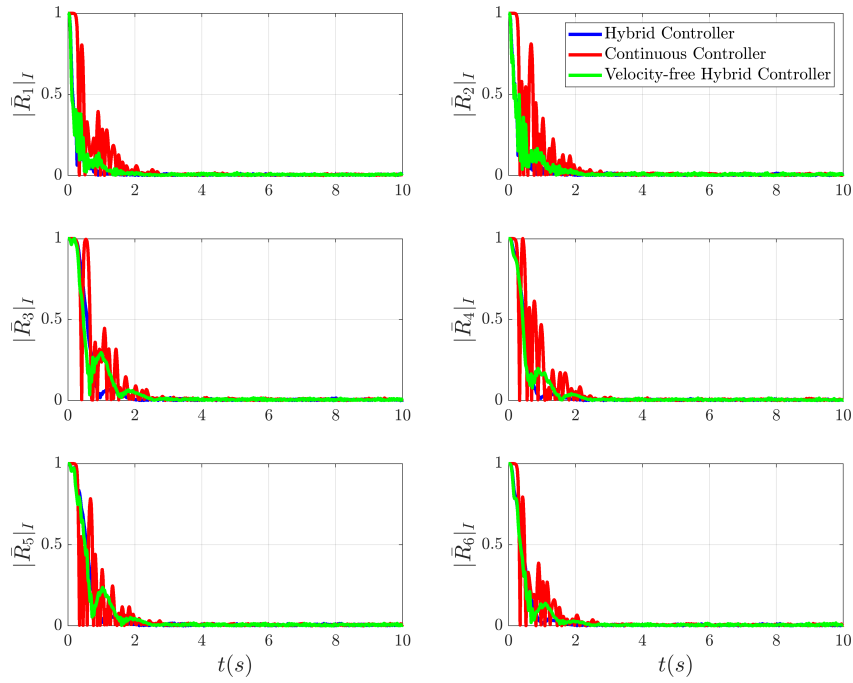
Figure 5.8: Time evolution of the relative attitude associated with each edge.
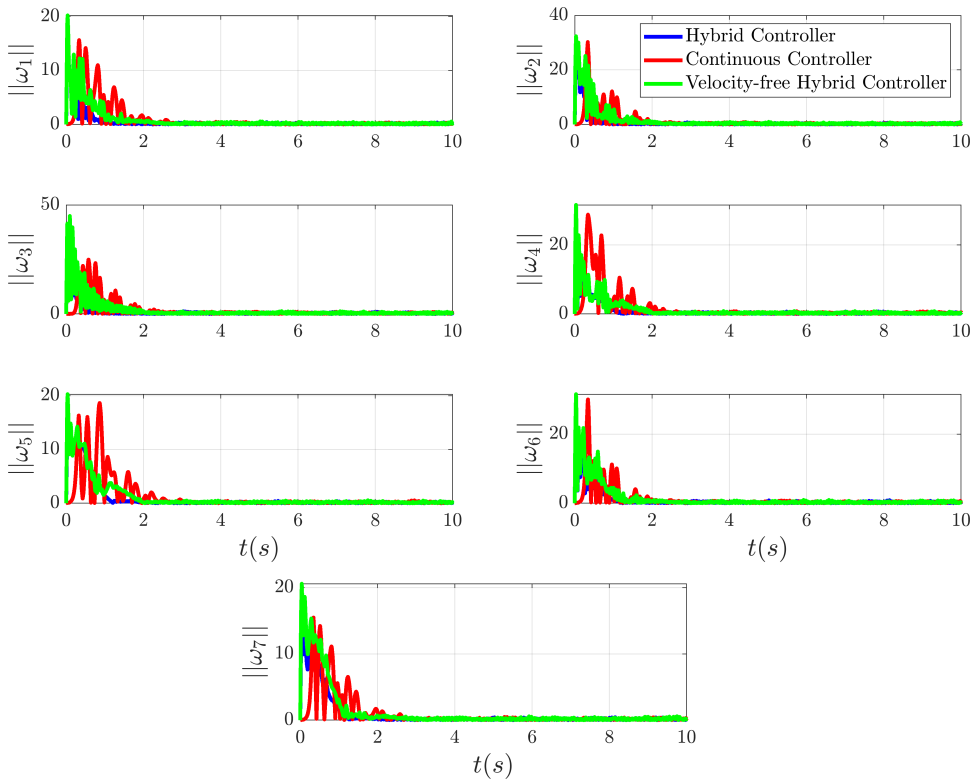
Figure 5.9: Time evolution of the angular velocity of each agent.
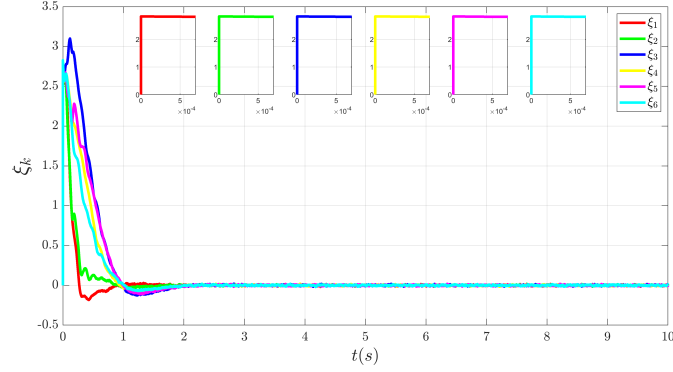
Figure 5.10: Time evolution of the hybrid variable ξ_k associated with each edge.
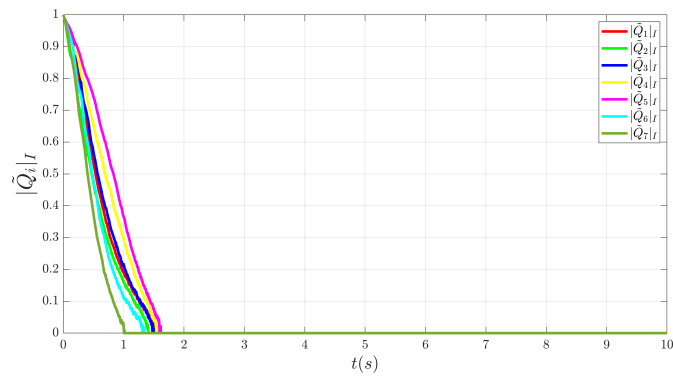
Figure 5.11: Time evolution of the auxiliary state $\tilde{Q}_i$ associated with each agent.
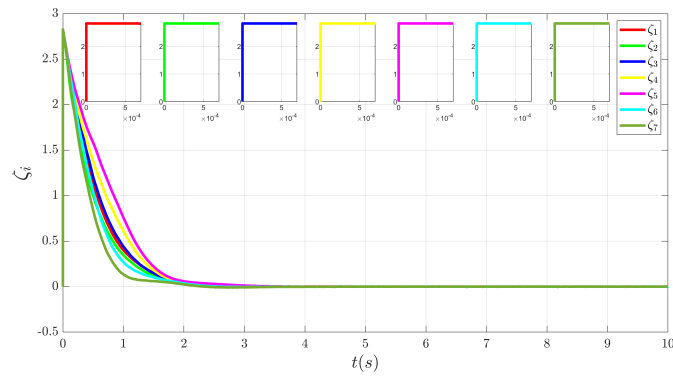
Figure 5.12: Time evolution of the hybrid variable ζ_i associated with each agent.

5.7 Conclusion

In this chapter, we addressed the problem of attitude synchronization for a group of rigid body systems evolving on $SO(3)$. We assumed that these systems can interact with each other through an undirected, connected, and acyclic graph topology. Accordingly, we

proposed two distributed hybrid attitude synchronization schemes on $SO(3)$. The first hybrid control law, relying on individual angular velocities and relative orientations, guarantees global attitude alignment to a common orientation. In the second hybrid control, we obviate the need for the angular velocities through the introduction of some dynamic auxiliary variables, while guaranteeing global asymptotic attitude synchronization. The proposed velocity-free control scheme relies only on the relative attitude information.

Designing a distributed attitude tracking and synchronization feedback control scheme that allows the agents to globally align their attitudes and track a time-varying reference trajectory, considering both the availability and non-availability of individual angular velocity information, is an interesting extension of this work.

Chapter 6

Conclusions

6.1 Summary

In this dissertation, three topics relevant to distributed cooperative state estimation and control for multi-agent rigid-body systems have been addressed. The first topic explored the problem of distributed pose estimation using local relative bearings as well as angular and linear velocity measurements. As a second topic, the problem of distributed attitude observer design on $SO(3)$ relying on relative orientation and angular velocity measurements has been investigated. Finally, the third topic is related to the problem of global attitude synchronization on $SO(3)$ with and without angular velocity measurements.

We addressed the first topic, related to the distributed pose estimation problem, by considering two practical scenarios for multi-agent systems: agents with fixed positions and time-varying orientations, and agents with time-varying positions and orientations. For both scenarios, we assumed that the agents interact with each other according to a directed graph topology, where two agents have access to their respective poses. In addition, the individual angular velocities and local inter-agent bearing measurements are assumed to be available. Under the scenario of agents having fixed positions and time-varying orientations, we first proposed two stand-alone AGAS nonlinear distributed attitude observers evolving on $SO(3)$ and $SO(3) \times \mathbb{R}^3$, respectively. Although both estimation schemes enjoy the same stability properties, the attitude observer evolving on $SO(3) \times \mathbb{R}^3$ incorporates a low pass filter on the bearing measurements, which makes it more suitable for practical applications. Thereafter, we proposed an almost globally asymptotically stable bearing-based distributed pose estimation scheme which consists of a cascade of an almost globally asymptotically stable distributed attitude observer and an ISS distributed position observer. On the other hand, considering agents with time-varying positions and orientations, we proposed a locally exponentially stable bearing-based distributed nonlinear pose estimation scheme composed of a cascade of a stand-alone locally exponentially stable bearing-based distributed attitude observer, and a bearing-based distributed position observer.

Regarding the second topic, we proposed two nonlinear distributed attitude estimation schemes $SO(3)$. These estimation schemes assume that each agent measures its own angular velocity in the respective body frame, measures the relative orientation

with respect to its neighbors, and that the agents interact with each other according to an undirected tree graph topology. The first estimation scheme is an AGAS continuous distributed attitude observer evolving on $SO(3)$. The second estimation scheme is a hybrid distributed attitude observer evolving on $SO(3) \times \mathbb{R}$, endowed with global asymptotic stability guarantees. Note that both estimation scheme provide estimates of the agents orientations up to a common constant orientation which can be uniquely determined if at least one agent has access to its absolute attitude. The second proposed scheme relies on some auxiliary time-varying scalar variables, namely ξ_k, which are governed by hybrid dynamics (4.13)-(4.14), where each variable is associated with one edge. These auxiliary variables are appropriately designed to prevent the relative attitude errors from reaching the undesired equilibrium set $\Upsilon_h \setminus \mathcal{A}_h$ generated by smooth vector fields. Moreover, the hybrid distributed attitude estimation scheme has been used to design a globally asymptotically stable bearing-based hybrid distributed pose estimation scheme for n-agent rigid-body systems.

Finally, the last topic dealt with in this dissertation is the global attitude synchronization on $SO(3)$. We proposed two distributed hybrid attitude synchronization schemes evolving on $SO(3)$, guarantee global synchronization of the individual orientations to a common orientation, under undirected, connected, and acyclic graph topologies. The first synchronization scheme relies on individual angular velocities and relative orientations to achieve global attitude synchronization, while the second scheme achieves the same result without individual angular velocity measurements, which is interesting in applications involving expensive and prone-to-failure gyroscopes.

6.2 Perspectives

Building upon the findings of this dissertation, there are several future directions related to the problems of distributed cooperative state estimation and control design for multi-agent autonomous systems that warrant further exploration.

With regards to the distributed pose estimation problem for multi-agent systems where agents have static positions and time-varying orientations, an interesting direction for future work would be to strengthen the stability properties of the proposed solutions using the hybrid systems framework to achieve global asymptotic stability. In the case of multi-agent systems with time-varying positions and orientations, the proposed attitude observer, although designed directly on $SO(3)$, is endowed with only local exponential stability guarantees, and the basin of attraction shrinks as the number of agents in the network increases. Therefore, the design of a bearing-based distributed attitude estimation scheme with strong stability guarantees, regardless of the number of agents, would be an interesting extension to our proposed scheme.

The problems of distributed attitude estimation and synchronization on $SO(3)$ have been studied in this dissertation under the assumption that the interaction graph topology is an undirected tree, which is practical in terms of communication and sensing costs. However, the main drawback of this graph topology is its vulnerability to failure, since the failure of one agent will engender the disconnection of successive agents. Relaxing this assumption, by considering connected undirected graphs or weakly (strongly) connected

directed graphs, is an interesting future direction that deserves further investigations.

In this dissertation, all proposed distributed cooperative state estimation and control schemes are designed under the assumption that the inter-agent interaction topology is fixed with no communication time-delays. Unfortunately, this is not the case in many real-world multi-agent application scenarios. Hence, redesigning our algorithms for multi-agent rigid body systems under dynamically changing and delayed inter-agent communication topology is an interesting future work.

Bibliography

Abdessameud, A. and Tayebi, A. (2009). Attitude synchronization of a group of space-craft without velocity measurements. *IEEE Transactions on Automatic Control*, 54(11):2642–2648.

Abdessameud, A., Tayebi, A., and Polushin, I. G. (2012). Attitude synchronization of multiple rigid bodies with communication delays. *IEEE Transactions on Automatic Control*, 57(9):2405–2411.

Absil, P.-A., Mahony, R., and Sepulchre, R. (2007). *Optimization Algorithms on Matrix Manifolds*. Princeton University Press.

Angeli, D. (2004). An almost global notion of input-to-state stability. *IEEE Transactions on Automatic Control*, 49(6):866–874.

Angeli, D. and Praly, L. (2011). Stability robustness in the presence of exponentially unstable isolated equilibria. *IEEE Transactions on Automatic Control*, 56(7):1582–1592.

Bai, H., Arcak, M., and Wen, J. T. (2008). Rigid body attitude coordination without inertial frame information. *Automatica*, 44(12):3170–3175.

Bayezit, I. and Fidan, B. (2013). Distributed cohesive motion control of flight vehicle formations. *IEEE Transactions on Industrial Electronics*, 60(12):5763–5772.

Berkane, S. (2017). *Hybrid Attitude Control and Estimation On SO(3)*. PhD thesis, University of Western Ontario.

Berkane, S. and Tayebi, A. (2017). Construction of synergistic potential functions on so(3) with application to velocity-free hybrid attitude stabilization. *IEEE Transactions on Automatic Control*, 62(1):495–501.

Bhat, S. P. and Bernstein, D. S. (2000). A topological obstruction to continuous global stabilization of rotational motion and the unwinding phenomenon. *Systems & Control Letters*, 39(1):63–70.

Bishop, A. N., Shames, I., and Anderson, B. D. (2011). Stabilization of rigid formations with direction-only constraints. In *2011 50th IEEE Conference on Decision and Control and European Control Conference*, pages 746–752.

Boughellaba, M. and Tayebi, A. (2022). Leader-follower bearing-based distributed pose estimation for multi-vehicle networks. In *2022 IEEE 61st Conference on Decision and Control (CDC)*, pages 6562–6567.

Boughellaba, M. and Tayebi, A. (2023a). Bearing-based distributed pose estimation for multi-agent networks. *IEEE Control Systems Letters*, 7:2617–2622.

Boughellaba, M. and Tayebi, A. (2023b). Comments on "pose localization of leader–follower networks with direction measurements" [automatica 120 (2020) 109125]. *Automatica*, 151:110949.

Boughellaba, M. and Tayebi, A. (2023d). Distributed hybrid attitude estimation for multi-agent systems on so(3). In *2023 American Control Conference (ACC)*, pages 1048–1053.

Boughellaba, M. and Tayebi, A. (accepted, 2024). Global attitude alignment for multi-agent systems on *so*(3) without angular velocity measurements. In *American Control Conference (ACC), Toronto, Canada*.

Boughellaba, M. and Tayebi, A. (under review, 2023c). Distributed attitude estimation for multi-agent systems on *so*(3). *IEEE Transactions on Automatic Control*.

Casau, P., Cunha, R., Sanfelice, R. G., and Silvestre, C. (2020). Hybrid control for robust and global tracking on smooth manifolds. *IEEE Transactions on Automatic Control*, 65(5):1870–1885.

Chen, T., Shan, J., and Wen, H. (2019). Distributed adaptive attitude control for networked underactuated flexible spacecraft. *IEEE Transactions on Aerospace and Electronic Systems*, 55(1):215–225.

Darryl D Holm., Tanya Schmah., C. S. (2009). *Geometric mechanics and symmetry: from finite to infinite dimensions*. volume 12. Oxford University Press.

Dimarogonas, D. V., Tsiotras, P., and Kyriakopoulos, K. J. (2009). Leader–follower cooperative attitude control of multiple rigid bodies. *Systems & Control Letters*, 58(6):429–435.

Eren, T. (2012). Formation shape control based on bearing rigidity. *International Journal of Control*, 85(9):1361–1379.

Goebel, R., Sanfelice, R., and Teel, A. (2012). *Hybrid Dynamical Systems: Modeling, Stability, and Robustness*. Princeton University Press.

Goebel, R., Sanfelice, R. G., and Teel, A. R. (2009). Hybrid dynamical systems. *IEEE Control Systems Magazine*, 29(2):28–93.

Gui, H. and de Ruiter, A. H. (2018). Global finite-time attitude consensus of leader-following spacecraft systems based on distributed observers. *Automatica*, 91:225–232.

Hamel, T. and Samson, C. (2018). Riccati observers for the nonstationary pnp problem. *IEEE Transactions on Automatic Control*, 63(3):726–741.

Huang, Y. and Meng, Z. (2021). Global finite-time distributed attitude synchronization and tracking control of multiple rigid bodies without velocity measurements. *Automatica*, 132:109796.

Jin, X., Shi, Y., Tang, Y., and Wu, X. (2020). Event-triggered attitude consensus with absolute and relative attitude measurements. *Automatica*, 122:109245.

Khalil, H. K. (1996). *Nonlinear Systems*. Prentice Hall, 2nd edition.

Koditschek, D. (1989). The application of total energy as a lyapunov function for mechanical control systems. *Contemporary Mathematics, American Mathematical Society, 1989*, 97.

Lee, B.-H. and Ahn, H.-S. (2016a). Distributed estimation for the unknown orientation of the local reference frames in n-dimensional space. In *2016 14th International Conference on Control, Automation, Robotics and Vision (ICARCV)*, pages 1–6.

Lee, B.-H. and Ahn, H.-S. (2016b). Distributed formation control via global orientation estimation. *Automatica*, 73:125–129.

Lee, B.-H., Kang, S.-M., and Ahn, H.-S. (2019). Distributed orientation estimation in so(d) and applications to formation control and network localization. *IEEE Transactions on Control of Network Systems*, 6(4):1302–1312.

Li, X., Luo, X., and Zhao, S. (2020). Globally convergent distributed network localization using locally measured bearings. *IEEE Transactions on Control of Network Systems*, 7(1):245–253.

Liu, T. and Huang, J. (2018). Leader-following attitude consensus of multiple rigid body systems subject to jointly connected switching networks. *Automatica*, 92:63–71.

Loria, A. and Panteley, E. (2002). Uniform exponential stability of linear time-varying systems: revisited. *Systems and Control Letters*, 47(1):13–24.

Maadani, M., Butcher, E. A., and Sanyal, A. K. (2020). Finite-time attitude consensus control of a multi-agent rigid body system. In *2020 American Control Conference (ACC)*, pages 877–882.

Mahony, R., Hamel, T., and Pflimlin, J. (2008). Nonlinear complementary filters on the special orthogonal group. *IEEE Transactions on Automatic Control*, 53(5):1203–1218.

Mao, G., Fidan, B., and Anderson, B. D. (2007). Wireless sensor network localization techniques. *Computer Networks*, 51(10):2529–2553.

Markdahl, J. (2021). Synchronization on riemannian manifolds: Multiply connected implies multistable. *IEEE Transactions on Automatic Control*, 66(9):4311–4318.

Mayhew, C. G., Sanfelice, R. G., Sheng, J., Arcak, M., and Teel, A. R. (2012). Quaternion-based hybrid feedback for robust global attitude synchronization. *IEEE Transactions on Automatic Control*, 57(8):2122–2127.

Mayhew, C. G. and Teel, A. R. (2011a). Hybrid control of rigid-body attitude with synergistic potential functions. In *Proceedings of the 2011 American Control Conference*, pages 287–292.

Mayhew, C. G. and Teel, A. R. (2011b). Synergistic potential functions for hybrid control of rigid-body attitude. In *Proceedings of the 2011 American Control Conference*, pages 875–880.

Mayhew, C. G. and Teel, A. R. (2013). Synergistic hybrid feedback for global rigid-body attitude tracking on *so*(3). *IEEE Transactions on Automatic Control*, 58(11):2730–2742.

Meng, Z., Ren, W., and You, Z. (2010). Distributed finite-time attitude containment control for multiple rigid bodies. *Automatica*, 46(12):2092–2099.

Mesbahi, M. and Egerstedt, M. (2010). *Graph Theoretic Methods in Multiagent Networks*. Princeton University Press, Princeton.

Morse, M. (1934). *The calculus of variations in the large*, volume 18. American Mathematical Soc.

Moshtagh, N., Michael, N., Jadbabaie, A., and Daniilidis, K. (2009). Vision-based, distributed control laws for motion coordination of nonholonomic robots. *IEEE Transactions on Robotics*, 25(4):851–860.

Oh, K.-K. and Ahn, H.-S. (2011). Formation control of mobile agents based on inter-agent distance dynamics. *Automatica*, 47(10):2306–2312.

Oh, K.-K. and Ahn, H.-S. (2014). Formation control and network localization via orientation alignment. *IEEE Transactions on Automatic Control*, 59(2):540–545.

Pereira, P. O., Boskos, D., and Dimarogonas, D. V. (2020). A common framework for complete and incomplete attitude synchronization in networks with switching topology. *IEEE Transactions on Automatic Control*, 65(1):271–278.

Perko, L. (2000). *Differential Equations and Dynamical Systems*. Springer, third edition.

Ren, W. (2007). Distributed attitude alignment in spacecraft formation flying. *International Journal of Adaptive Control and Signal Processing*, 21(2-3):95–113.

Ren, W. (2010). Distributed cooperative attitude synchronization and tracking for multiple rigid bodies. *IEEE Transactions on Control Systems Technology*, 18(2):383–392.

Ren, W. and Atkins, E. (2007). Distributed multi-vehicle coordinated control via local information exchange. *International Journal of Robust and Nonlinear Control: IFAC-Affiliated Journal*, 17(10-11):1002–1033.

Ren, W. and Beard, R. W. (2007). *Distributed Consensus in Multi-Vehicle Cooperative Control: Theory and Applications*. Springer Publishing Company, Incorporated, 1st edition.

Ren, W. and Cao, Y. (2011). Distributed coordination of multi-agent networks. communications and control engineering series.

Sanfelice, R., Copp, D., and Nanez, P. (2013). A toolbox for simulation of hybrid systems in matlab/simulink: Hybrid equations (hyeq) toolbox. In *Proceedings of the 16th International Conference on Hybrid Systems: Computation and Control*, page 101–106, New York, USA.

Sanfelice, R. G., Goebel, R., and Teel, A. R. (2007). Invariance principles for hybrid systems with connections to detectability and asymptotic stability. *IEEE Transactions on Automatic Control*, 52(12):2282–2297.

Sarlette, A. and Sepulchre, R. (2009a). Consensus optimization on manifolds. *SIAM journal on control and optimization*, 48(1).

Sarlette, A. and Sepulchre, R. (2009b). Consensus optimization on manifolds. *SIAM Journal on Control and Optimization*, 48(1):56–76.

Sarlette, A., Sepulchre, R., and Leonard, N. E. (2007). Cooperative attitude synchronization in satellite swarms: A consensus approach. *IFAC Proceedings Volumes*, 40(7):223–228. 17th IFAC Symposium on Automatic Control in Aerospace.

Sarlette, A., Sepulchre, R., and Leonard, N. E. (2009). Autonomous rigid body attitude synchronization. *Automatica*, 45(2):572–577.

Shuster, M. D. (1993). A survey of attitude representation. *Journal of The Astronautical Sciences*, 41:439–517.

Tang, Z. (2023). Distributed bearing-based localization under switching graph topologies. *IFAC-PapersOnLine*, 56(2):9487–9492. 22nd IFAC World Congress.

Tang, Z., Cunha, R., Hamel, T., and Silvestre, C. (2020b). Bearing-only formation control under persistence of excitation. In *2020 59th IEEE Conference on Decision and Control (CDC)*, pages 4011–4016.

Tang, Z., Cunha, R., Hamel, T., and Silvestre, C. (2021). Formation control of a leader–follower structure in three dimensional space using bearing measurements. *Automatica*, 128:109567.

Tang, Z., Cunha, R., Hamel, T., and Silvestre, C. (2022). Relaxed bearing rigidity and bearing formation control under persistence of excitation. *Automatica*, 141:110289.

Tang, Z., Cunha, R., Hamel, T., and Silvestre, C. (Accepted, 2020.a). Bearing leader-follower formation control under persistence of excitation. *in 2020 IFAC World congress*.

Tang, Z. and Loría, A. (2023a). Localization and tracking control of autonomous vehicles in time-varying bearing formation. *IEEE Control Systems Letters*, 7:1231–1236.

Tang, Z. and Loría, A. (2023b). Localization and tracking control of autonomous vehicles in time-varying bearing formation. *IEEE Control Systems Letters*, 7:1231–1236.

Tayebi, A. (2008). Unit quaternion-based output feedback for the attitude tracking problem. *IEEE Transactions on Automatic Control*, 53(6):1516–1520.

Tran, Q. V., Anderson, B. D., and Ahn, H.-S. (2020). Pose localization of leader–follower networks with direction measurements. *Automatica*, 120:109125.

Tran, Q. V., Anderson, B. D., and Ahn, H.-S. (2023). Authors' reply to 'comments on "pose localization of leader-follower networks with direction measurements" [automatica 120 (2020) 109125]'. *Automatica*, 151:110950.

Tran, Q. V., Anderson, B. D. O., and Ahn, H.-S. (2019). Pose localization of leader-follower networks with direction measurements. *arXiv:1910.03978*.

Tron, R., Afsari, B., and Vidal, R. (2011). Average consensus on riemannian manifolds with bounded curvature. In *2011 50th IEEE Conference on Decision and Control and European Control Conference*, pages 7855–7862.

Tron, R., Afsari, B., and Vidal, R. (2012). Intrinsic consensus on so(3) with almost-global convergence. In *2012 IEEE 51st IEEE Conference on Decision and Control (CDC)*, pages 2052–2058.

Tron, R., Afsari, B., and Vidal, R. (2013). Riemannian consensus for manifolds with bounded curvature. *IEEE Transactions on Automatic Control*, 58(4):921–934.

Tron, R., Thomas, J., Loianno, G., Daniilidis, K., and Kumar, V. (2016). A distributed optimization framework for localization and formation control: Applications to vision-based measurements. *IEEE Control Systems Magazine*, 36(4):22–44.

Tron, R. and Vidal, R. (2014). Distributed 3-d localization of camera sensor networks from 2-d image measurements. *IEEE Transactions on Automatic Control*, 59(12):3325–3340.

Van Tran, Q. and Ahn, H.-S. (2020). Distributed formation control of mobile agents via global orientation estimation. *IEEE Transactions on Control of Network Systems*, 7(4):1654–1664.

Van Tran, Q., Ahn, H.-S., and Kim, J. (2022). Direction-only orientation alignment of leader-follower networks. In *2022 American Control Conference (ACC)*, pages 2142–2147.

Van Tran, Q., Ahn, H.-S., and O. Anderson, B. D. (2018). Distributed orientation localization of multi-agent systems in 3-dimensional space with direction-only measurements. In *2018 IEEE Conference on Decision and Control (CDC)*, pages 2883–2889.

Van Tran, Q., Trinh, M. H., Zelazo, D., Mukherjee, D., and Ahn, H.-S. (2019). Finite-time bearing-only formation control via distributed global orientation estimation. *IEEE Transactions on Control of Network Systems*, 6(2):702–712.

Wang, M., Berkane, S., and Tayebi, A. (2021). Nonlinear observers design for vision-aided inertial navigation systems. *IEEE Transactions on Automatic Control*, pages 1–1.

Wang, M. and Tayebi, A. (2021). Nonlinear attitude estimation using intermittent linear velocity and vector measurements. In *2021 60th IEEE Conference on Decision and Control (CDC)*, pages 4707–4712.

Wang, M. and Tayebi, A. (2022). Hybrid feedback for global tracking on matrix lie groups *so*(3) and *se*(3). *IEEE Transactions on Automatic Control*, 67(6):2930–2945.

Wei, J., Zhang, S., Adaldo, A., Thunberg, J., Hu, X., and Johansson, K. H. (2018). Finite-time attitude synchronization with distributed discontinuous protocols. *IEEE Transactions on Automatic Control*, 63(10):3608–3615.

Zhang, D., Tang, Y., Jin, X., and Kurths, J. (2022). Quaternion-based attitude synchronization with an event-based communication strategy. *IEEE Transactions on Circuits and Systems I: Regular Papers*, 69(3):1333–1346.

Zhao, S. and Zelazo, D. (2015). Bearing-based formation stabilization with directed interaction topologies. In *2015 54th IEEE Conference on Decision and Control (CDC)*, pages 6115–6120.

Zhao, S. and Zelazo, D. (2016). Bearing rigidity and almost global bearing-only formation stabilization. *IEEE Transactions on Automatic Control*, 61(5):1255–1268.

Zhao, S. and Zelazo, D. (2016). Localizability and distributed protocols for bearing-based network localization in arbitrary dimensions. *Automatica*, 69:334–341.

Zhao, S. and Zelazo, D. (2019). Bearing rigidity theory and its applications for control and estimation of network systems: Life beyond distance rigidity. *IEEE Control Systems Magazine*, 39(2):66–83.

Appendix A

Proofs of Chapter 3

A.1 Proof of Lemma 3.1

Consider the following Lyapunov function candidate:

$$\mathcal{L}_i = \frac{1}{4}\text{tr}\left(M_i\left(I_3 - \tilde{R}_i\right)\right), \tag{A.1}$$

whose time-derivative, along the trajectories of (3.7), is given by

$$\dot{\mathcal{L}}_i = \frac{k_R}{2}\text{tr}\left(M_i\tilde{R}_i\left[\psi(M_i\tilde{R}_i)\right]^\times\right). \tag{A.2}$$

Using identities (2.23) and (2.33), one has

$$\dot{\mathcal{L}}_i = -k_R||\psi(M_i\tilde{R}_i)||^2 \leq 0. \tag{A.3}$$

Since system (3.7) is autonomous, by virtue of LaSalle's invariance theorem, the attitude error $\tilde{R}_i$ should converge to the largest invariant set contained in the set characterized by $\dot{\mathcal{L}}_i = 0$, *i.e.*, $\psi(M_i\tilde{R}_i) = 0$. As per Lemma 2.4, $\psi(M_i\tilde{R}_i) = 0$ implies that $\tilde{R}_i \in \Upsilon$. Since the matrix M_i is positive semi-definite with three distinct eigenvalues, it follows that the equilibrium points, in the set Υ, are isolated. Moreover, following the same arguments as in (Wang et al., 2021, Theorem 1), one can show that the desired equilibrium $\tilde{R}_i = I_3$ is locally exponentially stable and the dynamics of the first order approximation of $\tilde{R}_i$ around each undesired equilibrium has at least one positive eigenvalue. Accordingly, the desired equilibrium $\tilde{R}_i = I_3$ of (3.7) is AGAS. This completes the proof.

A.2 Proof of Lemma 3.2

Since system (3.6), subject to the bounded input $\sum_{j\in\mathcal{N}_i} k_{ij}g_{ij}(\tilde{R}_j)$, evolves on the compact manifold $SO(3)$, Assumption 2.1 is fulfilled. Moreover, according to Lemma 3.1, Assumptions 2.2 and 2.3 are also fulfilled. Now, consider the following real-valued function:

$$|\tilde{R}_i|_I^2 = \frac{1}{4}\text{tr}(I_3 - \tilde{R}_i), \tag{A.4}$$

whose time-derivative, along the trajectories of (3.6), is given by

$$\frac{d}{dt}|\tilde{R}_i|_I^2 = -k_R\psi(\tilde{R}_i)^T\left(\psi(M_i\tilde{R}_i) - \frac{1}{2}\sum_{j\in\mathcal{N}_i}k_{ij}g_{ij}(\tilde{R}_j)\right). \tag{A.5}$$

The last equation was obtained using identities (2.23) and (2.33). Moreover, since $\psi(\tilde{R}_i)^T$ $\psi(M_i\tilde{R}_i) = \psi(\tilde{R}_i)^T Q_i\psi(\tilde{R}_i)$, with $Q_i := \sum_{j\in\mathcal{N}_i}k_{ij}\left([b_{ij}]^\times\right)^T[b_{ij}]^\times$, one has

$$\frac{d}{dt}|\tilde{R}_i|_I^2 = -k_R\psi(\tilde{R}_i)^T\left(Q_i\psi(\tilde{R}_i) - \frac{1}{2}\sum_{j\in\mathcal{N}_i}k_{ij}g_{ij}(\tilde{R}_j)\right). \tag{A.6}$$

Using the fact that $||\psi(\tilde{R}_i)||^2 = 4(1 - |\tilde{R}_i|_I^2)|\tilde{R}_i|_I^2 \le 1$ and at least two bearing vectors are noncollinear, one obtains

$$\frac{d}{dt}|\tilde{R}_i|_I^2 \le -4k_R\underline{\lambda}^{Q_i}(1 - |\tilde{R}_i|_I^2)|\tilde{R}_i|_I^2 + \frac{k_R}{2}||\sum_{j\in\mathcal{N}_i}k_{ij}g_{ij}(\tilde{R}_j)||$$

$$\le -4k_R\underline{\lambda}^{Q_i}|\tilde{R}_i|_I^2 + 4k_R\underline{\lambda}^{Q_i} + \frac{k_R}{2}\sum_{j\in\mathcal{N}_i}k_{ij}||g_{ij}(\tilde{R}_j)||. \tag{A.7}$$

Recall that $\underline{\lambda}^{Q_i}$ is the smallest eigenvalue of Q_i, which is positive definite under the assumption that at least two bearing vectors are noncollinear. Furthermore, using the fact given in (2.36), one verifies that $||g_{ij}(\tilde{R}_j)|| \le 2\sqrt{2}|\tilde{R}_j|_I$. Hence, it follows from (A.7) that

$$\frac{d}{dt}|\tilde{R}_i|_I^2 \le -4k_R\underline{\lambda}^{Q_i}|\tilde{R}_i|_I^2 + 4k_R\underline{\lambda}^{Q_i} + \sqrt{2}k_R\sum_{j\in\mathcal{N}_i}k_{ij}|\tilde{R}_j|_I. \tag{A.8}$$

It is clear that, in view of (A.8), system (3.6) satisfies the ultimate boundedness property according to Lemma 2.5. Consequently, as per Theorem 2.4, one can conclude that system (3.6) is almost globally ISS with respect to I_3 and inputs $\tilde{R}_j$.

A.3 Proof of Theorem 3.1

Consider the following cascaded attitude dynamics of n-agent rigid-body system:

$$\dot{\tilde{R}}_3 = -2k_R\tilde{R}_3\left[\psi(M_3\tilde{R}_3)\right]^\times \tag{A.9}$$

$$\dot{\tilde{R}}_4 = -2k_R\tilde{R}_4\left[\psi(M_4\tilde{R}_4)\right]^\times + k_R\tilde{R}_4\left[\sum_{j\in\mathcal{N}_4}k_{4j}g_{4j}(\tilde{R}_j)\right]^\times \tag{A.10}$$

$$\vdots$$

$$\dot{\tilde{R}}_{n-1} = -2k_R\tilde{R}_{n-1}\left[\psi(M_{n-1}\tilde{R}_{n-1})\right]^\times + k_R\tilde{R}_{n-1}\left[\sum_{j\in\mathcal{N}_{n-1}}k_{(n-1)j}g_{(n-1)j}(\tilde{R}_j)\right]^\times \tag{A.11}$$

$$\dot{\tilde{R}}_n = -2k_R\tilde{R}_n \left[\psi(M_n\tilde{R}_n)\right]^\times + k_R\tilde{R}_n \left[\sum_{j\in\mathcal{N}_n} k_{nj}g_{nj}(\tilde{R}_j)\right]^\times, \tag{A.12}$$

where M_i is positive semi-definite with three distinct eigenvalues and $\hat{R}_l = R_l$ (*i.e.*, $\tilde{R}_l = I_3$), $l \in \{1,2\}$, as per Assumption 3.2. Next, consider the following result, which will be used in the stability analysis of the cascaded system (A.9)-(A.12):

Proposition A.1 *Under Assumption 3.2, the equilibrium point $(\tilde{R}_3 = I_3, \tilde{R}_4 = I_3)$ of system* (A.9)-(A.10) *is AGAS.*

Proof According to Assumption 3.2, one has either $3 \in \mathcal{N}_4$ or $3 \notin \mathcal{N}_4$. In the case where $3 \notin \mathcal{N}_4$, the $\tilde{R}_3$-subsystem and the $\tilde{R}_4$-subsystem are independent, and the AGAS of the equilibrium point $(\tilde{R}_3 = I_3, \tilde{R}_4 = I_3)$ can be directly deduced from Lemma 3.1. On the other hand, if $3 \in \mathcal{N}_4$, the two subsystems ($\tilde{R}_3$-subsystem and $\tilde{R}_4$-subsystem) are cascaded, and as such, in view of Lemma 3.1 and Lemma 3.2, it follows that the $\tilde{R}_4$-subsystem is almost globally ISS with respect to I_3 and input $\tilde{R}_3$, and the equilibrium $\tilde{R}_3 = I_3$ of the $\tilde{R}_3$-subsystem is AGAS. Finally, in view of Theorem 2.5, it follows that the cascaded system (A.9)-(A.10) is AGAS at $(\tilde{R}_3 = I_3, \tilde{R}_4 = I_3)$.

Now, we will establish the stability properties of the n-agent cascaded system (A.9)-(A.12). Due to the cascaded structure of the inter-agent interaction, a mathematical induction procedure is used to prove that the equilibrium point $(\tilde{R}_3 = I_3, \tilde{R}_4 = I_3, \ldots, \tilde{R}_n = I_3)$ of the n-agent cascaded system (A.9)-(A.12) is AGAS. First, it follows from Lemma 3.1 that the equilibrium point $\tilde{R}_3 = I_3$ of the subsystem (A.9) is AGAS. Moreover, according to Proposition A.1, the equilibrium point $(\tilde{R}_3 = I_3, \tilde{R}_4 = I_3)$ of system (A.9)-(A.10) is AGAS. Second, we assume that the equilibium $(\tilde{R}_3 = I_3, \tilde{R}_4 = I_3, \ldots, \tilde{R}_{n-1} = I_3)$ of the cascaded $(n-1)$-agent subsystem (A.9)-(A.11) is AGAS. Finally, using the facts that the $\tilde{R}_n$-subsystem is almost globally ISS with respect to I_3 and inputs from the cascaded $(n-1)$-agent subsystem (A.9)-(A.11) as per Lemma 3.2 and the equilibrium $(\tilde{R}_3 = I_3, \tilde{R}_4 = I_3, \ldots, \tilde{R}_{n-1} = I_3)$ of the cascaded $(n-1)$-agent subsystem (A.9)-(A.11) is AGAS by the induction assumption, one can show that the equilibrium $(\tilde{R}_3 = I_3, \tilde{R}_4 = I_3, \ldots, \tilde{R}_n = I_3)$ of the n-agent cascaded system is AGAS according to Theorem 2.5 . This completes the proof.

A.4 Proof of Lemma 3.3

Consider the following Lyapunov function candidate:

$$\mathcal{L}_i = \text{tr}\left(M_i\left(I_3 - \tilde{R}_i\right)\right) + \frac{1}{2}\Omega_i^T\Omega_i, \tag{A.13}$$

whose time-derivative, along the trajectories of (3.12)-(3.13) is given by

$$\dot{\mathcal{L}}_i = -\text{tr}\left(M_i\tilde{R}_i[\Omega_i]^\times\right) + \Omega_i^T\left(-k_\Omega\Omega_i - 2\psi\left(M_i\tilde{R}_i\right)\right)$$
$$= -k_\Omega||\Omega_i||^2 \leq 0. \tag{A.14}$$

Since system (3.12)-(3.13) is autonomous, according to LaSalle's invariance theorem, $\tilde{R}_i$ and Ω_i will converge to the largest invariant set contained in the set characterized by $\dot{\mathcal{L}}_i = 0$. Through a simple signal chasing, one can show that $\dot{\mathcal{L}}_i = 0 \Rightarrow \Omega_i = 0 \Rightarrow \dot{\Omega}_i = 0 \Rightarrow \psi(M_i\tilde{R}_i) = 0$. Consequently, the solution of (3.12)-(3.13) converges to the set Υ_1. This completes the proof of item (i).

Now, we will establish the stability properties of each equilibrium point. We start with the desired one, and we define the following first order approximation of $\tilde{R}_i$ and Ω_i around $(I_3, 0)$ as $\tilde{R}_i = I_3 + [x_i^s]^\times$ and $\Omega_i = y_i^s$, respectively, where $x_i^s, y_i^s \in \mathbb{R}^3$ are sufficiently small. By neglecting the cross terms and using property (2.24), one obtains the dynamics of x_i^s and y_i^s as follows:

$$\begin{pmatrix} \dot{x}_i^s \\ \dot{y}_i^s \end{pmatrix} = A_i^s \begin{pmatrix} x_i^s \\ y_i^s \end{pmatrix}, \tag{A.15}$$

where $A_i^s := \begin{pmatrix} 0_{3\times 3} & I_3 \\ -\bar{M}_i & -k_\Omega I_3 \end{pmatrix}$ with $\bar{M}_i := \text{tr}(M_i)I_3 - M_i$. The eigenvalues of A_i^s are given by $\lambda_{i\pm}^l = \frac{-k_\Omega \pm \sqrt{k_\Omega^2 + 4\mu_i^l}}{2}$, where μ_i^l is the lth eigenvalue of $-\bar{M}_i$. Since $\bar{M}_i$ is positive definite, the matrix A_i^s is Hurwitz. This completes the proof of item (ii).

Next, we define $\tilde{R}_i = R_i^*(I_3 + [x_i^u]^\times)$ and $\Omega_i = y_i^u$, for each $v_i \in \mathcal{E}(K_i)$, to be the first order approximation of $\tilde{R}_i$ and Ω_i around the three undesired equilibria $\Upsilon_1/(I_3, 0)$, such that $R_i^* := \mathcal{R}(\pi, v_i) = -I_3 + 2v_i v_i^T$ and $x_i^u, y_i^u \in \mathbb{R}^3$ are sufficiently small. Again, by neglecting the cross terms and using property (2.24), the dynamics of x_i^u and y_i^u are given by

$$\begin{pmatrix} \dot{x}_i^u \\ \dot{y}_i^u \end{pmatrix} = A_i^u \begin{pmatrix} x_i^u \\ y_i^u \end{pmatrix} \tag{A.16}$$

where $A_i^u := \begin{pmatrix} 0_{3\times 3} & I_3 \\ -\bar{\bar{M}}_i & -k_\Omega I_3 \end{pmatrix}$ with $\bar{\bar{M}}_i := \text{tr}(M_i R_i^*)I_3 - (M_i R_i^*)^T$. The eigenvalues of A_i^u are given by $\bar{\lambda}_{i\pm}^l = \frac{-k_\Omega \pm \sqrt{k_\Omega^2 + 4\bar{\mu}_i^l}}{2}$, where $\bar{\mu}_i^l$ is the lth eigenvalue of $-\bar{\bar{K}}_i$. Using the fact that M_i is positive semi-definite with three distinct eigenvalues, one verifies that $-v_i^T \bar{\bar{M}}_i v_i = \text{tr}(M_i) - v_i^T M_i v_i > 0$, which implies that, for each $v_i \in \mathcal{E}(M_i)$, the matrix A_i^u has at least one positive eigenvalue, and hence, the equilibria $\Upsilon_1/\{(I_3, 0)\}$ are unstable. Finally, due to the fact that A_i^u has at least one positive eigenvalue, invoking the stable manifold theorem (Perko, 2000), one can conclude that the stable manifold associated to the undesired equilibria has zero Lebesgue measure, and as such, the equilibrium $(I_3, 0)$ is AGAS. This completes the proof of items (iii) and (iv).

A.5 Proof of Lemma 3.4

First, we show that system (3.10)-(3.11) satisfies Assumption 2.1-2.3. It follows from (3.11) that

$$\Omega_i(t) = e^{-k_\Omega t}\Omega_i(0) + \int_0^t e^{-k_\Omega(t-\tau)}u_i(\tau)d\tau, \tag{A.17}$$

where $u_i(t) := -2\psi(M_i\tilde{R}_i) + \sum_{j\in\mathcal{N}_i} k_{ij}g_{ij}(\tilde{R}_j)$. Using the fact that $||g_{ij}(\tilde{R}_j)|| \leq 2\sqrt{2}|\tilde{R}_j|_I$ and identity (2.48), one has

$$||\Omega_i(t)|| \leq e^{-k_\Omega t}||\Omega_i(0)|| + \frac{\bar{u}_i}{k_\Omega}\left(1 - e^{-k_\Omega t}\right), \tag{A.18}$$

where $\bar{u}_i := 4\sqrt{\bar{\lambda}_{\bar{M}_i}} + 2\sqrt{2}\bar{k}_{ij}|\mathcal{N}_i|$ with $\bar{k}_{ij} := \max_{j\in\mathcal{N}_i}\{k_{ij}\}$ and $\bar{M}_i := \frac{1}{2}(\text{tr}(M_i)I_3 - M_i)$. From the last inequality, one can deduce that $||\Omega_i(t)||$ is upper bounded since $||\Omega_i(t)||$ is either increasing from $||\Omega_i(0)||$ to $\bar{u}_i/k_\Omega$ (if $||\Omega_i(0)|| \leq \bar{u}_i/k_\Omega$), or decreasing from $||\Omega_i(0)||$ to $\bar{u}_i/k_\Omega$ (if $||\Omega_i(0)|| \geq \bar{u}_i/k_\Omega$). Therefore, in both cases and for every $\epsilon_\Omega > 0$, picking $k_\Omega > \bar{u}_i/(||\Omega_i(0)|| + \epsilon_\Omega)$, one can verify that $||\Omega_i(t)|| \leq ||\Omega_i(0)|| + \epsilon_\Omega := \bar{\Omega}_i$. Since $||\Omega_i(t)||$ is bounded, one concludes that Ω_i belongs to a compact set $\mathcal{A} \subset \mathbb{R}^3$. Consequently, Assumption 2.1 holds since system (3.10)-(3.11), subject to the bounded inputs $d_i(t)$, evolves on the compact manifold $SO(3)\times\mathcal{A}$. Moreover, according to Lemma 3.3, Assumptions 2.2 and 2.3 are also fulfilled.

Now, consider the following real-valued function:

$$W_i = k_i\text{tr}\left(M_i(I_3 - \tilde{R}_i)\right) + \frac{1}{2}k_i\Omega_i^T\Omega_i + \Omega_i^T\psi(\tilde{R}_i),$$

with $k_i > 0$. Using the fact that $||\psi(\tilde{R}_i)|| \leq 2|\tilde{R}_i|_I$ and identity (2.46), and letting $\zeta_i := [|\tilde{R}_i|_I \ \ ||\tilde{\Omega}_i||]^T$, one has $\zeta_i^T P_1\zeta_i \leq W_i \leq \zeta_i^T P_2\zeta_i$, where

$$P_1 := \begin{pmatrix} 4k_i\underline{\lambda}^{\bar{M}_i} & -1 \\ -1 & \frac{k_i}{2} \end{pmatrix}, \quad P_2 := \begin{pmatrix} 4k_i\bar{\lambda}^{\bar{M}_i} & 1 \\ 1 & \frac{k_i}{2} \end{pmatrix},$$

with $\bar{M}_i := \text{tr}(M_i)I_3 - M_i$. The time derivative of W_i along the trajectories of (3.10)-(3.11) satisfies

$$\dot{W}_i = -k_i\text{tr}\left(M_i\tilde{R}_i[\Omega_i]^\times\right) + \left(k_i\Omega_i^T + \psi(\tilde{R}_i)^T\right)\left(-k_\Omega\Omega_i - 2\psi(M_i\tilde{R}_i) + \sum_{j\in\mathcal{N}_i} k_{ij}g_{ij}(\tilde{R}_j)\right)$$

$$+ \Omega_i^T E(\tilde{R}_i)\Omega_i$$

$$= -k_ik_\Omega\Omega_i^T\Omega_i - k_\Omega\psi(\tilde{R}_i)^T\Omega_i - 2\psi(\tilde{R}_i)^T\psi(M_i\tilde{R}_i) + k_i\Omega_i^T\sum_{j\in\mathcal{N}_i} k_{ij}g_{ij}(\tilde{R}_j)$$

$$+ \psi(\tilde{R}_i)^T\sum_{j\in\mathcal{N}_i} k_{ij}g_{ij}(\tilde{R}_j) + \Omega_i^T E(\tilde{R}_i)\Omega_i, \tag{A.19}$$

where $E(\tilde{R}_i) := \frac{1}{2}(\text{tr}(\tilde{R}_i)I_3 - \tilde{R}_i)$. Using the fact that $||E(\tilde{R}_i)||_F \leq \sqrt{3}$, $\psi(\tilde{R}_i)^T\psi(M_i\tilde{R}_i) = \psi(\tilde{R}_i)^T Q_i\psi(\tilde{R}_i)$, with $Q_i := \sum_{j\in\mathcal{N}_i} k_{ij}([b_{ij}]^\times)^T[b_{ij}]^\times$, one has

$$\dot{W}_i \leq -k_ik_\Omega||\Omega_i||^2 + k_\Omega||\psi(\tilde{R}_i)||||\Omega_i|| - 2\underline{\lambda}^{Q_i}||\psi(\tilde{R}_i)||^2 + k_i||\Omega_i||\sum_{j\in\mathcal{N}_i} k_{ij}||g_{ij}(\tilde{R}_j)||$$

$$+ ||\psi(\tilde{R}_i)||\sum_{j\in\mathcal{N}_i} k_{ij}||g_{ij}(\tilde{R}_j)|| + \sqrt{3}||\Omega_i||^2 \tag{A.20}$$

Furthermore, according to identity (2.48) and the fact that $|\tilde{R}_i|_I^2 \leq 1$, it follows that

$$
\begin{aligned}
\dot{W}_i &\leq -k_i k_\Omega ||\Omega_i||^2 + 2k_\Omega |\tilde{R}_i|_I ||\Omega_i|| - 8\underline{\lambda}^{Q_i}(1 - |\tilde{R}_i|_I^2)|\tilde{R}_i|_I^2 + k_i \bar{\Omega}_i \sum_{j \in \mathcal{N}_i} k_{ij} ||g_{ij}(\tilde{R}_j)|| \\
&\quad + 2 \sum_{j \in \mathcal{N}_i} k_{ij} ||g_{ij}(\tilde{R}_j)|| + \sqrt{3}||\Omega_i||^2 \\
&\leq -k_i k_\Omega ||\Omega_i||^2 + 2k_\Omega |\tilde{R}_i|_I ||\Omega_i|| - 8\underline{\lambda}^{Q_i}(1 - |\tilde{R}_i|_I^2)|\tilde{R}_i|_I^2 + 2\sqrt{2} k_i \bar{\Omega}_i \sum_{j \in \mathcal{N}_i} k_{ij} |\tilde{R}_j|_I \\
&\quad + 4\sqrt{2} \sum_{j \in \mathcal{N}_i} k_{ij} |\tilde{R}_j|_I + \sqrt{3}||\Omega_i||^2 \quad\quad\quad\quad\quad\quad\quad\quad\quad\quad\quad\quad\quad\quad (A.21) \\
&\leq -\zeta_i^T P_3 \zeta_i + 8\underline{\lambda}^{Q_i} + 2\sqrt{2}(2 + k_i \bar{\Omega}_i) \sum_{j \in \mathcal{N}_i} k_{ij} |\tilde{R}_j|_I, \quad\quad\quad\quad\quad\quad\quad (A.22)
\end{aligned}
$$

where $P_3 := \begin{pmatrix} 8\underline{\lambda}^{Q_i} & -k_\Omega \\ -k_\Omega & k_i k_\Omega - \sqrt{3} \end{pmatrix}$. Inequality (A.21) was obtained using the fact that $||g_{ij}(\tilde{R}_j)|| \leq 2\sqrt{2}|\tilde{R}_j|_I$. Choosing $k_i > 0$ such that $k_i > \max\{\frac{\sqrt{3}}{k_\Omega}, \frac{k_\Omega^2 + 8\sqrt{3}\underline{\lambda}^{Q_i}}{8\underline{\lambda}^{Q_i} k_\Omega}, \frac{1}{\sqrt{2\underline{\lambda}^{M_i}}}\}$, one verifies that P_1, P_2 and P_3 are positive definite matrices. It follows from (A.22) that the system (3.10)-(3.11) satisfies the ultimate boundedness property as per Lemma 2.5. Hence, system (3.10)-(3.11) is almost globally ISS with respect to $(I_3, 0)$ and inputs $\tilde{R}_j$ according to Theorem 2.4.

A.6 Proof of Theorem 3.2

According to (3.10)-(3.11), one has the following cascaded dynamics:

$$
\begin{aligned}
\dot{\tilde{R}}_3 &= \tilde{R}_3 [\Omega_3]^\times & (A.23) \\
\dot{\Omega}_3 &= -k_\Omega \Omega_3 - 2\psi(M_3 \tilde{R}_3) & (A.24) \\
\dot{\tilde{R}}_4 &= \tilde{R}_4 [\Omega_4]^\times & (A.25) \\
\dot{\Omega}_4 &= -k_\Omega \Omega_4 - 2\psi(M_4 \tilde{R}_4) + \sum_{j \in \mathcal{N}_4} k_{4j} g_{4j}(\tilde{R}_j) & (A.26) \\
&\quad\vdots \\
\dot{\tilde{R}}_{n-1} &= \tilde{R}_{n-1} [\Omega_{n-1}]^\times & (A.27) \\
\dot{\Omega}_{n-1} &= -k_\Omega \Omega_{n-1} - 2\psi(M_{n-1} \tilde{R}_{n-1}) + \sum_{j \in \mathcal{N}_{n-1}} k_{(n-1)j} g_{(n-1)j}(\tilde{R}_j) & (A.28) \\
\dot{\tilde{R}}_n &= \tilde{R}_n [\Omega_n]^\times & (A.29) \\
\dot{\Omega}_n &= -k_\Omega \Omega_n - 2\psi(M_n \tilde{R}_n) + \sum_{j \in \mathcal{N}_n} k_{nj} g_{nj}(\tilde{R}_j) & (A.30)
\end{aligned}
$$

where M_i, $i \in \mathcal{V}_f$, is positive semi-definite with three distinct eigenvalues and $\hat{R}_l = R_l$ (i.e., $\tilde{R}_l = I_3$), $l \in \{1, 2\}$, as per Assumption 3.2. Again, relying on the cascaded

structure of the inter-agent interaction, a proof by induction, similar to the proof of Theorem 3.1, will be used, along with Lemma 3.3 and Lemma 3.4, to show that the equilibrium point $(\tilde{R}_3 = I_3, \Omega_3 = 0, \tilde{R}_4 = I_3, \Omega_4 = 0, \dots, \tilde{R}_n = I_3, \Omega_n = 0)$ of the n-agent rigid-body system, governed by the cascaded dynamics (A.23)-(A.30), is AGAS. First, according to Lemma 3.3, it is clear that the equilibrium point $(\tilde{R}_3 = I_3, \Omega_3 = 0)$ of the subsystem (A.23)-(A.24) is AGAS. Furthermore, following similar arguments as in the proof of Proposition A.1, one can show that the equilibrium point $(\tilde{R}_3 = I_3, \Omega_3 = 0, \tilde{R}_4 = I_3, \Omega_4 = 0)$ of the subsystem (A.23)-(A.26) is AGAS. Second, we assume that the equilibrium $(\tilde{R}_3 = I_3, \Omega_3 = 0, \tilde{R}_4 = I_3, \Omega_4 = 0, \dots, \tilde{R}_{n-1} = I_3, \Omega_{n-1} = 0)$ of the cascaded $(n-1)$-agent subsystem (A.23)-(A.28) is AGAS. Finally, based on the facts that the subsystem (A.29)-(A.30) is almost globally ISS with respect to I_3 and inputs from the cascaded $(n-1)$-agent subsystem (A.23)-(A.28), and the equilibrium $(\tilde{R}_3 = I_3, \Omega_3 = 0, \tilde{R}_4 = I_3, \Omega_4 = 0, \dots, \tilde{R}_{n-1} = I_3, \Omega_{n-1} = 0)$ of the cascaded $(n-1)$-agent subsystem (A.23)-(A.28) is AGAS as per the induction assumption, one can show that the equilibrium $(\tilde{R}_3 = I_3, \Omega_3 = 0, \tilde{R}_4 = I_3, \Omega_4 = 0 \dots, \tilde{R}_n = I_3, \Omega_n = 0)$ of the cascaded n-agent system (A.23)-(A.30) is AGAS according to Theorem 2.5. This completes the proof.

A.7 Proof of Lemma 3.5

Consider the following Lyapunov function candidate:

$$V_i = \frac{1}{2}\tilde{p}_i^T \tilde{p}_i, \tag{A.31}$$

whose time-derivative, along the trajectories of (3.16), is given by

$$\dot{V}_i = \tilde{p}_i^T \left(-k_p \sum_{j \in \mathcal{N}_i} P_{b_{ij}} \tilde{p}_i + k_p \sum_{j \in \mathcal{N}_i} P_{b_{ij}} f_j(\tilde{p}_j, \tilde{R}_j, \tilde{R}_i) \right).$$

Since $||Ax|| \leq ||A||_F ||x||$, for every $A \in \mathbb{R}^{3 \times 3}$ and $x \in \mathbb{R}^3$, and in view of the positive definitness of the matrix $\sum_{j \in \mathcal{N}_i} P_{b_{ij}}$ (implied from Assumption 3.2), one has

$$\dot{V}_i \leq -k_p \underline{\lambda}_i^P ||\tilde{p}_i||^2 + k_p \bar{P} \sum_{j \in \mathcal{N}_i} ||\tilde{p}_i|| \, ||f_j(\tilde{p}_j, \tilde{R}_j, \tilde{R}_i)||, \tag{A.32}$$

where $\underline{\lambda}_i^P$ denotes the smallest eigenvalue of the matrix $\sum_{j \in \mathcal{N}_i} P_{b_{ij}}$ and $\bar{P}$ denotes the upper bound of the projection matrix norm, i.e., $||P_{b_{ij}}||_F \leq \bar{P}$. Applying Young's inequality on the last two terms of (A.32), leads to

$$\dot{V}_i \leq - k_p \underline{\lambda}_i^P ||\tilde{p}_i||^2 + k_p \bar{P} \sum_{j \in \mathcal{N}_i} \left(\xi_i ||\tilde{p}_i||^2 + \frac{1}{4\xi_i} ||f_j(\tilde{p}_j, \tilde{R}_j, \tilde{R}_i)||^2 \right) \tag{A.33}$$

$$\leq - k_p \left(\underline{\lambda}_i^P - \bar{P}\xi_i |\mathcal{N}_i| \right) ||\tilde{p}_i||^2 + \frac{k_p \bar{P}}{4\xi_i} \sum_{j \in \mathcal{N}_i} ||f_j(\tilde{p}_j, \tilde{R}_j, \tilde{R}_i)||^2. \tag{A.34}$$

Choosing $0 < \xi_i < \frac{\lambda_i^P}{P|\mathcal{N}_i|}$, for every $i \in \mathcal{V}_f$, and using the fact that $8|R|_I^2 = ||I - R||_F^2$ and $|R|_I \leq 1$, for every $R \in SO(3)$, one can show that

$$\dot{V}_i \leq -\alpha_1(||\tilde{p}_i||) + \sum_{j \in \mathcal{N}_i} \left(\alpha_2(||\tilde{p}_j||) + \alpha_3(|\tilde{R}_j|_I) + \alpha_4(|\tilde{R}_i|_I) \right), \tag{A.35}$$

where $\alpha_k(.) \in \mathcal{K}_\infty$, for every $k \in \{1, 2, 3, 4\}$. It follows from (A.35) that system (3.16) is ISS with respect to inputs $\tilde{p}_j$, $\tilde{R}_j$ and $\tilde{R}_i$.

A.8 Proof of Theorem 3.3

Consider the error dynamics (A.9)-(A.12) (or (A.23)-(A.30)) cascaded with the following position error dynamics:

$$\dot{\tilde{p}}_3 = -k_p \sum_{j \in \mathcal{N}_3} P_{b_{3j}} \tilde{p}_3 + k_p \sum_{j \in \mathcal{N}_3} P_{b_{3j}} f_j(\tilde{p}_j, \tilde{R}_j, \tilde{R}_3) \tag{A.36}$$

$$\dot{\tilde{p}}_4 = -k_p \sum_{j \in \mathcal{N}_4} P_{b_{4j}} \tilde{p}_4 + k_p \sum_{j \in \mathcal{N}_4} P_{b_{4j}} f_j(\tilde{p}_j, \tilde{R}_j, \tilde{R}_4) \tag{A.37}$$

$$\vdots$$

$$\dot{\tilde{p}}_{n-1} = -k_p \sum_{j \in \mathcal{N}_{n-1}} P_{b_{(n-1)j}} \tilde{p}_{n-1} + k_p \sum_{j \in \mathcal{N}_{n-1}} P_{b_{(n-1)j}} f_j(\tilde{p}_j, \tilde{R}_j, \tilde{R}_{n-1}) \tag{A.38}$$

$$\dot{\tilde{p}}_n = -k_p \sum_{j \in \mathcal{N}_n} P_{b_{nj}} \tilde{p}_n + k_p \sum_{j \in \mathcal{N}_n} P_{b_{nj}} f_j(\tilde{p}_j, \tilde{R}_j, \tilde{R}_n). \tag{A.39}$$

Once again, due to the cascaded nature of the inter-agent interaction, a proof by induction will be used, together with Proposition 3.1 and Lemma 3.5 as well as a result from Theorem 3.1 (resp. Theorem 3.3), to establish the stability property of the equilibrium point $(\tilde{R}_3 = I_3, \tilde{R}_4 = I_3, \ldots, \tilde{R}_n = I_3, \tilde{p}_3 = 0, \tilde{p}_4 = 0, \ldots, \tilde{p}_n = 0)$ (resp. $(\tilde{R}_3 = I_3, \Omega_3 = 0, \tilde{R}_4 = I_3, \Omega_4 = 0 \ldots, \tilde{R}_n = I_3, \Omega_n = 0, \tilde{p}_3 = 0, \tilde{p}_4 = 0, \ldots, \tilde{p}_n = 0))$ of the n-agent network governed by the cascaded dynamics (A.9)-(A.12) (resp. (A.23)-(A.30))) and (A.36)-(A.39). Before that, let us introduce the following two propositions:

Proposition A.2 *Suppose Assumption 3.2 is satisfied. Then, the following statements hold:*

   i) The equilibrium $(\tilde{R}_3 = I_3, \tilde{p}_3 = 0)$ is AGAS for the cascaded system (A.9) and (A.36).

   ii) The equilibrium $(\tilde{R}_3 = I_3, \Omega_3 = 0, \tilde{p}_3 = 0)$ of the cascaded system (A.23)-(A.24) and (A.36) is AGAS.

Proof From Lemma 3.1 and Proposition 3.1, one can conclude that the equilibrium $\tilde{R}_3 = I_3$ of subsystem (A.9) is AGAS and the equilibrium $\tilde{p}_3 = 0$ of the $\tilde{p}_3$-subsystem,

with $\tilde{R}_3 = I_3$, is GES. Thus, as per Lemma 3.5, the equilibrium $(\tilde{R}_3 = I_3, \tilde{p}_3 = 0)$ of the cascaded system (A.9) and (A.36) is AGAS. This completes the proof of item (i). The proof of item (ii) can be established using the same steps as those for item (i), including Lemma 3.3, Proposition 3.1, and Lemma 3.5.

Proposition A.3 *Suppose Assumption 3.2 is satisfied. Then, the following statements hold:*

i) *The equilibrium $(\tilde{R}_3 = I_3, \tilde{R}_4 = I_3, \tilde{p}_3 = 0, \tilde{p}_4 = 0)$ for the cascaded system (A.9)-(A.10) and (A.36)-(A.37) is AGAS.*

ii) *The equilibrium $(\tilde{R}_3 = I_3, \Omega_3 = 0, \tilde{R}_4 = I_3, \Omega_4 = 0, \tilde{p}_3 = 0, \tilde{p}_4 = 0)$ of the cascaded system (A.23)-(A.26) and (A.36)-(A.37) is AGAS.*

Proof Using the facts that the equilibrium point $(\tilde{R}_3 = I_3, \tilde{R}_4 = I_3)$ of subsystem (A.9)-(A.10) is AGAS, and the equilibrium point $(\tilde{R}_3 = I_3, \tilde{p}_3 = 0)$ of subsystem (A.9) and (A.36) is AGAS, together with the fact that the $\tilde{p}_4$-subsystem is ISS with respect to $\tilde{p}_3$, $\tilde{R}_3$, and $\tilde{R}_4$, one can establish the claim in item (i). Similarly, one can also establish the proof of item (ii).

Now, let us proceed with a proof by induction to complete the proof of Theorem 3.3. First, from Proposition A.2, the equilibrium point $(\tilde{R}_3 = I_3, \tilde{p}_3 = 0)$ of subsystem (A.9) and (A.36) is AGAS. Second, we assume that the equilibrium $(\tilde{R}_3 = I_3, \tilde{R}_4 = I_3, \ldots, \tilde{R}_{n-1} = I_3, \tilde{p}_3 = 0, \tilde{p}_4 = 0, \ldots, \tilde{p}_{n-1} = 0)$ of the cascaded $(n-1)$-agent subsystem (A.9)-(A.11) and (A.36)-(A.38) is AGAS. Finally, considering the result from Theorem 3.1, and using the following facts:

- the $\tilde{p}_n$-subsystem is ISS with respect to $\tilde{R}_n$ and the inputs from the cascaded $(n-1)$-agent subsystem (A.9)-(A.11) and (A.36)-(A.38),

- the equilibrium $(\tilde{R}_3 = I_3, \tilde{R}_4 = I_3, \ldots, \tilde{R}_{n-1} = I_3, \tilde{p}_3 = 0, \tilde{p}_4 = 0, \ldots, \tilde{p}_{n-1} = 0)$ of the cascaded subsystem (A.9)-(A.11) and (A.36)-(A.38) is AGAS by the induction assumption,

one can show that the equilibrium point $(\tilde{R}_3 = I_3, \tilde{R}_4 = I_3, \ldots, \tilde{R}_n = I_3, \tilde{p}_3 = 0, \tilde{p}_4 = 0, \ldots, \tilde{p}_n = 0)$ of the cascaded system (A.9)-(A.12) and (A.36)-(A.39) is AGAS. This completes the proof of the first item in Theorem 3.3. For the second item of Theorem 3.3, considering Theorem 3.2 and following similar induction arguments used in the proof of the first item, it can also be shown that the equilibrium point $(\tilde{R}_3 = I_3, \Omega_3 = 0, \tilde{R}_4 = I_3, \Omega_4 = 0, \ldots, \tilde{R}_n = I_3, \Omega_n = 0, \tilde{p}_3 = 0, \tilde{p}_4 = 0, \ldots, \tilde{p}_n = 0)$ of the cascaded system (A.23)-(A.30) and (A.36)-(A.39) is AGAS.

A.9 Proof of Theorem 3.4

Consider the following real-valued function

$$\mathcal{L}_i = \frac{1}{4}\text{tr}(I - \tilde{R}_i) = |\tilde{R}_i|_I^2, \tag{A.40}$$

whose time-derivative, along the trajectories generated by dynamics (3.24), is given by

$$\dot{\mathcal{L}}_i = \frac{1}{4}k_i^R\text{tr}\left(\tilde{R}_i\left[2\psi(M_i\tilde{R}_i) - \sum_{j \in \mathcal{N}_i}(\tilde{R}_j^T - I)b_{ij} \times \hat{R}_ib_{ij}^i\right]^\times\right). \tag{A.41}$$

In view of (2.33), it follows from equation (A.41) that

$$\dot{\mathcal{L}}_i = \frac{1}{4}k_i^R\text{tr}\left(\mathbb{P}_a(\tilde{R}_i)\left[2\psi(M_i\tilde{R}_i)\right]^\times\right) - \frac{1}{4}k_i^R\text{tr}\left(\mathbb{P}_a(\tilde{R}_i)\left[\sum_{j \in \mathcal{N}_i}(\tilde{R}_j^T - I)b_{ij} \times \hat{R}_ib_{ij}^i\right]^\times\right). \tag{A.42}$$

Using property (2.23) and the fact that $\mathbb{P}_a(B) = \frac{1}{2}(B - B^T)$, $\forall B \in \mathbb{R}^{3\times3}$, equation (A.42) can be written as follows:

$$\dot{\mathcal{L}}_i = -\frac{k_i^R}{2}\sum_{j \in \mathcal{N}_i}(\mathbb{P}_a(\tilde{R}_i)b_{ij})^T\mathbb{P}_a(\tilde{R}_i)b_{ij} + \frac{k_i^R}{2}\psi(\tilde{R}_i)^T\left(\sum_{j \in \mathcal{N}_i}(\tilde{R}_j^T - I)b_{ij} \times \hat{R}_ib_{ij}^i\right) \tag{A.43}$$

$$= -\frac{k_i^R}{2}\psi(\tilde{R}_i)^TQ_i\psi(\tilde{R}_i) + \frac{k_i^R}{2}\psi(\tilde{R}_i)^T\left(\sum_{j \in \mathcal{N}_i}(\tilde{R}_j^T - I)b_{ij} \times \hat{R}_ib_{ij}^i\right), \tag{A.44}$$

where $Q_i = \sum_{j \in \mathcal{N}_i}[b_{ij}]^{\times T}[b_{ij}]^\times = \sum_{j \in \mathcal{N}_i}(I - b_{ij}b_{ij}^T)$. To obtain (A.44) from (A.43), we used the fact that $\mathbb{P}_a(B)x = \psi(B) \times x = -x \times \psi(B)$, $\forall x \in \mathbb{R}^3$ and $B \in \mathbb{R}^{3\times3}$. Since $Q_i(t)$ is a uniformly positive definite matrix under Assumption 3.4, there exists a constant $\nu^{Q_i} > 0$ such that $Q_i(t) - \nu^{Q_i}I$ is positive definite. Therefore, it follows from (A.44) that

$$\dot{\mathcal{L}}_i \leq -\frac{k_i^R}{2}\nu^{Q_i}||\psi(\tilde{R}_i)||^2 + \frac{k_i^R}{2}||\psi(\tilde{R}_i)||\sum_{j \in \mathcal{N}_i}||\tilde{R}_j^T - I||_F$$

$$\leq -\frac{k_i^R}{2}\nu^{Q_i}||\psi(\tilde{R}_i)||^2 + \frac{k_i^R}{2}||\psi(\tilde{R}_i)||\sum_{j=1}^{i-1}||\tilde{R}_j^T - I||_F. \tag{A.45}$$

Now, consider the following Lyapunov function candidate:

$$\mathcal{L}(x) = ||x||^2 = \sum_{i=3}^n|\tilde{R}_i|_I^2 = \sum_{i=3}^n\mathcal{L}_i. \tag{A.46}$$

It follows from inequality (A.45) that the time-derivative of $\mathcal{L}$ satisfies

$$\dot{\mathcal{L}} \leq -\sum_{i=3}^{n} \frac{k_i^R}{2}\nu^{Q_i}||\psi(\tilde{R}_i)||^2 + \sum_{i=3}^{n}\sum_{j=3}^{i-1} \frac{k_i^R}{2}||\psi(\tilde{R}_i)||||\tilde{R}_j^T - I||_F$$
$$+\sum_{i=3}^{n}\sum_{j=1}^{2} \frac{k_i^R}{2}||\psi(\tilde{R}_i)||||\tilde{R}_j^T - I||_F. \tag{A.47}$$

Since, according to Assumption 3.2.a, R_1 and R_2 are known and $\hat{R}_l = R_l$, $l \in \{1,2\}$, the last term of (A.47) is equal to zero. Consequently, one has

$$\dot{\mathcal{L}} \leq -\sum_{i=3}^{n} \frac{k_i^R}{2}\nu^{Q_i}||\psi(\tilde{R}_i)||^2 + \sum_{i=3}^{n}\sum_{j=3}^{i-1} \frac{k_i^R}{2}||\psi(\tilde{R}_i)||||\tilde{R}_j^T - I||_F. \tag{A.48}$$

Applying Young's inequality on the second term of (A.48), one has

$$\dot{\mathcal{L}} \leq -\sum_{i=3}^{n} \frac{k_i^R}{2}\nu^{Q_i}||\psi(\tilde{R}_i)||^2 + \sum_{i=3}^{n}\sum_{j=3}^{i-1} \frac{k_i^R \epsilon_{ij}}{2}||\psi(\tilde{R}_i)||^2$$
$$+\sum_{i=3}^{n}\sum_{j=3}^{i-1} \frac{k_i^R}{8\epsilon_{ij}}||\tilde{R}_j^T - I||_F^2, \tag{A.49}$$

where ϵ_{ij} are positive scalars obtained from Young's inequality as follows:

$$||\psi(\tilde{R}_i)||||\tilde{R}_j^T - I||_F \leq \epsilon_{ij}||\psi(\tilde{R}_i)||^2 + \frac{1}{4\epsilon_{ij}}||\tilde{R}_j^T - I||_F^2.$$

Considering the last term of (A.49) and letting $k = i - 1$, one has

$$\sum_{i=3}^{n}\sum_{j=3}^{i-1} \frac{k_i^R}{8\epsilon_{ij}}||\tilde{R}_j^T - I||_F^2 = \sum_{k=2}^{n}\sum_{j=3}^{k} \frac{k_{k+1}^R}{8\epsilon_{k+1\,j}}||\tilde{R}_j^T - I||_F^2$$
$$= \sum_{j=3}^{n}\sum_{k=j}^{n} \frac{k_{k+1}^R}{8\epsilon_{k+1\,j}}||\tilde{R}_j^T - I||_F^2$$
$$= \sum_{j=3}^{n}\sum_{i=j+1}^{N} \frac{k_i^R}{8\epsilon_{ij}}||\tilde{R}_j^T - I||_F^2$$
$$= \sum_{i=3}^{n}\sum_{j=i+1}^{n} \frac{k_j^R}{8\epsilon_{ji}}||\tilde{R}_i^T - I||_F^2. \tag{A.50}$$

We have performed an exchange between the indices to obtain the last equality. We have also changed the order of the double summation to get the second equality and substituted $k + 1$ by i to get the third equality.
From (A.49) and (A.50), one has

$$\dot{\mathcal{L}} \leq -\sum_{i=3}^{n} \frac{k_i^R}{2}\nu^{Q_i}||\psi(\tilde{R}_i)||^2 + \sum_{i=3}^{n}\sum_{j=3}^{i-1} \frac{k_i^R \epsilon_{ij}}{2}||\psi(\tilde{R}_i)||^2$$

$$+ \sum_{i=3}^{n} \sum_{j=i+1}^{n} \frac{k_j^R}{8\epsilon_{ji}} ||\tilde{R}_i^T - I||_F^2. \tag{A.51}$$

According to (2.36) and (2.48), inequality (A.51) can rewritten as follows:

$$\dot{\mathcal{L}} \leq \sum_{i=3}^{n} \left(-2k_i^R \left(1 - |\tilde{R}_i|_I^2 \right) \left(\nu^{Q_i} - \sum_{j=3}^{i-1} \epsilon_{ij} \right) \right) |\tilde{R}_i|_I^2$$

$$+ \sum_{i=3}^{n} \sum_{j=i+1}^{n} \frac{k_j^R}{\epsilon_{ji}} |\tilde{R}_i|_I^2. \tag{A.52}$$

Now, let us show that the set $\Upsilon = \{x \in [0,1]^{n-2} | \mathcal{L}(x) \leq \epsilon\}$ is forward invariant. Assume that $x(t) \in \Upsilon$ for some $t \geq 0$, which implies that $|\tilde{R}_i(t)|_I^2 \leq \varepsilon^2$ for all $i \in \{3, 4, \ldots, n\}$, and consequently

$$\dot{\mathcal{L}} \leq \sum_{i=3}^{n} \left(-2k_i^R \left(1 - \varepsilon^2 \right) \left(\nu^{Q_i} - \sum_{j=3}^{i-1} \epsilon_{ij} \right) + \sum_{j=i+1}^{n} \frac{k_j^R}{\epsilon_{ji}} \right) |\tilde{R}_i|_I^2. \tag{A.53}$$

Choosing the positive scalars k_i^R, for all $i \in \{3, 4, \ldots, n\}$, such that

$$k_i^R > \frac{\sum_{j=i+1}^{n} \frac{k_j^R}{\epsilon_{ji}}}{2(1 - \varepsilon^2)(\nu^{Q_i} - \sum_{j=3}^{i-1} \epsilon_{ij})} \quad \text{with} \quad \sum_{j=3}^{i-1} \epsilon_{ij} < \nu^{Q_i}, \tag{A.54}$$

it follows that $\mathcal{L}(t)$ is non-increasing and the set Υ is forward invariant, and consequently $|\tilde{R}_i(t)|_I^2 \leq \varepsilon^2$ for all $t \geq 0$ and $i \in \{3, 4, \ldots, n\}$. Hence, from (A.53), one has

$$\dot{\mathcal{L}} \leq - \sum_{i=3}^{n} \beta_i |\tilde{R}_i|_I^2, \tag{A.55}$$

where $\beta_i := 2k_i^R(1 - \varepsilon^2)(\nu^{Q_i} - \sum_{j=3}^{i-1} \epsilon_{ij}) - \sum_{j=i+1}^{n} \frac{k_j^R}{\epsilon_{ji}}$. Based on the gain conditions (A.54), one has $\beta_i > 0$ for all $i \in \{3, 4, \ldots, n\}$. Moreover, letting $\underline{\beta} := \min_{3 \leq i \leq n} \beta_i$, it follows from (A.55) that

$$\dot{\mathcal{L}} \leq -\underline{\beta} \sum_{i=3}^{n} |\tilde{R}_i|_I^2 = -\underline{\beta} \mathcal{L}. \tag{A.56}$$

The exponential stability of $x = 0$ follows immediately from (A.56). This completes the proof of Theorem 3.4.

A.10 Proof of Lemma 3.6

Consider the following Lyapunov function candidate:

$$V_i = \frac{1}{2} \tilde{p}_i^T \tilde{p}_i, \tag{A.57}$$

whose time-derivative, along the trajectories of the closed-loop system (3.27), is given by

$$\dot{V}_i = \tilde{p}_i^T \left(-k_p \sum_{j \in \mathcal{N}_i} P_{b_{ij}} \tilde{p}_i + k_p \sum_{j \in \mathcal{N}_i} h_{ij}(t, \tilde{p}_j, \tilde{R}_j, \tilde{R}_i) \right). \tag{A.58}$$

Since $\sum_{j \in \mathcal{N}_i} P_{b_{ij}}$ is a uniformly positive definite matrix (as per Assumption 3.4), there exists a constant $\nu^{P_i} > 0$ such that $\sum_{j \in \mathcal{N}_i} P_{b_{ij}} - \nu^{P_i} I$ is positive definite. Consequently, one has

$$\dot{V}_i \leq -k_p \nu^{P_i} ||\tilde{p}_i||^2 + k_p \sum_{j \in \mathcal{N}_i} ||\tilde{p}_i^T|| \, ||h_{ij}(t, \tilde{p}_j, \tilde{R}_j, \tilde{R}_i)||, \tag{A.59}$$

which, after applying Young's inequality to the term within the summation, leads to

$$\dot{V}_i \leq -k_p \nu^{P_i} ||\tilde{p}_i||^2 + k_p \sum_{j \in \mathcal{N}_i} \left(\xi_i ||\tilde{p}_i||^2 + \frac{1}{4\xi_i} ||h_{ij}(t, \tilde{p}_j, \tilde{R}_j, \tilde{R}_i)||^2 \right)$$

$$\leq -k_p \left(\nu^{P_i} - |\mathcal{N}_i| \xi_i \right) ||\tilde{p}_i||^2 + \frac{k_p}{4\xi_i} \sum_{j \in \mathcal{N}_i} ||h_{ij}(t, \tilde{p}_j, \tilde{R}_j, \tilde{R}_i)||^2. \tag{A.60}$$

Moreover, since the bearings $b_{ij}(t)$, for every $(i,j) \in \mathcal{E}$, are bounded, $\forall t \geq 0$, it follows that $P_{b_{ij}}(t)$ is bounded as well. Using this fact together with property (2.36) and the fact that $|R|_I \leq 1$, for every $R \in SO(3)$, and choosing $0 < \xi < \frac{\nu^{P_i}}{|\mathcal{N}_i|}$, one can verify that

$$\dot{V}_i \leq -\alpha_1(||\tilde{p}_i||) + \sum_{j \in \mathcal{N}_i} \left(\alpha_2(||\tilde{p}_j||) + \alpha_3(|\tilde{R}_j|_I) + \alpha_4(|\tilde{R}_i|_I) \right), \tag{A.61}$$

where $\alpha_k(.) \in \mathcal{K}_\infty$, for every $k \in \{1, 2, 3, 4\}$. It follows from (A.61) that system (3.27) is ISS with respect to inputs $\tilde{p}_j$, $\tilde{R}_j$ and $\tilde{R}_i$ for every $i \in \mathcal{V}_f$ and $j \in \mathcal{N}_i$.

A.11 Proof of Theorem 3.5

Consider the attitude estimation error dynamics (3.24) cascaded with the following position error dynamics:

$$\dot{\tilde{p}}_3 = -k_p \sum_{j \in \mathcal{N}_3} P_{b_{3j}} \tilde{p}_3 + k_p \sum_{j \in \mathcal{N}_3} h_{3j}(t, \tilde{p}_j, \tilde{R}_j, \tilde{R}_3) \tag{A.62}$$

$$\dot{\tilde{p}}_4 = -k_p \sum_{j \in \mathcal{N}_4} P_{b_{4j}} \tilde{p}_4 + k_p \sum_{j \in \mathcal{N}_4} h_{4j}(t, \tilde{p}_j, \tilde{R}_j, \tilde{R}_4) \tag{A.63}$$

$$\vdots$$

$$\dot{\tilde{p}}_{n-1} = -k_p \sum_{j \in \mathcal{N}_{n-1}} P_{b_{(n-1)j}} \tilde{p}_{n-1} + k_p \sum_{j \in \mathcal{N}_{n-1}} h_{(n-1)j}(t, \tilde{p}_j, \tilde{R}_j, \tilde{R}_{n-1}) \tag{A.64}$$

$$\dot{\tilde{p}}_n = -k_p \sum_{j \in \mathcal{N}_n} P_{b_{nj}} \tilde{p}_n + k_p \sum_{j \in \mathcal{N}_n} h_{nj}(t, \tilde{p}_j, \tilde{R}_j, \tilde{R}_n). \tag{A.65}$$

Here, we will also use a proof by induction due to the cascaded structure of the system. To do so, we will first establish the stability properties of the closed-loop system of the first follower. Using the results of Lemma 3.6 and Theorem 3.4 as well as the fact that the equilibrium $\tilde{p}_3 = 0$ of $\tilde{p}_3-$subsystem (A.62), with $h_{3j}(t, \tilde{p}_j, \tilde{R}_j, \tilde{R}_3) = 0$ for every $j \in \mathcal{N}_i$, is UGES, one can show, as per (Khalil, 1996, Lemma 5.6), that the equilibrium $(\tilde{R}_3 = I_3, \tilde{R}_4 = I_3, \ldots, \tilde{R}_n = I_3, \tilde{p}_3 = 0)$ of the system (3.24) cascaded with (A.62) is exponentially stable. Next, we assume that the equilibrium $(\tilde{R}_3 = I_3, \tilde{R}_4 = I_3, \ldots, \tilde{R}_n = I_3, \tilde{p}_3 = 0, \tilde{p}_4 = 0, \ldots, \tilde{p}_{n-1} = 0)$ is exponentially stable for the system (3.24) cascaded with (A.62)-(A.64). Finally, based on the latter assumption and the result of Theorem 3.4, along with the fact that the $\tilde{p}_n$-subsystem is ISS with respect to the inputs from the system (3.24) and (A.62)-(A.64), one can conclude, according to (Khalil, 1996, Lemma 5.6), that the equilibrium $(\tilde{R}_3 = I_3, \tilde{R}_4 = I_3, \ldots, \tilde{R}_n = I_3, \tilde{p}_3 = 0, \tilde{p}_4 = 0, \ldots, \tilde{p}_n = 0)$ is exponentially stable for the system (3.24) cascaded with (A.62)-(A.65). This completes the proof.

Appendix B

Proofs of Chapter 4

B.1   Proof of Lemma 4.1

We will prove the claimed result by contradiction. Assume that there exists $t \geq 0$ such that $\bar{H}(t)x = 0$ does not imply $x = 0$, which means that $\bar{H}(t)$ is not full column rank. Since the graph is a tree, according to Assumption 4.2, one has $\text{rank}\big(\bar{H}(t)\big) \leq 3n - 3$. Furthermore, suppose that $y = [y_1^T, \ldots, y_n^T]^T \in \mathbb{R}^{3n}$ is a vector that belongs to the null space of $\bar{H}(t)^T$, i.e., $\bar{H}(t)^T y = 0$. Then, one can verify that $y_j = \bar{R}_k y_i$, for all $i \in \mathcal{V}$, $j \in \mathcal{N}_i$ and $k = \mathcal{M}_i^+ \cap \mathcal{M}_j^-$. Since the graph is connected, it follows that $y = Q(\bar{R}_1, \ldots, \bar{R}_m)y_1$ where the map $Q : (SO(3))^m \to \mathbb{R}^{3n \times 3}$. It is clear that the dimension of the null space of $\bar{H}(t)^T$ is three since all components of y depend only on y_1. Therefore, the matrix $\bar{H}(t)$ is full column rank, i.e., $\text{rank}\big(\bar{H}(t)\big) = 3n - 3$. This contradicts the assumption in the beginning of the proof. This completes the proof.

B.2   Proof of Theorem 4.1

According to the definition of the absolute position error, the observer correcting term given in (4.8) can be rewritten as follows:

$$\sigma_i = -\sum_{j \in \mathcal{N}_i} \psi(A\tilde{R}_j^T \tilde{R}_i). \tag{B.1}$$

Since the graph $\mathcal{G}$ is an undirected graph with an orientation, one can verify that $\mathcal{N}_i = \mathcal{I}_i \cup \mathcal{O}_i$, with $\mathcal{I}_i := \{j \in \mathcal{N}_i : j \text{ is the tail of the oriented edge } (i, j) \in \mathcal{E}\}$ and $\mathcal{O}_i := \{j \in \mathcal{N}_i : j \text{ is the head of the oriented edge } (i, j) \in \mathcal{E}\}$. Therefore, it follows from (B.1) that

$$
\begin{aligned}
\sigma_i &= -\left(\sum_{j \in \mathcal{I}_i} \psi(A\tilde{R}_j^T \tilde{R}_i) + \sum_{j \in \mathcal{O}_i} \psi(A\tilde{R}_j^T \tilde{R}_i)\right) \\
&= -\left(\sum_{j \in \mathcal{I}_i} \psi(A\tilde{R}_j^T \tilde{R}_i) - \sum_{j \in \mathcal{O}_i} \psi(\tilde{R}_i^T \tilde{R}_j M)\right)
\end{aligned} \tag{B.2}
$$

$$= -\left(\sum_{j\in\mathcal{I}_i}\psi(A\tilde{R}_j^T\tilde{R}_i) - \sum_{j\in\mathcal{O}_i}\tilde{R}_i^T\tilde{R}_j\psi(A\tilde{R}_i^T\tilde{R}_j)\right) \tag{B.3}$$

$$= -\left(\sum_{p\in\mathcal{M}_i^+}\psi(A\bar{R}_p) - \sum_{l\in\mathcal{M}_i^-}\bar{R}_l\psi(A\bar{R}_l)\right)$$

$$= -\sum_{k=1}^{m}H_{ik}\psi(A\bar{R}_k), \tag{B.4}$$

where H_{ik} is given in (4.7). Equations (B.2) and (B.3) are obtained using the facts that $\psi(BR) = -\psi(R^T B)$ and $\psi(GR) = R^T\psi(RG)$, $\forall G, B = B^T \in \mathbb{R}^{3\times3}$ and $R \in SO(3)$. Moreover, one can verify that

$$\sigma = -\boldsymbol{H}\Psi, \tag{B.5}$$

where $\Psi := \left[\psi(A\bar{R}_1)^T, \psi(A\bar{R}_2)^T, \ldots, \psi(A\bar{R}_m)^T\right]^T \in \mathbb{R}^{3m}$. For the sake of simplicity, we write the block matrix $\bar{H}$ without the time argument. Consider the following Lyapunov function candidate:

$$V(x) = \sum_{k=1}^{m}\operatorname{tr}\left(A(I_3 - \bar{R}_k)\right), \tag{B.6}$$

which is positive definite on $\mathcal{S}$ with respect to $\mathcal{A}$. Note that

$$\Psi = \left[\psi\left(\bar{R}_1^T\nabla_{\bar{R}_1}V\right)^T, \psi\left(\bar{R}_2^T\nabla_{\bar{R}_2}V\right)^T, \ldots, \psi\left(\bar{R}_m^T\nabla_{\bar{R}_m}V\right)^T\right]^T \in \mathbb{R}^{3m},$$

where $\nabla_{\bar{R}_k}V$ is the gradients of V with respect to $\bar{R}_k$ for all $k \in \mathcal{M}$. The time-derivative of $V(x)$, along the trajectories of the closed-loop system (4.9), is given by

$$\dot{V}(x) = -k_R\sum_{k=1}^{m}\operatorname{tr}\left(A\bar{R}_k[\bar{\sigma}_k]^\times\right)$$

$$= 2k_R\sum_{k=1}^{m}\bar{\sigma}_k^T\psi(A\bar{R}_k).$$

Identities (2.23) and (2.33) were used to obtain the last equality. In view of (4.6), one obtains

$$\dot{V}(x) = 2k_R\bar{\sigma}^T\Psi = 2k_R\sigma^T\boldsymbol{H}\Psi. \tag{B.7}$$

Furthermore, since $\sigma = -\boldsymbol{H}\Psi$, one has

$$\dot{V}(x) = -2k_R||\boldsymbol{H}\Psi||^2 \leq 0. \tag{B.8}$$

Thus, the desired equilibrium set $\mathcal{A}$ for system (4.9) is stable. Moreover, since the closed-loop system (4.9) is autonomous, as per LaSalle's invariance theorem, any solution x to the closed-loop system (4.9) must converge to the largest invariant set contained in the

set characterized by $\dot{V}(x) = 0$, *i.e.*, $\boldsymbol{H}\Psi = 0$. According to Lemma 4.1, $\boldsymbol{H}\Psi = 0$ implies $\Psi = 0$. This also implies that

$$A\bar{R}_k = \bar{R}_k^T A, \tag{B.9}$$

for every $k \in \mathcal{M}$. Since A is a real symmetric matrix, one can decompose A as $A = U\Lambda U^T$ where $\Lambda = \mathrm{diag}(\lambda_1, \lambda_2, \lambda_3)$ with λ_1, λ_2 and λ_3 are the distinct eigenvalues of A and $U \in O(3)$. Using steps similar to (Mahony et al., 2008) along with the fact that $A = U\Lambda U^T$, one can show that equation (B.9) further implies that $\bar{R}_k \in \{I_3, UD_1U^T, UD_2U^T, UD_3U^T\}$ for every $k \in \mathcal{M}$. It follows that every solution x of system (4.9) must converge to the set Υ. This completes the proof of item (i).

Now, we will establish the stability properties of each equilibrium set. We start with the desired equilibrium set $\mathcal{A}$, and we set $\tilde{R}_i = R_c \exp([\tilde{r}_i^s]^\times)$, where $\tilde{r}_i^s \in \mathbb{R}^3$ is sufficiently small and $R_c \in SO(3)$ is an arbitrary constant rotation matrix. Considering the later expression of $\tilde{R}_i$ together with the fact that $\exp([y]^\times) \approx I_3 + [y]^\times$, for sufficiently small y, one can get the following first-order approximation of $\tilde{R}_i$ around the desired equilibrium set $\mathcal{A}$:

$$\tilde{R}_i \approx R_c\left(I_3 + [\tilde{r}_i^s]^\times\right), \tag{B.10}$$

for every $i \in \mathcal{V}$. Moreover, it follows from (B.10), with the fact of A being symmetric, that

$$\mathbb{P}_a(A\tilde{R}_j^T\tilde{R}_i) \approx \frac{1}{2}\bigg(A\left(I_3 - [\tilde{r}_j]^\times\right)R_c^TR_c\left(I_3 + [\tilde{r}_i]^\times\right)$$
$$- \left(I_3 - [\tilde{r}_i]^\times\right)R_c^TR_c\left(I_3 + [\tilde{r}_j]^\times\right)A \bigg). \tag{B.11}$$

Since we are only interested in the first-order approximation of the estimated attitude errors, the last equation can be simplified by neglecting the cross terms as follows:

$$\mathbb{P}_a(A\tilde{R}_j^T\tilde{R}_i) \approx \frac{1}{2}\bigg(\left(A[\tilde{r}_i]^\times + [\tilde{r}_i]^\times A\right) - \left(A[\tilde{r}_j]^\times + [\tilde{r}_j]^\times A\right) \bigg). \tag{B.12}$$

Furthermore, using the fact given in (2.24), one has

$$\mathbb{P}_a(A\tilde{R}_j^T\tilde{R}_i) \approx \frac{1}{2}\left[\bar{A}(\tilde{r}_i - \tilde{r}_j)\right]^\times, \tag{B.13}$$

where $\bar{A} := \mathrm{tr}(A)I_3 - A$. From (B.10) and (B.13), one can derive the follwing linearization of (4.4):

$$R_c[\dot{\tilde{r}}_i]^\times = -\frac{k_R}{2}R_c\sum_{j\in\mathcal{N}_i}\left[\bar{A}(\tilde{r}_i - \tilde{r}_j)\right]^\times. \tag{B.14}$$

where $i \in \mathcal{V}$. After some mathematical manipulations, the following dynamics of $\tilde{r}_i^s$ is obtained:

$$\dot{\tilde{r}}_i^s = -\frac{k_R}{2}\bar{A}\sum_{j\in\mathcal{N}_i}(\tilde{r}_i^s - \tilde{r}_j^s). \tag{B.15}$$

Equation (B.15) represents the classical consensus protocol for multi-agent systems (Ren and Beard, 2007; Mesbahi and Egerstedt, 2010). Note that, at the equilibrium point of system (B.15) (*i.e.*, $\tilde{r}_i^s = \tilde{r}_j^s$, $\forall i, j \in \mathcal{V}$), one has $\bar{R}_k = I_3$, for all $k \in \mathcal{M}$, which in turns implies that $(\bar{R}_1, \bar{R}_2, \ldots, \bar{R}_m) \in \mathcal{A}$. Therefore, to show local asymptotic stability of the desired equilibrium set $\mathcal{A}$, one has to show that the equilibrium point $\tilde{r}_i^s = \tilde{r}_j^s$, for all $i \in \mathcal{V}$ and $j \in \mathcal{N}_i$, of the system (B.15), is asymptotically stable. Defining $\tilde{r}^s := \left[(\tilde{r}_1^s)^T, (\tilde{r}_2^s)^T, \ldots, (\tilde{r}_n^s)^T \right]^T$, it follows from (B.15) that

$$
\begin{aligned}
\dot{\tilde{r}}^s &= -\frac{k_R}{2} \left(I_n \otimes \bar{A} \right) \left(\mathcal{L} \otimes I_3 \right) \tilde{r}^s \\
&= -\frac{k_R}{2} \left(\mathcal{L} \otimes \bar{A} \right) \tilde{r}^s,
\end{aligned}
\tag{B.16}
$$

where $\mathcal{L} = HH^T \in \mathbb{R}^{n \times n}$ is the Laplacian matrix corresponding to the graph $\mathcal{G}$. Since $\mathcal{G}$ is undirected and connected (as per Assumption 4.2) and the matrix A is positive definite with three distinct eigenvalues, it follows that the equilibrium point $\tilde{r}^s = \mathbf{1}_n \otimes r_c$, for the multi-agent system (B.16), is asymptotically stable, where $r_c = \frac{1}{n} \sum_{j=1}^n \tilde{r}_j^s(0)$. Consequently, the set $\mathcal{A}$ is locally asymptotically stable. This completes the proof of item (ii).

To prove item (iii), we first evaluate the *Hessian* of $V(x)$, denoted by $HessV(x)$, to determine the nature of the points belonging to the undesired equilibrium set $\Upsilon \setminus \mathcal{A}$ (*i.e.*, whether they are global minima, global maxima, or saddle points). Given an open interval $\mathbb{O} \subset \mathbb{R}$ containing zero in its interior, $\forall k \in \mathcal{M}$, one defines a smooth curve $\varphi_k : \mathbb{O} \to SO(3)$ such that $\varphi_k(t) = \bar{R}_k^* \exp\left(t[\zeta_k]^\times \right)$ where $\zeta_k \in \mathbb{R}^3$ and $x^* = (\bar{R}_1^*, \bar{R}_2^*, \ldots, \bar{R}_m^*) \in \Upsilon \setminus \mathcal{A}$. Let $x_\varphi(t) := (\varphi_1(t), \varphi_2(t), \ldots, \varphi_m(t)) \in \mathcal{S}$, one has

$$
\begin{aligned}
\frac{d}{dt} V(x_\varphi) &= -\sum_{k=1}^m \mathrm{tr} \left(A \bar{R}_k^* \exp\left(t[\zeta_k]^\times \right) [\zeta_k]^\times \right) \\
\frac{d^2}{dt^2} V(x_\varphi) &= -\sum_{k=1}^m \mathrm{tr} \left(A \bar{R}_k^* \exp\left(t[\zeta_k]^\times \right) \left([\zeta_k]^\times \right)^2 \right) - \sum_{k=1}^m \mathrm{tr} \left(A \bar{R}_k^* \exp\left(t[\zeta_k]^\times \right) [\dot{\zeta}_k]^\times \right).
\end{aligned}
\tag{B.17}
$$

Since $x_\varphi(0) = x^*$, one verifies $\mathbb{P}_a(A\bar{R}_k^*) = 0$ for every $k \in \mathcal{M}$. Consequently, it follows from (B.17) that

$$
\left. \frac{d^2}{dt^2} V(x_\varphi) \right|_{t=0} = -\sum_{k=1}^m \mathrm{tr} \left(A \bar{R}_k^* \left([\zeta_k]^\times \right)^2 \right).
\tag{B.18}
$$

Using the fact $([z]^\times)^2 = -z^T z I_3 + z z^T$ and $\mathrm{tr}(z_1 z_2^T) = z_1^T z_2$, $\forall z, z_1, z_2 \in \mathbb{R}^3$, one obtains

$$
\begin{aligned}
\left. \frac{d^2}{dt^2} V(x_\varphi) \right|_{t=0} &= \sum_{k=1}^m \zeta_k^T \left(\mathrm{tr}(A\bar{R}_k^*) I_3 - A\bar{R}_k^* \right) \zeta_k \\
&= \sum_{k=1}^m \zeta_k^T A_k^* \zeta_k = \zeta^T \boldsymbol{A}^* \zeta,
\end{aligned}
\tag{B.19}
$$

where $A_k^* = \text{tr}(A\bar{R}_k^*)I_3 - A\bar{R}_k^*$, $\zeta = [\zeta_1^T, \zeta_2^T, \ldots, \zeta_m^T]^T \in \mathbb{R}^{3m}$ and $\boldsymbol{A}^* = \text{diag}(A_1^*, A_2^*, \ldots, A_m^*)$ $\in \mathbb{R}^{3m \times 3m}$. In view of (B.19), according to (Absil et al., 2007), one has $HessV(x) = \boldsymbol{A}^*$ for every $x \in \Upsilon \setminus \mathcal{A}$. In other words, the matrix $\boldsymbol{A}^*$ represents the *Hessian* of $V(x)$ evaluated at the undesired equilibrium points. It is worth noting that the eigenvalues of the matrix $\boldsymbol{A}^*$ are actually the eigenvalues of the matrices A_k^*, for every $k \in \mathcal{M}$. Therefore, as a next step, we will explicitly find the eigenvalues of the matrices A_k^*, for every $k \in \mathcal{M}$. Using the fact that $A = U\Lambda U^T$, recall that $U^T U = I_3$ and $\Lambda = \text{diag}(\lambda_1, \lambda_2, \lambda_3)$ with $\lambda_1 \neq \lambda_2 \neq \lambda_3$ (according to Assumption 4.4), one has $A_k^* = U\left(\text{tr}(\Lambda U^T \bar{R}_k^* U)I_3 - \Lambda U^T \bar{R}_k^* U\right)U^T$. Now, for every $\bar{m} \in \mathcal{M}^I$, one can verify that $\text{tr}(\Lambda U^T \bar{R}_{\bar{m}}^* U)I_3 - \Lambda U^T \bar{R}_{\bar{m}}^* U = \text{diag}(\lambda_2 + \lambda_3, \lambda_1 + \lambda_3, \lambda_1 + \lambda_2)$. On the other hand, for every $\bar{n} \in \mathcal{M}^\pi$, one can verify that $\text{tr}(\Lambda U^T \bar{R}_{\bar{n}}^* U)I_3 - \Lambda U^T \bar{R}_{\bar{n}}^* U \in \{\text{diag}(-\lambda_2 - \lambda_3, \lambda_1 - \lambda_3, \lambda_1 - \lambda_2), \text{diag}(\lambda_2 - \lambda_3, -\lambda_1 - \lambda_3, \lambda_2 - \lambda_1), \text{diag}(\lambda_3 - \lambda_2, \lambda_3 - \lambda_1, -\lambda_1 - \lambda_2)\}$. Since $\lambda_1 \neq \lambda_2 \neq \lambda_3$, it follows that the eigenvalues of the matrix $\boldsymbol{A}^*$ are either all negative or some of them are positive and some are negative. Consequently, the critical points of $V(x)$ in $\Upsilon \setminus \mathcal{A}$ are either global maxima or saddle points of $V(x)$.

Now, we will show that the critical points of $V(x)$ in the set $\Upsilon \setminus \mathcal{A}$ are unstable. Consider the following real-valued function $\bar{V} : SO(3)^m \to \mathbb{R}$ inspired from (Tran et al., 2019):

$$\bar{V}(x) = 2 \sum_{\bar{n} \in \mathcal{M}^\pi} (\lambda_{p_{\bar{n}}} + \lambda_{d_{\bar{n}}}) - V(x). \tag{B.20}$$

where $\lambda_{p_{\bar{n}}}$ and $\lambda_{d_{\bar{n}}}$ are two distinct eigenvalues of A, i.e., $p_{\bar{n}}, d_{\bar{n}} \in \{1, 2, 3\}$ such that $p_{\bar{n}} \neq d_{\bar{n}}$. Let us consider an equilibrium point $x^* \in \Upsilon \setminus \mathcal{A}$ such that $\bar{R}_{\bar{n}} = UD_{l_{\bar{n}}}U^T$, $\bar{n} \in \mathcal{M}^\pi$, where $l_{\bar{n}} \in \{1, 2, 3\}$ such that $l_{\bar{n}} \neq p_{\bar{n}}$ and $l_{\bar{n}} \neq d_{\bar{n}}$. It is clear that $\bar{V}(x^*) = 0$. Moreover, since the set $\Upsilon \setminus \mathcal{A}$ contains only global maxima or saddle points of $V(x)$, one can find some $\bar{x}^* \in \mathcal{S}$ arbitrarily close to x^* such that $\bar{V}(\bar{x}^*) > 0$. Furthermore, it follows from (B.8) and (B.20) that $\dot{\bar{V}}(x) = -\dot{V}(x) > 0$. Consequently, one concludes that all points belonging to the undesired equilibrium set $\Upsilon \setminus \mathcal{A}$ are unstable. By virtue of the stable manifold theorem (Perko, 2000), one can conclude that the stable manifold associated to the undesired equilibrium set $\Upsilon \setminus \mathcal{A}$ has zero Lebesgue measure, and as such, the equilibrium set $\mathcal{A}$ is AGAS. This completes the proof of item (iii).

B.3 Proof of Lemma 4.2

Since the function U is continuous, one can verify that the flow set $\mathcal{F}$ and the jump set $\mathcal{J}$, given in (4.18), are closed sets. Moreover, one has $\mathcal{F} \cup \mathcal{J} = \mathcal{S}_h$.

The outer semicontinuity, local boundedness, and convexity properties of the flow map F follow from the fact that F is a single-valued continuous function.

Using the fact that U is continuous on $SO(3) \times \mathbb{R}$, one can show, following similar arguments as in (Casau et al., 2020, Proof of Lemma 1), that $\rho_k(\bar{R}_k) := \arg\min_{\bar{\xi}_k \in \Xi} U(\bar{R}_k, \bar{\xi}_k)$ for every $k \in \mathcal{M}$ is outer semicontinuous. Furthermore, it can be verified that for every $i \in \mathcal{V}$ and $k \in \mathcal{M}_i^+$, the set-valued mapping given in (4.20) has a closed graph relative to $\mathcal{J}_i$. According to (Goebel et al., 2012, Lemma 5.10), this implies that the set-valued mapping (4.20) is outer semi-continuous relative to $\mathcal{J}_i$. Consequently, in conjunction with the fact that $\rho_k(\bar{R}_k)$ is outer semi-continuous, it follows that the jump map G is

outer semi-continuous relative to $\mathcal{J}$. The local boundedness of G relative to $\mathcal{J}$ follows from the fact that ξ_k^*, for every $k \in \mathcal{M}$, takes values over a finite discrete set Ξ and the remaining components of G are single-valued continuous functions on $\mathcal{J}$.

B.4   Proof of Theorem 4.2

Consider the following Lyapunov function candidate:

$$U_R(x_h) = \sum_{k=1}^{m} U(\bar{R}_k, \xi_k), \tag{B.21}$$

whose time-derivative, along the trajectories generated by the flows of the hybrid closed-loop dynamics (4.22), is given by

$$\begin{aligned}
\dot{U}_R(x_h) &= \sum_{k=1}^{m} \langle \nabla_{\bar{R}_k} U_R, k_R \bar{R}_k [\bar{\sigma}_k]^\times \rangle_{\bar{R}_k} + \sum_{k=1}^{m} \langle \langle \nabla_{\xi_k} U_R, \dot{\xi}_k \rangle \rangle \\
&= \sum_{k=1}^{m} \langle \langle \bar{R}_k^T \nabla_{\bar{R}_k} U_R, k_R [\bar{\sigma}_k]^\times \rangle \rangle + \sum_{k=1}^{m} \langle \langle \nabla_{\xi_k} U_R, \dot{\xi}_k \rangle \rangle \\
&= 2k_R \sum_{k=1}^{m} \bar{\sigma}_k^T \psi \left(\bar{R}_k^T \nabla_{\bar{R}_k} U_R \right) + \sum_{k=1}^{m} \dot{\xi}_k \nabla_{\xi_k} U_R \\
&= 2k_R \bar{\sigma}^T \Psi_\nabla^{\bar{R}} + \dot{\xi}^T \Psi_\nabla^{\xi},
\end{aligned} \tag{B.22}$$

where $\Psi_\nabla^{\xi} := [\nabla_{\xi_1} U_R, \nabla_{\xi_2} U_R, \ldots, \nabla_{\xi_m} U_R]^T \in \mathbb{R}^m$. To derive the above equations, identities (2.23), (2.33) and (2.38) have been used. It follows from (4.13) and (4.21) that

$$\dot{U}_R(x_h) = -2k_R \|\boldsymbol{H}\Psi_\nabla^{\bar{R}}\|^2 - k_\xi \|\Psi_\nabla^{\xi}\|^2 \leq 0. \tag{B.23}$$

Consequently, $U_R(x_h)$ is non-increasing along the flows of (4.22). Moreover, in view of (4.22) and (4.10), one has

$$U_R(x_h) - U_R(x_h^+) = \sum_{k=1}^{m} \left(U(\bar{R}_k, \xi_k) - U(\bar{R}_k^+, \xi_k^+) \right) \geq \delta. \tag{B.24}$$

Thus, $U_R(x_h)$ is strictly decreasing over the jumps of (4.22). It follows from (B.23)-(B.24) and the result presented in Theorem 2.1 that the set $\mathcal{A}_h$ is stable. Consequently, every maximal solution of the hybrid closed-loop system (4.22) is bounded. In addition, from (B.23) and (B.24), one can verify that $U_R(x_h(t,j)) \leq U_R(x_h(t_j,j))$ and $U_R(x_h(t_j,j)) \leq U_R(x_h(t_j, j-1)) - \delta$, $\forall (t,j), (t_j,j), (t_j, j-1) \in \operatorname{dom} x_h$, with $(t,j) \geq (t_j,j) \geq (t_j, j-1)$. Thus, one has $0 \leq U_R(x_h(t,j)) \leq U_R(x_h(0,0)) - j\delta$, $\forall (t,j) \in \operatorname{dom} x_h$, which leads to $j \leq \lceil \frac{U_R(x_h(0,0))}{\delta} \rceil$, where $\lceil . \rceil$ denotes the ceiling function. This shows that the number of jumps is finite and depends on the initial conditions.

Now, we will show the global attractivity of $\mathcal{A}_h$ using the invariance principle for hybrid

systems (Goebel et al., 2012, Section 8.2), presented in Section 2.6. Consider the following functions:

$$u_{\mathcal{F}}(x_h) := \begin{cases} -2k_R||\boldsymbol{H}\Psi_{\triangledown}^{\bar{R}}||^2 - k_\xi||\Psi_{\triangledown}^\xi||^2 & \text{if } x_h \in \mathcal{F}, \\ -\infty & \text{otherwise}, \end{cases} \tag{B.25}$$

$$u_{\mathcal{J}}(x_h) := \begin{cases} -\delta & \text{if } x_h \in \mathcal{J}, \\ -\infty & \text{otherwise}, \end{cases} \tag{B.26}$$

In view of (B.23)-(B.26), one can notice that the growth of U_R is upper bounded during the flows by $u_{\mathcal{F}}(x_h) \leq 0$ and during the jumps by $u_{\mathcal{J}}(x_h) \leq 0$ for every $x_h \in \mathcal{S}_h$. It follows from Theorem 2.2 that every maximal solution of the hybrid system (4.22) converges to the following largest weakly[1] invariant subset:

$$U_R^{-1}(r) \cap \mathcal{S}_h \cap \left[\overline{u_{\mathcal{F}}^{-1}(0)} \cup \left(u_{\mathcal{J}}^{-1}(0) \cap G\left(u_{\mathcal{J}}^{-1}(0)\right) \right) \right],$$

for some $r \in \mathbb{R}$. Moreover, one can verify that

$$u_{\mathcal{F}}^{-1}(0) = \{x_h \in \mathcal{F} : \boldsymbol{H}\Psi_{\triangledown}^{\bar{R}} = 0, \ \Psi_{\triangledown}^\xi = 0\}$$
$$u_{\mathcal{J}}^{-1}(0) = \emptyset.$$

Furthermore, according to Lemma 4.1, one has

$$u_{\mathcal{F}}^{-1}(0) = \{x_h \in \mathcal{F} : \Psi_{\triangledown}^{\bar{R}} = 0, \ \Psi_{\triangledown}^\xi = 0\}$$
$$= \mathcal{F} \cap \Upsilon_h,$$

where the set Υ_h is defined in (4.11). Given $x_h \in \mathcal{A}_h$, one obtains, for all $k \in \mathcal{M}$, $U(\bar{R}_k, \xi_k) - \min_{\bar{\xi}_k \in \Xi} U(\bar{R}_k, \bar{\xi}_k) = -\min_{\bar{\xi}_k \in \Xi} U(\bar{R}_k, \bar{\xi}_k) \leq 0$. Therefore, from (4.18), and according to Condition 4.1, one can verify that $\mathcal{A}_h \subset \mathcal{F} \cap \Upsilon_h$ and $\mathcal{F} \cap (\Upsilon_h \backslash \mathcal{A}_h) = \emptyset$. In addition, applying some set-theoretic arguments, one has $\mathcal{F} \cap \Upsilon_h \subset (\mathcal{F} \cap (\Upsilon_h \backslash \mathcal{A}_h)) \cup (\mathcal{F} \cap \mathcal{A}_h) = \emptyset \cup \mathcal{A}_h$. It follows from $\mathcal{A}_h \subset \mathcal{F} \cap \Upsilon_h$ and $\mathcal{F} \cap \Upsilon_h \subset \mathcal{A}_h$ that $\mathcal{F} \cap \Upsilon_h = \mathcal{A}_h$. Hence, $u_{\mathcal{F}}^{-1}(0) = \mathcal{A}_h$. Consequently, every maximal solution of the hybrid system (4.22) converges to the largest weakly invariant subset $U_R^{-1}(0) \cap \mathcal{A}_h = \mathcal{A}_h$. Since every maximal solution of the hybrid closed-loop system (4.22) is bounded, $G(x_h) \in \mathcal{F} \cup \mathcal{J}$ for every $x_h \in \mathcal{J}$, and $F(x_h) \subset T_{\mathcal{F}}(x_h)$, for every $x_h \in \mathcal{F} \backslash \mathcal{J}$, where $T_{\mathcal{F}}(x_h)$ denotes the tangent cone to $\mathcal{F}$ at the point x_h, according to Proposition 2.1, one can conclude that every maximal solution of the hybrid closed-loop system (4.22) is complete. This, together with Lemma 4.2, allows us to conclude, as per Theorem 2.3, that the set $\mathcal{A}_h$ is globally asymptotically stable for the hybrid closed-loop system (4.22). This completes the proof.

---

[1]The reader is referred to (Goebel et al., 2012) for the definition of *weakly invariant* sets in the hybrid systems context.

B.5 Proof of Proposition 4.1

The time derivative of U_R, along the trajectories of the hybrid closed-loop system (4.22), is given by

$$\dot{U}_R(x_h) = -\sum_{k=1}^{m} \mathrm{tr}\big(A\bar{R}_k\mathcal{R}_\alpha(\xi_k, u)[k_R\mathcal{R}_\alpha(\xi_k, u)^T\bar{\sigma}_k + \dot{\xi}_k u]^\times\big) + \gamma \sum_{k=1}^{m} \dot{\xi}_k\xi_k. \qquad (B.27)$$

Using identities (2.23) and (2.33), one obtains

$$\begin{aligned}
\dot{U}_R(x_h) =& 2k_R \sum_{k=1}^{m} \bar{\sigma}_k^T\mathcal{R}_\alpha(\xi_k, u)\psi\big(A\bar{R}_k\mathcal{R}_\alpha(\xi_k, u)\big) \\
&+ \sum_{k=1}^{m} \dot{\xi}_k\Big(\gamma\xi_k + 2u^T\psi\big(A\bar{R}_k\mathcal{R}_\alpha(\xi_k, u)\big)\Big). \qquad (B.28)
\end{aligned}$$

It follows from (B.22) and (B.28) that $\psi\big(\bar{R}_k^T\nabla_{\bar{R}_k}U_R\big) = \mathcal{R}_\alpha(\xi_k, u)\psi(A\bar{R}_k\mathcal{R}_\alpha(\xi_k, u))$ and $\nabla_{\xi_k}U_R = \gamma\xi_k + 2u^T\psi(A\bar{R}_k\mathcal{R}_\alpha(\xi_k, u))$ for all $k \in \mathcal{M}$. Considering the last two expressions $(\psi\big(\bar{R}_k^T\nabla_{\bar{R}_k}U_R\big)$ and $\nabla_{\xi_k}U_R)$ and the definition of the set of all critical points of U_R, given in (4.11), one can conclude that Υ_h is the set of all critical points of U_R. Moreover, one can conclude that $\mathcal{A}_h \subset \Upsilon_h$. This completes the proof.

B.6 Proof of Theorem 4.3

Define $e := \big[e_1^T, e_2^T, \ldots, e_n^T\big]^T \in \mathbb{R}^{3n}$. According to the flows of (4.37), one has

$$\dot{e} = -k_p\boldsymbol{L}_B(t)e. \qquad (B.29)$$

Notice that $(\boldsymbol{1}_n \otimes I_3)^T e(0) = 0$ and $(\boldsymbol{1}_n \otimes I_3)^T\dot{e} = 0$. Moreover, since the bearings $b_{ij}(t)$, for every $(i, j) \in \mathcal{E}$, are bounded, $\forall t \geq 0$, one also has that $\boldsymbol{L}_B(t)$ is bounded. With all of these and Assumption 4.6, it follows from (Loria and Panteley, 2002, Lemma 5) that

$$||e(t)||^2 \leq ||e(0)||^2\mathrm{e}^{-\beta t}, \qquad (B.30)$$

where β is a positive scalar. Again, using the fact that $\boldsymbol{L}_B(t)$ is bounded, $\forall t \geq 0$, together with inequality (B.30), it follows from the converse theorem (Khalil, 1996) that there is exist a real-valued function $U_e : [0, \infty) \times \mathbb{R}^{3n} \to \mathbb{R}$ such that the following inequalities hold:

$$c_1||e||^2 \leq U_e(t, e) \leq c_2||e||^2 \qquad (B.31)$$

$$\dot{U}_e(t, e) \leq -c_3||e||^2, \qquad (B.32)$$

where c_1, c_2 and c_3 are positive constant. Now, consider the following Lyapunov function candidate:

$$\mathcal{U}(\bar{x}_h) = U_R(x_h) + U_e(t, e) = \sum_{k=1}^{m} U(\bar{R}_k, \xi_k) + U_e(t, e)$$

$$= \sum_{k=1}^{m} \left(\text{tr} \Big(A \left(I_3 - \bar{R}_k \mathcal{R}_\alpha(\xi_k, u) \right) \Big) + \frac{\gamma}{2} \xi_k^2 \right) + U_e(t, e).$$

Recall that $U_R(x_h)$ is a potential function on $\mathcal{S}_h$ with respect to $\mathcal{A}_h$. Combining this fact with the inequality (B.31), one can verify that $\mathcal{U}(\bar{x}_h)$ is positive definite on $\bar{\mathcal{S}}_h$ with respect to $\bar{\mathcal{A}}_h$. The time-derivative of $\mathcal{U}(\bar{x}_h)$, along the trajectories generated by the flows of the hybrid closed-loop system (4.37), is given by

$$\dot{\mathcal{U}}(\bar{x}_h) = -2k_R||\boldsymbol{H}\Psi_\nabla^{\bar{R}}||^2 - k_\xi||\Psi_\nabla^\xi||^2 + \dot{U}_e(t, e)$$
$$\leq -2k_R||\boldsymbol{H}\Psi_\nabla^{\bar{R}}||^2 - k_\xi||\Psi_\nabla^\xi||^2 - c_3||e||^2 \tag{B.33}$$
$$\leq 0, \tag{B.34}$$

where the elements of the vectors $\Psi_\nabla^{\bar{R}}$ and Ψ_∇^ξ are explicitly given in Proposition 4.1. Inequality (B.33) was obtained using the fact given in (B.32). This implies the non-increasing of $\mathcal{U}(\bar{x}_h)$ along the flows of (4.37). Furthermore, one has

$$\mathcal{U}(\bar{x}_h) - \mathcal{U}(\bar{x}_h^+) = U_R(x_h) - U_R(x_h^+) \tag{B.35}$$
$$= \sum_{k=1}^{m} \left(U(\bar{R}_k, \xi_k) - U(\bar{R}_k^+, \xi_k^+) \right)$$
$$\geq \delta, \tag{B.36}$$

where we have used the fact that $U_e(t, e) - U_e(t^+, e^+) = 0$ to obtain the equality (B.35). Inequality (B.36) shows the strict decrease of $\mathcal{U}(\bar{x}_h)$ over the jumps of (4.37). Moreover, using arguments similar to the first part of the proof of theorem 4.2, one can show that the set $\bar{\mathcal{A}}_h$ is stable, every maximal solution of the hybrid closed-loop dynamics (4.37) is complete, and the number of jumps is finite.

Now, let us prove the global asymptotic stability of the set $\bar{\mathcal{A}}_h$. Following the same steps as in the proof of Theorem 4.2, with

$$u_{\bar{\mathcal{F}}}(\bar{x}_h) := \begin{cases} -2k_R||\boldsymbol{H}\Psi_\nabla^{\bar{R}}||^2 - k_\xi||\Psi_\nabla^\xi||^2 - c_3||e||^2 & \text{if } \bar{x}_h \in \bar{\mathcal{F}}, \\ -\infty & \text{otherwise}, \end{cases} \tag{B.37}$$

$$u_{\bar{\mathcal{J}}}(\bar{x}_h) := \begin{cases} -\delta & \text{if } \bar{x}_h \in \bar{\mathcal{J}}, \\ -\infty & \text{otherwise}, \end{cases} \tag{B.38}$$

one can show that every maximal solution of the hybrid system (4.37) converges to the largest weakly invariant subset $\bar{\mathcal{A}}_h$. Furthermore, using the fact that every maximal solution of (4.37) is bounded, $\bar{G}(\bar{x}_h) \in \bar{\mathcal{F}} \cup \bar{\mathcal{J}}$ for every $\bar{x}_h \in \bar{\mathcal{J}}$, and $\bar{F}(\bar{x}_h) \subset T_{\bar{\mathcal{F}}}(\bar{x}_h)$, for every $\bar{x}_h \in \bar{\mathcal{F}} \setminus \bar{\mathcal{J}}$, according to Proposition 2.1, one can verify that every maximal solution of (4.37) is complete. This, together with the fact that (4.37) satisfies the basic hybrid conditions as per Lemma 4.3, implies that the set $\bar{\mathcal{A}}_h$ is globally asymptotically stable for the hybrid system (4.37). This completes the proof.

Appendix C

Proofs of Chapter 5

C.1 Proof of Theorem 5.1

Consider the following Lyapunov function candidate:

$$\mathcal{V}(\bar{x}) = k_R U_R(x) + \omega^T J^d \omega. \tag{C.1}$$

where $J^d := \mathrm{diag}(J_1, J_2, \ldots, J_n) \in \mathbb{R}^{3n \times 3n}$, $J_i = J_i^\top > 0$, $i = 1, \ldots, n$. Note that $\mathcal{V}$ is positive definite on $\bar{\mathcal{S}}$ with respect to $\bar{\mathcal{A}}$. The time-derivative of $\mathcal{V}$, along the trajectories generated by the flows of the hybrid closed-loop dynamics (5.8), is given by

$$\dot{\mathcal{V}}(\bar{x}) = k_R \dot{U}_R(x) + 2\omega^T J^d \dot{\omega}. \tag{C.2}$$

The time-derivative of the first term of (C.2) can be calculated as follows

$$\dot{U}_R(x) = \sum_{k=1}^{m} \langle \nabla_{\bar{R}_k} U_R, \bar{R}_k [\bar{\omega}_k]^\times \rangle_{\bar{R}_k} + \sum_{k=1}^{m} \langle\langle \nabla_{\xi_k} U_R, \dot{\xi}_k \rangle\rangle$$

$$= \sum_{k=1}^{m} \langle\langle \bar{R}_k^T \nabla_{\bar{R}_k} U_R, [\bar{\omega}_k]^\times \rangle\rangle + \sum_{k=1}^{m} \langle\langle \nabla_{\xi_k} U_R, \dot{\xi}_k \rangle\rangle \tag{C.3}$$

$$= 2 \sum_{k=1}^{m} \bar{\omega}_k^T \psi \left(\bar{R}_k^T \nabla_{\bar{R}_k} U_R \right) + \sum_{k=1}^{m} \dot{\xi}_k \nabla_{\xi_k} U_R \tag{C.4}$$

$$= 2\, \bar{\omega}^T \Psi_\nabla^{\bar{R}} + \dot{\xi}^T \Psi_\nabla^{\xi} = 2\, \omega^T \bar{H} \Psi_\nabla^{\bar{R}} - k_\xi \|\Psi_\nabla^{\xi}\|^2, \tag{C.5}$$

where

$$\Psi_\nabla^{\xi} := [\nabla_{\xi_1} U_R, \nabla_{\xi_2} U_R, \ldots, \nabla_{\xi_m} U_R]^T \in \mathbb{R}^m,$$

and

$$\Psi_\nabla^{\bar{R}} := \left[\psi \left(\bar{R}_1^T \nabla_{\bar{R}_1} U_R \right)^T, \psi \left(\bar{R}_2^T \nabla_{\bar{R}_2} U_R \right)^T, \ldots, \psi \left(\bar{R}_m^T \nabla_{\bar{R}_m} U_R \right)^T \right]^T \in \mathbb{R}^{3m}.$$

To derive equations (C.3)-(C.5), identities (2.23), (2.33) and (2.38) have been used. Furthermore, from (5.4), (5.6) and (C.5), one obtains

$$\dot{\mathcal{V}}(\bar{x}) = -k_R k_\xi \|\Psi_\nabla^{\xi}\|^2 - 2k_\omega \|\omega\|^2, \tag{C.6}$$

which implies that $\mathcal{V}$ is non-increasing along the flows of (5.8). Moreover, in view of (5.8) and (C.1), one has

$$
\begin{aligned}
\mathcal{V}(\bar{x}) - \mathcal{V}(\bar{x}^+) &= k_R \left(U_R(x) - U_R(x^+) \right) \\
&= k_R \sum_{k=1}^{m} \left(U(\bar{R}_k, \xi_k) - U(\bar{R}_k^+, \xi_k^+) \right) \\
&\geq k_R \delta_{\bar{R}},
\end{aligned} \tag{C.7}
$$

which indicates that $\mathcal{V}(\bar{x})$ is strictly decreasing over the jumps of (5.8). In view of (C.6) and (C.7), it follows from Theorem 2.1 that the set $\bar{\mathcal{A}}$ is stable. Thus, all maximal solutions of (5.8) are bounded. This, together with the facts that $\bar{F}(\bar{x}) \subset T_{\bar{\mathcal{F}}}(\bar{x})$, for every $\bar{x} \in \bar{\mathcal{F}} \setminus \bar{\mathcal{J}}$, and $\bar{G}(\bar{x}) \in \bar{\mathcal{F}} \cup \bar{\mathcal{J}}$, for every $\bar{x} \in \bar{\mathcal{J}}$, implies, as per Proposition 2.1, that every maximal solution of the hybrid closed-loop dynamics (5.8) is complete. In addition, in view of (C.6) and (C.7), one can verify that $\mathcal{V}(\bar{x}(t, j)) \leq \mathcal{V}(\bar{x}(t_j, j))$ and $\mathcal{V}(\bar{x}(t_j, j)) \leq \mathcal{V}(\bar{x}(t_j, j-1)) - k_R \delta_{\bar{R}}, \forall (t, j), (t_j, j), (t_j, j-1) \in \text{dom } \bar{x}$, with $(t, j) \geq (t_j, j) \geq (t_j, j-1)$. Thus, one has $0 \leq \mathcal{V}(\bar{x}(t, j)) \leq \mathcal{V}(\bar{x}(0, 0)) - j k_R \delta_{\bar{R}}, \forall (t, j) \in \text{dom } \bar{x}$, which leads to $j \leq \lceil \frac{\mathcal{V}(\bar{x}(0,0))}{k_R \delta_{\bar{R}}} \rceil$, where $\lceil . \rceil$ denotes the ceiling function. The last inequality implies that the number of jumps is finite and depends on the initial conditions.

Now, we will proceed with the proof of the global attractivity of $\bar{\mathcal{A}}$ using the invariance principle for hybrid systems presented in Section 2.6. Consider the following two functions:

$$
u_{\bar{\mathcal{F}}}(\bar{x}) := \begin{cases} -k_R k_\xi \|\Psi_{\bar{\nabla}}^\xi\|^2 - 2k_\omega \|\omega\|^2 & \text{if } \bar{x} \in \bar{\mathcal{F}}, \\ -\infty & \text{otherwise}, \end{cases} \tag{C.8}
$$

$$
u_{\bar{\mathcal{J}}}(\bar{x}) := \begin{cases} -k_R \delta_{\bar{R}} & \text{if } \bar{x} \in \bar{\mathcal{J}}, \\ -\infty & \text{otherwise}. \end{cases} \tag{C.9}
$$

It follows from (C.6)-(C.9) that the Lyapunov function candidate $\mathcal{V}$ is upper bounded by $u_{\bar{\mathcal{F}}}(\bar{x}) \leq 0$ and $u_{\bar{\mathcal{J}}}(\bar{x}) \leq 0$ during the flows and jumps, respectively, for every $\bar{x} \in \bar{\mathcal{S}}$. Consequently, as per Theorem 2.2, every maximal solution of the hybrid system (5.8) converges to the following largest weakly invariant subset:

$$
\mathcal{V}^{-1}(r) \cap \bar{\mathcal{S}} \cap \left[\overline{u_{\bar{\mathcal{F}}}^{-1}(0)} \cup \left(u_{\bar{\mathcal{J}}}^{-1}(0) \cap G\left(u_{\bar{\mathcal{J}}}^{-1}(0) \right) \right) \right],
$$

for some $r \in \mathbb{R}$. Moreover, one can find that $u_{\bar{\mathcal{J}}}^{-1}(0) = \emptyset$ and $u_{\bar{\mathcal{F}}}^{-1}(0) = \{\bar{x} \in \bar{\mathcal{F}} : \Psi_{\bar{\nabla}}^\xi = 0, \omega = 0\}$. Note that, for every $\bar{x} \in u_{\bar{\mathcal{F}}}^{-1}(0)$, one has $\omega = 0$ which implies that $\dot{\omega} = 0$. Moreover, it follows from (5.4) and (5.6) that $\bar{H}\Psi_{\bar{\nabla}}^{\bar{R}} = 0$ which also implies, as per Lemma 4.1, that $\Psi_{\bar{\nabla}}^{\bar{R}} = 0$. Since $\Psi_{\bar{\nabla}}^\xi = 0$ and $\Psi_{\bar{\nabla}}^{\bar{R}} = 0$, one has $x \in \bar{\Upsilon}$. Consequently, one has $u_{\bar{\mathcal{F}}}^{-1}(0) = \{\bar{x} \in \bar{\mathcal{F}} : x \in \mathcal{F} \cap \bar{\Upsilon}, \omega = 0\}$. On the other hand, given $x \in \mathcal{A}$, one has, for all $k \in \mathcal{M}$, $U(\bar{R}_k, \xi_k) - \min_{\bar{\xi}_k \in \Xi} U(\bar{R}_k, \bar{\xi}_k) = -\min_{\bar{\xi}_k \in \Xi} U(\bar{R}_k, \bar{\xi}_k) \leq 0$. Therefore, from (5.9), and according to Condition 4.1, one can verify that $\mathcal{A} \subset \mathcal{F} \cap \bar{\Upsilon}$ and $\mathcal{F} \cap (\bar{\Upsilon} \setminus \mathcal{A}) = \emptyset$. In addition, applying some set-theoretic arguments, one has $\mathcal{F} \cap \bar{\Upsilon} \subset (\mathcal{F} \cap (\bar{\Upsilon} \setminus \mathcal{A})) \cup (\mathcal{F} \cap \mathcal{A}) = \emptyset \cup \mathcal{A}$. It follows from $\mathcal{A} \subset \mathcal{F} \cap \bar{\Upsilon}$ and $\mathcal{F} \cap \bar{\Upsilon} \subset \mathcal{A}$ that $\mathcal{F} \cap \bar{\Upsilon} = \mathcal{A}$. This implies that $u_{\bar{\mathcal{F}}}^{-1}(0) = \bar{\mathcal{A}}$.

Hence, every maximal solution of the hybrid system (5.8) converges to the largest weakly invariant subset $\mathcal{V}^{-1}(0) \cap \bar{\mathcal{A}} = \bar{\mathcal{A}}$. Since every maximal solution of the hybrid closed-loop system (5.8) is complete and (5.8) satisfies the basic hybrid conditions as per Lemma 5.1, it follows from Theorem 2.3 that the set $\bar{\mathcal{A}}$ is globally asymptotically stable for the hybrid closed-loop system (5.8). This completes the proof.

C.2 Proof of Theorem 5.2

Consider the following Lyapunov function candidate:

$$\hat{\mathcal{V}}(\hat{x}) = k_R \sum_{i=1}^{m} U(\bar{R}_k, \xi_k) + k_{\tilde{Q}} \sum_{i=1}^{n} U(\tilde{Q}_i, \zeta_i) + \sum_{i=1}^{n} \omega_i^T J_i \omega_i. \tag{C.10}$$

One can verify that the above Lyapunov function candidate is positive definite on $\hat{\mathcal{S}}$ with respect to $\hat{\mathcal{A}}$, and its time-derivative, along the trajectories generated by the flows of the hybrid closed-loop dynamics (5.18), is given by

$$\dot{\hat{\mathcal{V}}}(\hat{x}) = -k_R k_\xi \|\Psi_\nabla^\xi\|^2 - 2k_{\tilde{Q}} k_Q \|\Psi_\nabla^{\tilde{Q}}\|^2 - k_{\tilde{Q}} k_\zeta \|\Psi_\nabla^\zeta\|^2, \tag{C.11}$$

where $\zeta := [\zeta_1, \zeta_2, \ldots, \zeta_n]^T \in \mathbb{R}^n$, and $\Psi_\nabla^{\tilde{Q}} \in \mathbb{R}^{3n}$ and $\Psi_\nabla^\zeta \in \mathbb{R}^n$ are given by

$$\Psi_\nabla^{\tilde{Q}} := \left[\psi\left(\tilde{Q}_1^T \nabla_{\tilde{Q}_1} U(\tilde{Q}_1, \zeta_1)\right)^T, \psi\left(\tilde{Q}_2^T \nabla_{\tilde{Q}_2} U(\tilde{Q}_2, \zeta_2)\right)^T, \ldots, \psi\left(\tilde{Q}_n^T \nabla_{\tilde{Q}_n} U(\tilde{Q}_n, \zeta_n)\right)^T \right]^T,$$

$$\Psi_\nabla^\zeta := \left[\nabla_{\zeta_1} U(\tilde{Q}_1, \zeta_1), \nabla_{\zeta_2} U(\tilde{Q}_2, \zeta_2), \ldots, \nabla_{\zeta_n} U(\tilde{Q}_n, \zeta_n) \right]^T.$$

This implies that $\hat{\mathcal{V}}$ is non-increasing along the flow of (5.18). Furthermore, one has

$$\hat{\mathcal{V}}(\hat{x}) - \hat{\mathcal{V}}(\hat{x}^+) = k_R \sum_{k=1}^{m} \left(U(\bar{R}_k, \xi_k) - U(\bar{R}_k^+, \xi_k^+) \right) + k_{\tilde{Q}} \sum_{i=1}^{n} \left(U(\tilde{Q}_i, \zeta_i) - U(\tilde{Q}_i^+, \zeta_i^+) \right)$$
$$\geq \underline{k}\, \underline{\delta} \tag{C.12}$$

where $\underline{k} := \min\{k_R, k_Q\}$ and $\underline{\delta} := \min\{\delta_{\bar{R}}, \delta_{\tilde{Q}}\}$. Following the same steps as in the proof of Theorem 5.1, it can be shown that the set $\hat{\mathcal{A}}$ is stable, every maximal solution of the hybrid closed-loop dynamics (5.18) is complete, and the number of jumps is finite. Furthermore, consider the following two functions:

$$u_{\hat{\mathcal{F}}}(\hat{x}) := \begin{cases} -k_R k_\xi \|\Psi_\nabla^\xi\|^2 - 2k_{\tilde{Q}} k_Q \|\Psi_\nabla^{\tilde{Q}}\|^2 - k_{\tilde{Q}} k_\zeta \|\Psi_\nabla^\zeta\|^2 & \text{if } \hat{x} \in \hat{\mathcal{F}}, \\ -\infty & \text{otherwise}, \end{cases} \tag{C.13}$$

$$u_{\hat{\mathcal{J}}}(\hat{x}) := \begin{cases} -\underline{k}\, \underline{\delta} & \text{if } \hat{x} \in \hat{\mathcal{J}}, \\ -\infty & \text{otherwise}. \end{cases} \tag{C.14}$$

It follows from the invariance principle for hybrid systems given in Section 2.6 that every maximal solution of the hybrid system (5.18) converges to the following largest weakly invariant subset:

$$\hat{\mathcal{V}}^{-1}(r) \cap \hat{\mathcal{S}} \cap \left[\overline{u_{\hat{\mathcal{F}}}^{-1}(0)} \cup \left(u_{\hat{\mathcal{J}}}^{-1}(0) \cap G\left(u_{\hat{\mathcal{J}}}^{-1}(0) \right) \right) \right],$$

for some $r \in \mathbb{R}$, where $u_{\hat{\mathcal{J}}}^{-1}(0) = \emptyset$ and $u_{\hat{\mathcal{F}}}^{-1}(0) = \{\hat{x} \in \hat{\mathcal{F}} : \ \Psi_{\nabla}^{\xi} = 0, \ \Psi_{\nabla}^{\tilde{Q}} = 0, \ \Psi_{\nabla}^{\zeta} = 0\}$. Note that, for every $\hat{x} \in u_{\hat{\mathcal{F}}}^{-1}(0)$, one has $\Psi_{\nabla}^{\xi} = 0$ and, for $i \in \mathcal{V}$, $(\tilde{Q}_i, \zeta_i) \in \mathcal{F}_i^{\tilde{Q}} \cap \Upsilon$. According to (Wang and Tayebi, 2022), along with Condition 5.1, it can be shown that $\mathcal{F}_i^{\tilde{Q}} \cap \Upsilon = \{(I_3, 0)\}$. Moreover, from the fact that $\dot{\tilde{Q}}_i = 0$ (since $\tilde{Q}_i = I_3$), one has $\omega_i = k_Q \psi \left(\tilde{Q}_i^T \nabla_{\tilde{Q}_i} U(\tilde{Q}_i, \zeta_i) \right) = 0$. This implies that $k_R \bar{H} \Psi_{\nabla}^{\bar{R}} = 0$. This fact together with $\Psi_{\nabla}^{\xi} = 0$ and considering the last part of the proof of Theorem 5.1, one has $\bar{x} \in \bar{\mathcal{A}}$. Finally, one concludes that $u_{\hat{\mathcal{F}}}^{-1}(0) = \hat{\mathcal{A}}$ and every maximal solution of the hybrid system (5.18) converges to the largest weakly invariant subset $\hat{\mathcal{V}}^{-1}(0) \cap \hat{\mathcal{A}} = \hat{\mathcal{A}}$. This, together with the fact that every maximal solution of the hybrid closed-loop system (5.18) is complete and (5.18) satisfies the basic hybrid conditions given in Section 2.6.2, implies that the set $\hat{\mathcal{A}}$ is globally asymptotically stable for the hybrid closed-loop system (5.18). This completes the proof.